

การพัฒนาต้นแบบระบบผลิตเชื้อเพลิงจากวัสดุเหลือทิ้งทางการเกษตรแบบเคลื่อนย้ายได้ระดับชุมชน



นางสาวจุฬารัตน์ นิสามณีเนตร

จุฬาลงกรณ์มหาวิทยาลัย

บทคัดย่อและแฟ้มข้อมูลฉบับเต็มของวิทยานิพนธ์ตั้งแต่ปีการศึกษา 2554 ที่ให้บริการในคลังปัญญาจุฬาฯ (CUIR)  
เป็นแฟ้มข้อมูลของนิสิตเจ้าของวิทยานิพนธ์ ที่ส่งผ่านทางบัณฑิตวิทยาลัย

The abstract and full text of theses from the academic year 2011 in Chulalongkorn University Intellectual Repository (CUIR)  
are the thesis authors' files submitted through the University Graduate School.

วิทยานิพนธ์นี้เป็นส่วนหนึ่งของการศึกษาตามหลักสูตรปริญญาวิทยาศาสตรดุษฎีบัณฑิต

สาขาวิชาวิศวกรรมสิ่งแวดล้อม ภาควิชาวิศวกรรมสิ่งแวดล้อม

คณะวิศวกรรมศาสตร์ จุฬาลงกรณ์มหาวิทยาลัย

ปีการศึกษา 2560

ลิขสิทธิ์ของจุฬาลงกรณ์มหาวิทยาลัย

Prototype development of small scale transportable fuel production system for  
agricultural byproducts



A Dissertation Submitted in Partial Fulfillment of the Requirements  
for the Degree of Doctor of Philosophy Program in Environmental Engineering

Department of Environmental Engineering

Faculty of Engineering

Chulalongkorn University

Academic Year 2017

Copyright of Chulalongkorn University

Thesis Title	Prototype development of small scale transportable fuel production system for agricultural byproducts
By	Miss Jurarat Nisamaneenate
Field of Study	Environmental Engineering
Thesis Advisor	Associate Professor Viboon Sricharoenchaikul, Ph.D.
Thesis Co-Advisor	Duangduen Atong, Ph.D.

---

Accepted by the Faculty of Engineering, Chulalongkorn University in Partial Fulfillment of the Requirements for the Doctoral Degree

..... Dean of the Faculty of Engineering  
(Associate Professor Supot Teachavorasinskun, D.Eng.)

THESIS COMMITTEE

..... Chairman  
(Associate Professor Orathai Chavalparit, Ph.D.)

..... Thesis Advisor  
(Associate Professor Viboon Sricharoenchaikul, Ph.D.)

..... Thesis Co-Advisor  
(Duangduen Atong, Ph.D.)

..... Examiner  
(Associate Professor Pichaya Rachdawong, Ph.D.)

..... Examiner  
(Assistant Professor Manaskorn Rachakornkij, Ph.D.)

..... External Examiner  
(Kanit Soongprasit, Ph.D.)

จุฬารัตน์ นิตามณีเนตร : การพัฒนาต้นแบบระบบผลิตเชื้อเพลิงจากวัสดุเหลือทิ้งทางการเกษตรแบบเคลื่อนย้ายได้ระดับชุมชน (Prototype development of small scale transportable fuel production system for agricultural byproducts) อ.ที่ปรึกษาวิทยานิพนธ์หลัก: รศ. ดร.วิบูลย์ ศรีเจริญชัยกุล, อ.ที่ปรึกษาวิทยานิพนธ์ร่วม: ดร.ดวงเดือน อางองค์, 180 หน้า.

วัตถุประสงค์ของงานวิจัยนี้เพื่อศึกษาศักยภาพการแปรสภาพเปลือกถั่วลิสงและเหง้ามันสำปะหลังโดยใช้เตาปฏิกรณ์ชนิดเบตนิ่งแบบเคลื่อนย้ายได้ที่มีปรับปรุงด้วยหน่วยบูรณาการความร้อน จากการทดลองพบว่าหน่วยบูรณาการความร้อนสามารถช่วยปฏิกิริยาแกซิฟิเคชัน โดยสามารถลดปริมาณน้ำมันทาร์ และเพิ่มคุณภาพของแก๊สผลิตภัณฑ์ อัตราการไหลของอากาศมีผลต่อปริมาณและคุณภาพแก๊สผลิตภัณฑ์ ที่อัตราการไหลของอากาศสูงจะส่งผลให้ปริมาณแก๊สมาก และมีน้ำมันทาร์และผลิตภัณฑ์ถ่านชาร์ต่ำ ที่สภาวะเหมาะสมโดยไม่ใช้ตัวเร่งปฏิกิริยาของเปลือกถั่วลิสงให้ค่าการแปรสภาพของคาร์บอนเท่ากับ 87.10% ไฮโดรเจน 57.21% ค่าความร้อน  $3.95 \text{ MJ/m}^3$  และประสิทธิภาพเชิงความร้อน 56.10% ที่อัตราการไหลของอากาศ  $3.06 \text{ m}^3/\text{hr}$  และเหง้ามันสำปะหลัง ให้ค่าการแปรสภาพของคาร์บอนเท่ากับ 92.39% ไฮโดรเจน 65.92% ค่าความร้อน  $4.46 \text{ MJ/m}^3$  และประสิทธิภาพเชิงความร้อน 54.86% ที่อัตราการไหลของอากาศ  $2.50 \text{ m}^3/\text{hr}$

เพื่อปรับปรุงคุณภาพของแก๊สผลิตภัณฑ์จากกระบวนการแกซิฟิเคชันโดยใช้ตัวเร่งปฏิกิริยา พบว่าเมื่อใช้ตัวเร่งปฏิกิริยา 5%Ni/char และ 5%Ni/dolomite สามารถเพิ่มการสลายตัวของน้ำทาร์ไปเป็นแก๊สผลิตภัณฑ์ที่มีคุณภาพ เพิ่มค่าความร้อน และประสิทธิภาพเชิงความร้อนของระบบ ตัวเร่งปฏิกิริยา 5%Ni/dolomite นอกจากจะช่วยให้ปฏิกิริยาการแตกตัวแล้วยังเป็นตัวกรองน้ำมันทาร์ได้อีกด้วย ประสิทธิภาพของการใช้แก๊สเชื้อเพลิงเหลวในการผลิตกระแสไฟฟ้าเท่ากับ 16.88% ลดลงเหลือ 11.03% เมื่อใช้แก๊สเชื้อเพลิงจากเปลือกถั่วลิสง และ 11.61% เมื่อใช้แก๊สเชื้อเพลิงจากเหง้ามันสำปะหลัง ประสิทธิภาพรวมของทั้งระบบผลิตแก๊สชีวมวลและผลิตกระแสไฟฟ้า เมื่อใช้เปลือกถั่วลิสง เท่ากับ 12.69% และ 12.40% เมื่อใช้เหง้ามันสำปะหลัง ผลการทำนายองค์ประกอบแก๊สจากโมเดลพบว่าค่าจากการทำนายของเปลือกถั่วลิสงสามารถทำนายได้ใกล้เคียงกับค่าจากการทดลองมากกว่าเหง้ามันสำปะหลัง โมเดลที่ได้รับการปรับปรุงนี้สามารถใช้ประเมินประสิทธิภาพของเตาปฏิกรณ์ และปริมาณแก๊สได้

CHULALONGKORN UNIVERSITY

ภาควิชา วิศวกรรมสิ่งแวดล้อม

สาขาวิชา วิศวกรรมสิ่งแวดล้อม

ปีการศึกษา 2560

ลายมือชื่อนิสิต .....

ลายมือชื่อ อ.ที่ปรึกษาหลัก .....

ลายมือชื่อ อ.ที่ปรึกษาร่วม .....

# # 5571403821 : MAJOR ENVIRONMENTAL ENGINEERING

KEYWORDS: DOWN DRAFT GASIFIER / BIOMASS GASIFICATION / CASSAVA RHIZOME / PEANUT SHELL / NI / DOLOMITE / CHAR

JURARAT NISAMANEENATE: Prototype development of small scale transportable fuel production system for agricultural byproducts. ADVISOR: ASSOC. PROF. VIBOON SRICHAROENCHAIKUL, Ph.D., CO-ADVISOR: DUANGDUEN ATONG, Ph.D., 180 pp.

The objective is to study the potential of peanut shell waste and cassava rhizome conversion using a modular fixed bed gasifier coupled with thermal integration unit. The thermal integration unit improved gasification reaction in which lower tar content and high gas production efficiency can be achieved. The air flow rate had integrated effects on product yield and composition; higher air flow rate resulted in higher gas yield with less tar and char. The result from peanut shell gasification indicated the optimal conditions without catalyst addition at air flow rate of  $3.06 \text{ m}^3/\text{hr}$  where carbon and hydrogen conversions were 87.10% and 57.21%, respectively. The lower heating value and cold gas efficiency were  $3.95 \text{ MJ/m}^3$  and 56.10%, respectively. In case of cassava rhizome, carbon and hydrogen conversion were 92.36%, and 65.92%, respectively at  $2.5 \text{ m}^3/\text{hr}$  air flow. The lower heating value and cold gas efficiency were  $4.46 \text{ MJ/m}^3$  and 54.86%, respectively.

For improve quality of product gas from gasification, the 5%Ni/char and 5%Ni/dolomite catalyst enhanced condensable tar reforming to smaller gases resulting in increased gas heating value and cold gas efficiency with greater synthesis gas yield. The 5%Ni/dolomite catalyst can be employed as both the tar filter and also enhanced catalytic cracking reactions. With product gas connection to a generator, the conversion to electricity was 11.03% with peanut shell and 11.29% with cassava rhizome. The efficiency of the gasifier-cogeneration system from peanut shell and cassava rhizome waste was 11.84% and 12.12%, respectively. The predicted gas composition results from ASPEN PLUS simulation model for peanut shell waste were better than those of cassava rhizome. Generally, developed model is able to simulate the performance of the gasifier with acceptable gas yield estimation.

Department: Environmental Engineering

Field of Study: Environmental Engineering

Academic Year: 2017

Student's Signature .....

Advisor's Signature .....

Co-Advisor's Signature .....

## ACKNOWLEDGEMENTS

This doctoral dissertation could not be accomplished without the support of several people. It is an honor to thank those who helped make this possible. First of all, I would like to express my sincere gratitude to my advisor, Associate Professor Viboon Sricharoenchaikul, and my co-advisor, Dr. Duangduen Atong, for their continuous support of my Ph.D. study and research in addition to their patience and worth advice which gave me the guidance and constant encouragement throughout the research. My special thanks also to the thesis committee namely Associate Professor Orathai Chavalparit, Chairman of the committee; Assistant Professor Manaskorn Rachakornkij, Examiner; Associate Professor Pichaya Rachdawong, Examiner and Dr. Kanit Soongprasit, External Examiner.

I would like to thank the National Metal and Materials Technology Center (MTEC) for providing related facilities and equipment. Especially, I also need to express my gratitude to my school, Department of Environmental Engineering, Faculty of Engineering, Chulalongkorn University, for giving me the chance in the advanced study.

I must acknowledge my friends at Chulalongkorn University and authorities at MTEC for advising in a part of characteristics analysis along with continuous support on my research over the years. I would also like to thank all other people who have helped me during my research study at both the Department of Environmental Engineering and MTEC. These include laboratory technicians, other respected lecturers, and other staffs; without their help, this study would not have been possible.

Last but not the least, I would like to thank my family for giving birth to me in the first place and supporting me throughout my life.

## CONTENTS

	Page
THAI ABSTRACT .....	iv
ENGLISH ABSTRACT .....	v
ACKNOWLEDGEMENTS .....	vi
CONTENTS .....	vii
LIST OF TABLES .....	xi
LIST OF FIGURES .....	xii
CHAPTER 1 Introduction.....	1
1.1 Thesis Topic.....	1
1.2 Keywords.....	1
1.3 Background .....	1
1.4 Research objectives .....	5
1.5 Research Hypothesis.....	5
1.6 Scope of work.....	6
1.7 Benefit of research.....	6
CHAPTER 2 Theory and Literature Review .....	7
2.1 Biomass Thermal Conversion Processes .....	7
2.2 Biomass .....	7
2.2.1 Structure of Biomass .....	8
2.2.2 Constituents of biomass cells .....	9
2.2.3 Biomass characteristics related to gasification.....	10
2.3 The gasification process.....	12
2.3.1 Gasifying Mediums .....	13

	Page
2.3.2 Gasification Reactions and Steps.....	14
2.4 Gasifier type.....	18
2.4.1 Updraft gasifier .....	20
2.4.2 Downdraft gasifiers.....	20
2.4.3 Cross draft gasifier.....	21
2.5 Gasification parameters.....	24
2.5.1 Gasification parameters .....	25
2.6 Gas conditioning .....	27
2.6.1 Tar removal and conversion.....	28
2.7 Catalytic Gasification.....	28
2.7.1 Catalyst Selection.....	30
2.7.2 Catalyst .....	31
2.8 Biomass Gasification Models.....	32
2.8.1 Kinetic rate models .....	32
2.8.2 Thermodynamic equilibrium models.....	33
2.9 Literature review.....	34
CHAPTER 3 Experimental Procedures.....	45
3.1 Biomass Fuel Analysis and Experimental setup.....	46
3.1.1 Biomass Preparation .....	47
3.1.2 Experimental setup .....	49
3.2 Gasifier test and modified .....	50
3.2.1 Characteristics of gas.....	51
3.2.2 Characteristics of char and tar .....	51



	Page
3.2.3 Modifier with the thermal integration unit .....	51
3.2.4 The effect of gasification parameter.....	52
3.3 Improvement of the gasification efficiency with metal catalyst .....	52
3.3.1 Catalyst Preparation .....	52
3.3.2 Characterization of catalyst.....	55
3.4 Power generation and predict product distribution from gasification unit. ....	55
CHAPTER 4 The Characteristic of Biomass and Catalyst.....	58
4.1 Characteristic of biomass.....	58
4.1.1 The cassava rhizome.....	58
4.1.2 The peanut shell waste.....	58
4.2 Characterization of catalyst.....	60
4.2.1 Ni/Char catalyst .....	60
4.2.2 Ni/dolomite Catalyst .....	63
4.3 Characteristic of spent catalyst .....	66
4.3.1 Ni/char catalyst.....	66
4.3.2 Ni/dolomite catalyst.....	68
CHAPTER 5 Biomass Gasification with a Downdraft Gasifier.....	70
5.1 Gasification performance of downdraft gasifier with peanut shell waste .....	70
5.1.1 The system performance and effect of heat recovery unit. ....	70
5.1.2 The effect of air flow rate.....	72
5.1.3 The effect of Ni/char catalyst addition .....	77
5.1.4 The effect of Ni/dolomite catalyst.....	78
5.2 Gasification performance of downdraft gasifier with Cassava rhizome.....	81

	Page
5.2.1 The system performance and effect of heat recovery unit. ....	81
5.2.2 The effect of air flow rate.....	84
5.2.3 The effect of biomass particle size.....	86
5.2.4 The effect of Ni/char catalyst.....	89
5.2.5 The effect of Ni/dolomite catalyst.....	91
5.3 Characteristic of char and tar from gasification.....	93
5.4 Power gas generation .....	94
5.5 ASPEN MODEL .....	98
5.5.1 Simulation Assumptions.....	98
5.5.2 Gasification model description.....	99
CHAPTER 6 Conclusions and Future work recommendations .....	106
REFERENCES .....	108
VITA.....	180

## LIST OF TABLES

Table 2.1 Heating value for production gas based on gasifying medium.....	14
Table 2.2 Typical gasification reaction at 25°C.....	16
Table 2.3 Review of the biomass gasification with downdraft gasifier.....	40
Table 2.4 Review of the biomass gasification with nickel Catalyst.....	42
Table 2.5 Review of biomass gasification models.....	43
Table 3.1 ASTM standard methods for analysis of biomass.....	47
Table 3.2 Specification of gas engine/generator.....	56
Table 4.1 Characteristic of cassava rhizome.....	59
Table 4.2 Characteristic of peanut shell.....	60
Table 5.1 Effects of heat thermal integration unit addition (1.62 m <sup>3</sup> /hr air flow rate).....	72
Table 5.2 Effects of air flow rate on biomass consumption and cold gas efficiency. .	76
Table 5.3 The mass input, mass output and the mass balance closures from peanut shell gasification. ....	76
Table 5.4 Effect of catalyst on carbon and hydrogen conversions. ....	81
Table 5.5 Effects of heat thermal integration unit with 1.98 m <sup>3</sup> /hr.....	84
Table 5.6 Effects of air flow rate on biomass consumption and cold gas efficiency. .	88
Table 5.7 The mass input, mass output and the mass balance closures from cassava rhizome gasification.....	89
Table 5.8 The simulation of operation condition gasification parameter. ....	100
Table 5.9 Description of the unit operation of the blocks in the simulation.....	100

Table 5.10 The gas composition from peanut shell gasification: experimental & simulation.....	102
Table 5.11 The gas composition from cassava rhizome (1-5 mm) gasification: experimental & simulation. ....	104
Table 5.12 The gas composition from cassava rhizome (5-10 mm) gasification: experimental & simulation. ....	105
Table 5.13 The gas composition from cassava rhizome (10-15 mm) gasification: experimental & simulation. ....	105

## LIST OF FIGURES

Figure 2.1 Biological and chemical processes for conversion of biomass into fuel, gases, or chemicals. ....	8
Figure 2.2 Major constituent of a woody biomass.....	9
Figure 2.3 Molecular structure of cellulose. ....	9
Figure 2.4 Molecular structure of a typical hemicellulose, xylan .....	10
Figure 2.5 Some structural unit of lignin.....	10
Figure 2.6 C-H-O diagram of the gasification process.....	13
Figure 2.7 Potential paths for gasification.....	14
Figure 2.8 Gasification technologies and their commercial supplier. ....	19
Figure 2.9 Range of applicability of biomass gasifier types.....	19
Figure 2.10 Schematics of (a) updraft (b) and (c) crossdraft gasifier. ....	21
Figure 2.11 Downdraft gasifier with open top (a), conventional doendraft (b), Imbert gasifier (c). ....	24
Figure 2.12 (a) V-heart Imbert gasifier, (b) Flat-plat hearth constriction, (c) The space between the nozzles .....	24
Figure 2.13 Equivalence ratio .....	25

Figure 3.1 Experimental plan .....	45
Figure 3.2 Grinding Machine.....	48
Figure 3.3 The particle sizes of cassava rhizome.....	48
Figure 3.4 The peanut shell waste.....	48
Figure 3.5 Schematic of a modular downdraft gasifier system used in the experiment.....	50
Figure 3.6 Portable analyzer.....	51
Figure 3.7 The thermal integration unit.....	52
Figure 3.8 Char support was prepare by slow pyrolysis of cassava rhizome (b) Char support.....	53
Figure 3.9 Ni/char catalyst was prepare by the impregnation method (a) char support (b) impregnation with $\text{Ni}(\text{NO}_3)_2 \cdot 6\text{H}_2\text{O}$ (c) drying (d) calcination. ....	53
Figure 3.10 (a) dolomite power (b) organic binder (c) kaolin power (d) extruder (e) and (f) extrusion dolomite.....	54
Figure 3.11 Ni/dolomite pellet catalyst was prepared by the impregnation method (a) dolomite support (b) impregnation with $\text{Ni}(\text{NO}_3)_2 \cdot 6\text{H}_2\text{O}$ (c) drying (d) calcination.....	54
Figure 3.12 The catalyst holder.....	55
Figure 3.13 Schematic diagram of the downdraft gasifier combined with power generation system.....	56
Figure 3.14 gas engine/generator system .....	57
Figure 4.1 X-Ray diffraction of char support and calained 5%Ni/char.....	61
Figure 4. 2 TGA results of (a) 5%Ni/char (b) calcined 5%Ni/char.....	62
Figure 4.2 TGA results of (a) 5%Ni/char (b) calcined 5%Ni/char .....	62
Figure 4.3 SEM of (a, b) char support, (c, d) 5%Ni/char and (e, f) calcined 5%Ni/char.....	63

Figure 4.4 XRD of the fresh catalyst; (a) dolomite (b) calcined dolomite (c) 5%Ni/dolomite and (d) calcined 5%Ni/dolomite. ....	64
Figure 4.5 TGA thermogram of (a) calcined dolomite (b) calcined 5%Ni/dolomite ....	65
Figure 4.5 TGA thermogram of (a) calcined dolomite (b) calcined 5%Ni/dolomite ....	65
Figure 4.6 SEM of (a) dolomite (b) calcined dolomite (c) 5%Ni/dolomite .....	66
Figure 4.7 TGA of (a) spent char and (b) spent 5%Ni/char .....	67
Figure 4.8 SEM of (a) spent char and (b) spent 5%Ni/char .....	67
Figure 4.9 TGA of (a) spent dolomite pellet and (b) spent 5%Ni/dolomite.....	68
Figure 4.10 SEM of (a) spent dolomite pellet and (b) spent 5% Ni/dolomite.....	69
Figure 5.1 Temperature distribution within gasifier w/o thermal integration unit. ....	71
Figure 5.2 Temperature distribution within gasifier with heat thermal integration unit.....	71
Figure 5.3 Effect of heat recovery addition on conversion and cold gas efficiency.....	72
Figure 5.4 Effect of air flow rate on conversion without heat thermal integration unit.....	74
Figure 5.5 Effect of air flow rate on conversion with heat thermal integration unit....	75
Figure 5.6 Effect of air flow rate on H <sub>2</sub> /CO and biomass consumption rate.....	75
Figure 5.7 Effect of Char, 5%Ni/Char and Activated carbon catalysts on gas composition to gas products. ....	78
Figure 5.8 Effect of dolomite catalyst on gas composition. ....	80
Figure 5.9 Effect of 5%Ni/dolomite and 10%Ni/dolomite catalyst on gas composition. ....	80
Figure 5.10 Temperature distribution within gasifier w/o thermal integration unit. ....	82
Figure 5.11 Temperature distribution within gasifier with heat thermal integration unit.....	83

Figure 5.12 Effect of heat recovery addition on conversion and cold gas efficiency. .	83
Figure 5.13 Effect of air flow rate on conversion of cassava rhizome ( $\leq 5$ mm).....	87
Figure 5.14 Effect of air flow rate on conversion of cassava rhizome (5-10 mm).....	87
Figure 5.15 Effect of air flow rate on conversion of cassava rhizome (10-15 mm). ....	88
Figure 5.16 Effect of 5%Ni/char catalyst on gas composition from cassava rhizome gasification.....	90
Figure 5.17 Effect of 5%Ni/char catalyst on C and H conversions from cassava rhizome gasification.....	91
Figure 5.18 Effect of 5%Ni/dolomite catalyst on gas composition from cassava rhizome gasification.....	93
Figure 5.19 Effect of 5%Ni/dolomite catalyst on C and H conversions from cassava rhizome gasification.....	93
Figure 5.20 Composition of gas produced from peanut shell gasification. ....	95
Figure 5.21 Composition of gas produced from cassava rhizome gasification. ....	95
Figure 5.22 The efficiency of the engine generator using LPG fuel.....	97
Figure 5.23 The efficiency of the engine generator using producer gas from cassava rhizome gasification.....	97
Figure 5.24 The efficiency of the engine generator using producer gas from peanut shell gasification.....	98
Figure 5.25 Flow chart of biomass gasification simulation using Aspen Plus.....	99
Figure 5.26 Comparison of gas composition from peanut shell gasification: experimental & simulation. ....	102
Figure 5.27 Comparison of gas composition from cassava rhizome (1-5 mm) gasification: experimental & simulation. ....	103
Figure 5.28 Comparison of gas composition from cassava rhizome (5-10 mm) gasification: experimental & simulation. ....	103

Figure 5.29 Comparison of gas composition from cassava rhizome (10-15 mm)  
gasification: experimental & simulation. .... 104





## CHAPTER 1

### Introduction

#### 1.1 Thesis Topic

ภาษาอังกฤษ Prototype development of small scale transportable fuel production system for agricultural byproducts

ภาษาไทย การพัฒนาต้นแบบระบบผลิตเชื้อเพลิงแบบเคลื่อนย้ายได้ขนาดเล็กสำหรับวัสดุเหลือทิ้งทางการเกษตร

#### 1.2 Keywords

Cassava rhizome

Peanut shells

Downdraft gasifier

Gasification

Nickel

Char

Dolomite

ASPEN PLUS



#### 1.3 Background

Fossil fuels resources are declining rapidly while their usages raising the problems of global warming and numerous other environmental impacts. To overcome these problems, expanding the use of biomass has been suggested as an alternative option to conventional ones (Basu, 2010b). Biomass can be converted into energy and other chemicals products via thermochemical processes. Combustion, pyrolysis and gasification are the three main thermochemical conversion methods. Gasification is partial thermal oxidation, which results in a high proportion of gaseous products. This technology is more proper to be applied to biomass than coal due to their comparatively high H/C ratio. The gas produced can be standardized in its quality and is easier and has more all-around usage than the

original biomass e.g. it can be used to power gas engines and gas turbines or as chemical feedstock for the production of liquid fuels (Olgun et al., 2011).

A downdraft gasifier is a co-current flow reactor where biomass is fed at the top and air intake enters at the top or throat section and flows in the same direction as that of biomass. The product gas flows downward and leaves through a bed of hot ash. This enables cracking of tar during the gasification process due to gas passage through a high-temperature zone. For this reason, the advantage of a downdraft gasifier was higher conversion efficiency with a low tar and particulate matter generations. Imbert downdraft gasifier is the close top gasifier with a throat section at the reactor core. The throat in the gasifier design plays important role in reducing the tar concentration in the producer gas. The downdraft gasifier was developed to convert high volatile raw materials to low tar fuel gas and has been proven to be one of the most effective design for power generation. The reasons for designing Imbert type gasifier as a modular (small scale transportable) downdraft gasifier used in this experiment are that a modular gasifier is suitable for remote area since collection and costly transportation of biomass raw material are not required while the capital cost can be kept low. Additional benefit in such a rural setup mechanism is the possibility of the utilization of various wastes from the local agriculture and industry. Lately, the researches in the downdraft gasification have been intensified in order to improve its performance, e.g., Dogru et al. (2002) studied gasification of hazelnut shells in a downdraft gasifier, the quality of product gas is found to be dependent on the smooth flow of fuel. Sheth and Babu (2010) have investigated on producer gas generated from wood waste in a downdraft biomass gasifier and examined the reliability of the results by performing material balance. In addition, Zainal et al. (2002) investigated the downdraft gasifier using wood chips and charcoal by varying the equivalence ratio. Skoulou et al. (2008) made a comparison study in performance of tree cutting and olive kernels. They reported that  $H_2$  yield in gas production of raw materials could be increased by rising temperature. In addition to the gasification by downdraft facility, many research teams applied this method on variety biomass (Jain et al., 2000), (Demirbaş, 2001), (Jayah et al., 2003; P. M. Lv et al., 2004), (Wander et al., 2004), (Hanaoka et al., 2005;

Yoon et al., 2012), (Tinaut et al., 2008), (Olgun et al., 2011; Sharma, 2009), (Martinez et al., 2012), (Gai et al., 2012), and (Pérez et al., 2012).

As feedstock of downdraft gasification, various biomasses have been intensively used in the previous works including many agricultural residues and wastes. However, cassava rhizome and peanut shell waste are rarely tested in downdraft gasification. Therefore, these agricultural residues will be applied as feedstock in this study. Cassava rhizome is a part of the neck between trunks and tuberous roots, which become the residue from cassava plantations. According to the recent survey in Thailand, approximately 7 million acres of cassava plantation could yield 25 million tons of cassava roots. Usually, the current practice of cassava rhizome residue management is open burning, which releases not only the greenhouse gases but also other pollutions as well as loss of energy. Therefore, utilization of cassava rhizome as energy source by gasification has potential to resolve this environmental problem while generating useful fuel gas products and power. Peanut plantation is a common agricultural in Asia. Worldwide peanut production was 40.18 million tons, of which 50,000 tons were produced in Thailand (El-Siddig et al., 2006). Thai peanut shell residues from peanut process plant were used as raw material for this study. Although these residues have high heating value, peanut shell wastes are usually burned by combustion, not gasification process which is a more efficient process. Their high heating value and low moisture content are appropriate with gasification process.

In order to improve gasification efficiency, a thermal integration and catalyst unit was coupled to the main reactor. Thermal integration unit is a gas circulating heat exchanger that returns hot fuel gas exiting the gasifier back to drying and pyrolysis zone in addition to increase residence time to cracking and reforming the product gas from the gasifier. The catalytic cracking is recognized as the most efficient method to eliminate the tar in the produced gas. Nickel catalysts are highly effective on tar removal and hydrogen yield improvement. These catalysts are normally supported by natural materials, for example, dolomite, olivine, and active charcoal (Bulushev et al., 2011; McKendry, 2002b). Char, a carbonaceous product of

pyrolysis, may also be applied as catalyst for tar reforming when used in the secondary reactor. Chars have been reported to be inexpensive support and also an excellent adsorbent (McKendry, 2002b). Many researchers have studied Ni and metal catalyst on char support for biomass gasification to reduced tar content in production gas. Wang et al. (2011) investigated char and char support nickel catalyst for secondary syngas cleanup and conditioning. Ni/Coal-char and Ni/wood-char convert 97% of tar in syngas at 800°C with 15% NiO loading. Shen et al. (2014) also studied the iron supported on biomass char and brown coal char which were used as a hot gas cleaning catalysts. The result suggested that catalysts would decrease CO<sub>2</sub> and CH<sub>4</sub> and increase H<sub>2</sub> and CO in the product gas. Miao et al. (2010) , studied decomposition of acetic acid using porous dolomite pellets catalyst at 800°C. They found that 99.70% of acetic acid was decomposed and the porous dolomite pellets were much more effective than the natural dolomite particles. Wang et al. (2012) observed the steam gasification of MSW with NiO supported on modified dolomite and reported that the catalysts could eliminate tar in the gas production and increased the hydrogen yield. Therefore, char from cassava rhizome pyrolysis and dolomite pellets were used as catalyst support in this study.

Simulations model can be helpful for prediction of operational behavior, efficiency of gasification system, startup, change of biomass, change of loading. The Advanced System for Process Engineering (ASPEN) process simulator has been used by different investigators to simulate the gasification process. Ramzan et al. (2011) established steady state simulation model for biomass gasification using ASPEN PLUS. They concluded that the model can be used as a predictive tool for optimization of the gasifier performance. Keche Amba et al. (2015) explored the simulation of biomass gasification in downdraft gasifier for different biomass using ASPEN PLUS. This model developed with ASPEN PLUS is validated with data obtained from four types of biomass. This model well predicted composition of H<sub>2</sub>, CO, and CO<sub>2</sub> while under predicted the CH<sub>4</sub>.

The objective of this research is to study the gasification of peanut shell waste and cassava rhizome with modular downdraft gasifier. The present study is to investigate the effects of air flow rate, biomass particles size, addition of thermal

integration unit and catalyst unit on biomass gasification efficiency. The performance of biomass gasification was evaluated in term of zone temperature, producer gas composition, conversion, air superficial velocity, biomass consumption rate, gasification efficiency, and specific gasification rate at various conditions.

The fuel gas produced from the gasification unit was combined with a small gas engine system (based on LPG fuels) for power generation. In addition, this research was to develop a steady state simulation for biomass gasifier to predict the gas composition using ASPEN PLUS. The results obtained through the model are validated with the experiment results from this modular downdraft gasifier.

#### **1.4 Research objectives**

1.4.1 To modify an Imbert typed small scale transportable downdraft gasifier system coupled with heat recovery and catalyst unit for upgrade fuel gas production and reduced tar content.

1.4.2 To investigate the effect of air flow rate and biomass particle size on conversion of raw material to fuel gas.

1.4.3 To study the effect of the secondary catalytic cleaning and upgrading with Ni/char and Ni/dolomite pellet catalysts on fuel gas produced from the gasification unit.

1.4.4 To study the potential of the power generation through gas engine using fuel gas produced from the gasification unit.

1.4.5 To predict product distribution from gasification of agricultural byproducts using Advanced System for Process Engineering (ASPEN).

#### **1.5 Research Hypothesis**

1.5.1 Imbert type downdraft gasifiers coupled with heat recovery and catalyst unit can convert more than 80% of carbon and hydrogen contents in selected agricultural by products to fuel gas.

1.5.2 Advanced System for Process Engineering (ASPEN) can be used to estimate the yield of fuel gas from gasification agricultural byproducts within +/- 15% of experimental measurement.

## 1.6 Scope of work

1.6.1 Modified a small scale downdraft gasifier.

- Build an Imbert typed downdraft gasifier with a throat section to reducing the tar content in the producer gas.

- Modified the gasifier with the thermal integration unit to improve heat recovery.

- Feeding system by auger motor with level fuel sensor.

1.6.2 Gasifier tests with agricultural by products.

- Use cassava rhizome and peanut shell waste as raw material.

- The effect of air flow rate at 1.62-3.05 m<sup>3</sup>/hr and biomass particle size.

1.6.3 Cleaning and upgrading with Ni catalyst on char and dolomite pellets support on fuel gas produced.

- Preparation of the char support from cassava rhizome with the tube reactor by slow pyrolysis.

- Preparation of dolomite pellets support by extrusion.

- Ni/char and Ni/dolomite pellet catalysts were prepared by the impregnation method using Ni(NO<sub>3</sub>)<sub>2</sub>·6H<sub>2</sub>O.

1.6.4 The gasification unit was combined with a small gas engine system and utilizing Advanced System for Process Engineering PLUS (ASPEN PLUS) model to predict the composition of gas from this downdraft gasifier.

## 1.7 Benefit of research

1.7.1 The optimal conditions for the production of fuel gas from agricultural by downdraft gasifier.

1.7.2 The added value of biomass from agricultural byproduct and approach to development the potential of biomass utilized to fuel gas.

1.7.3 Prototype development of small scale transportable fuel gas production system for agricultural by products at community level.

## CHAPTER 2

### Theory and Literature Review

#### 2.1 Biomass Thermal Conversion Processes

Biomass can be converted into useful forms of energy using a number of different processes. The choice of conversion process are the type and quality of biomass feed stock, the desired form of the energy, end used requirements, environmental standard, economic conditions, and project special factor (McKendry, 2002a). Conversion of biomass to energy is undertaken using two main process technologies: thermochemical and biochemical. In thermochemical conversion, the entire biomass is converted into gases, which are then synthesized into the desired chemicals or used directly. Production of thermal energy is the main driver for this conversion route that has four broad pathways: Combustion, Pyrolysis, Gasification, and Liquefaction. Combustion involves high-temperature conversion of biomass in excess air into carbon dioxide and steam. On the other hand, gasification involves a chemical reaction in an oxygen limited environment. Pyrolysis takes place at a relatively low temperature in the total absence of oxygen. In liquefaction, the large feedstock molecules are decomposed into liquids having smaller molecules. Gasification is partial thermal oxidation which results in a high proportion of combustible gaseous products. Biomass can be converted into various products via gasification processes. Thermal processes have high throughputs and can, in principle, operate on any biomass form (McKendry, 2002a, 2002b).

#### 2.2 Biomass

Biomass is a renewable energy source because the conversion formed through the process of photosynthesis, chlorophyll in the plants captures the sun energy by the absorption of carbon dioxide from the atmosphere and water from the ground into carbohydrates, complex compounds of carbon, hydrogen, and oxygen.

### 2.2.1 Structure of Biomass

Biomass is a complex mixture of organic materials such as carbohydrates, fats, and proteins. Additionally a small amounts of inorganics such as sodium, phosphorus, calcium, and iron. The main components of plant biomass are extractives, fiber or cell wall, and ash as shown in Figure 2.2.

- Extractives: Substances present in vegetable or animal tissue that can be separated by successive treatment with solvents and recovered by evaporation of the solution. These include protein, oil, starch, sugar, etc.

- Cell wall: Provides structural strength to the plant, allowing it to stand tall above the ground without support. A typical cell wall is made of carbohydrates and lignin. Carbohydrates are mainly cellulose or hemicellulose fiber, which impart strength to the plant structure; the lignin holds the fibers together. These constituents vary with types of plant.

- Ash: The inorganic component of the biomass after burning.

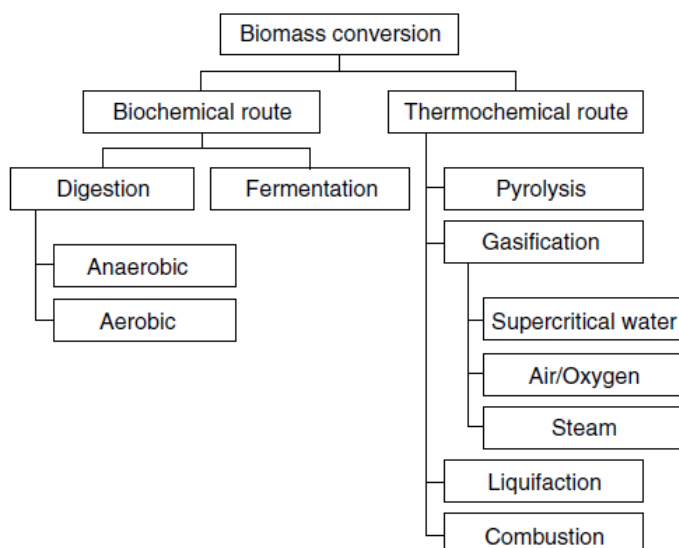


Figure 2.1 Biological and chemical processes for conversion of biomass into fuel, gases, or chemicals (Basu, 2010a).



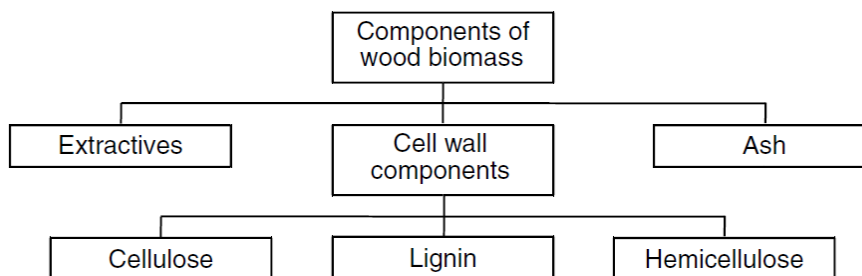


Figure 2.2 Major constituent of a woody biomass (Basu, 2010a).

## 2.2.2 Constituents of biomass cells

### 1. Cellulose

Cellulose is the primary structural parts of cell walls in biomass, and it can be represented by the generic formula  $(C_6H_{10}O_5)_n$ . Cellulose is a long chain polymer with a high degree of polymerization and a large molecular weight (Figure 2.3). It has a crystalline structure of thousands of unit, which is made up of many glucose molecules (Klass, 1998a). Cellulose is primarily composed of d-glucose, which is made of 6 carbons or hexose sugar. The cellulose is a dominant component of wood about 40-44% by dry weight.

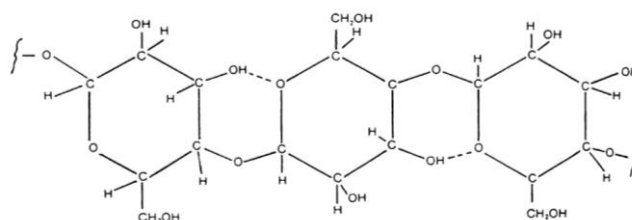


Figure 2.3 Molecular structure of cellulose (Basu, 2010b, 2013a).

### 2. Hemicellulose

Hemicellulose has a random, amorphous structure with little strength. It is a group of carbohydrates with a branched chain structure and a lower degree of polymerization, and may be represented by the generic formula  $(C_5H_8O_4)_n$ . In Figure 2.4 is shown the molecular arrangement of a typical hemicellulose molecule, or xylan. Hemicellulose molecule is smaller than that of cellulose, it breaks down more easily than cellulose and many hemicelluloses are soluble in alkaline solution such as NaOH and KOH. Hemicellulose tends to yield more gases and less tar than cellulose. It constitutes around 20-30% of dry weight.

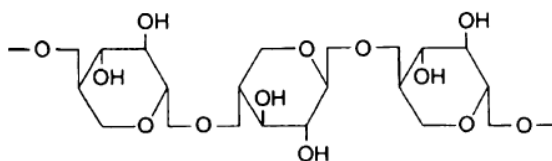


Figure 2.4 Molecular structure of a typical hemicellulose, xylan (Basu, 2010b, 2013a).

### 3. Lignin

Lignin is a complex highly branched polymer of phenyl propane units and is an integral part of the secondary cell walls of plants. It is primarily a three dimensional polymer of 4-propenyl phenol, 4-propenyl-2-methoxy phenol, and 4-propenyl-2,5-dimethoxy phenol (Figure 2.5). The complex three dimensional structures are decomposed with difficulty by microorganisms and chemicals, and its function is therefore thought to be conferring mechanical strength and protection. A typical hard wood contains about 18-25%, while range of 25-35% in softwood contains by dry weight.

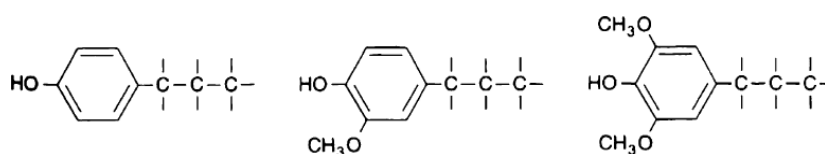


Figure 2.5 Some structural unit of lignin (Basu, 2010b, 2013a).

### 2.2.3 Biomass characteristics related to gasification

#### 1. Moisture content

The moisture content of biomass is defined as the quantity of water in the material expressed as a percentage of the material weight. This weight can be referred to on a wet basis, on a dry basis, and on a dry-and-ash free basis. For thermal conversion process like gasification, preference is given to relatively dry biomass feed stock because a higher quality gas is produced. Natural drying is cheap but requires long drying times. Artificial drying is more expensive but also more effective. In practice, artificial drying is often integrated with the gasification plant to ensure a feedstock of constant moisture content. Then biomass drying process using waste heat from engine/turbine industry plant.

#### 2. Ash content and composition

Ash is the inorganic or mineral content of the biomass, which remains after complete combustion. The amount of ash in different type of feed stock varies widely and influences the design of the reactor, and particularly the ash removal system. The chemical inorganic matter in biomass fuel, because it affects the melting behavior of the ash. In Combustion process, the ash can reacts to form a slag, a liquid phase formed at elevated temperatures.

### 3. Elemental composition

The generic formula for biomass is  $CH_{1.4}O_{0.6}$  on dry ash free basis. The elemental composition of the fuel is important with respect to the heating value and the emission levels in almost all application. The production of nitrogen and sulfur compounds is generally small in biomass gasification because of the low nitrogen and sulfur content in biomass.

### 4. Heating value

The biomass heating value is determined by the elemental composition, the ash content of the biomass and in particularly on the fuel moisture content. On a dry and ash free basis, the average heating value 19 MJ/kg. The heating value of any fuel can be measured with bomb calorimeter. Several empirical formulas exist to calculate the heating value from its elemental composition (Higman et al., 2008b). The higher heating value is the total energy content released when the fuel is burnt in air, including the latent heat contained in the water vapor and therefore represents the maximum amount of energy potentially recoverable from a given biomass source. The actual amount of energy recoverable energy will vary with the conversion technology, as with the form of that energy i.e. combustible gas, oil, steam, etc. In practical terms, the latent heat contained in the water vapor cannot be used effectively and therefore, the LHV is the appropriate value to use for the energy available for subsequent use.

### 5. Bulk density and morphology

The bulk density refers to the weight of material per unit of volume. It differs for various types of biomass. With the heating value, it determines the energy density of the gasifier feedstock. The importance of the as produced, bulk density is in relation to transport and storage costs. Apart from handling and storage behavior, the

bulk density is important for the performance of the biomass as a fuel inside fixed bed reactors: a high void age tends to result in channeling, bridging, incomplete conversion and decrease in the capacity of the gasifier. The biomass size distribution are important in determining the pressure drop over the fuel bed and for satisfactory operation. Uniform particle size and favorable particle properties are usefulness for avoid such problems.

#### 6. Volatile matter content

Volatile matter is important components for characterization of biomass fuel. The amount of volatile has an impact on the tar production levels in gasifier. Depending upon the gasifier design, the volatiles leave the reactor at low temperature. Normally, the volatile matter content in the biomass materials varies between 50 and 80 wt%.

### 2.3 The gasification process

Gasification is the conversion of solid or liquid feedstock into gaseous fuel or chemical feedstock which can be burned to release energy or used for production of value-added chemicals. Gasification and combustion are related thermochemical processes, but there is an important difference between them. Gasification packs energy into chemical bonds in the product gas while combustion breaks those bonds to release the energy. The gasification process adds hydrogen to and strips carbon away from the feedstock to produce gases with higher hydrogen-to carbon (H/C) ratio, whereas combustion oxidizes the hydrogen and carbon into water and carbon dioxide, respectively. Gasification processes convert biomass into combustible gases that ideally contain all the energy originally present in the biomass. In practice, gasification can convert for 60% to 90% of the energy in the biomass into energy in the gas phase. Gasification processes can be either direct (using air or oxygen mediate to generate heat through exothermic reactions) or indirect (transferring heat to the reactor from the outside). The gas can be burned to produce industrial or residential heat, to run engines mechanical or electrical power, or synthetic fuels (Basu, 2010b)

### 2.3.1 Gasifying Mediums

Gasifying agents react with solid carbonaceous and heavier hydrocarbons to convert them into low molecular weight gases for CO and H<sub>2</sub>. The main gasifying agent used for gasification are oxygen, steam, and air (Table 2.1). The heating value and the composition of the gas produced are strong functions of the nature and amount of gasifying agent used. The diagram of carbon, hydrogen, and oxygen demonstrates the conversion paths of formation of different products in a gasifier.

Oxygen is used as the gasifying agent, the conversion path moves toward the oxygen corner. Its products include CO for low oxygen, while CO<sub>2</sub> for high oxygen. When the amount of oxygen exceeds a stoichiometric amount, the process moves from gasification to combustion product is flue gas instead of fuel gas. If steam is used as the gasifier agent, the path is toward the hydrogen corner in Figure 2.6. Then the product gas contains more hydrogen per unit of carbon, resulting in higher H/C ratio. The gasifying agent affects the heating value of the product gas. If air is used instead of oxygen, the nitrogen in it greatly dilutes the product gas. The oxygen gasification has the highest heating value followed by steam and air gasification.

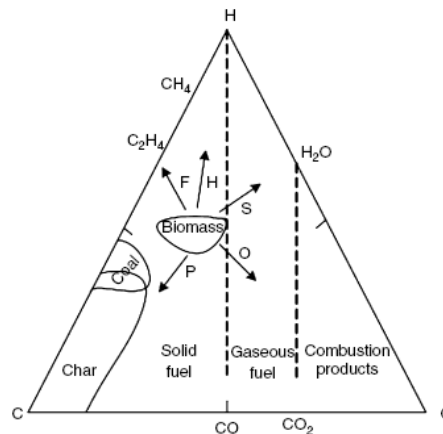


Figure 2.6 C-H-O diagram of the gasification process; H hydrogen; S steam; O oxygen;

P slow pyrolysis; F fast pyrolysis (Basu, 2010b).

Table 2.1 Heating value for production gas based on gasifying medium (Higman et al., 2008c).

Medium	Heating Value (MJ/Nm <sup>3</sup> )
Air	4-7
Steam	10-18
Oxygen	12-28

### 2.3.2 Gasification Reactions and Steps

A typical gasification process generally follows the sequence of steps shown in Figure 2.7. In a typical process, biomass is first dried and then it undertakes thermal degradation or pyrolysis. The products of pyrolysis react among themselves as well as with the gasifying medium to form the final gasification product.

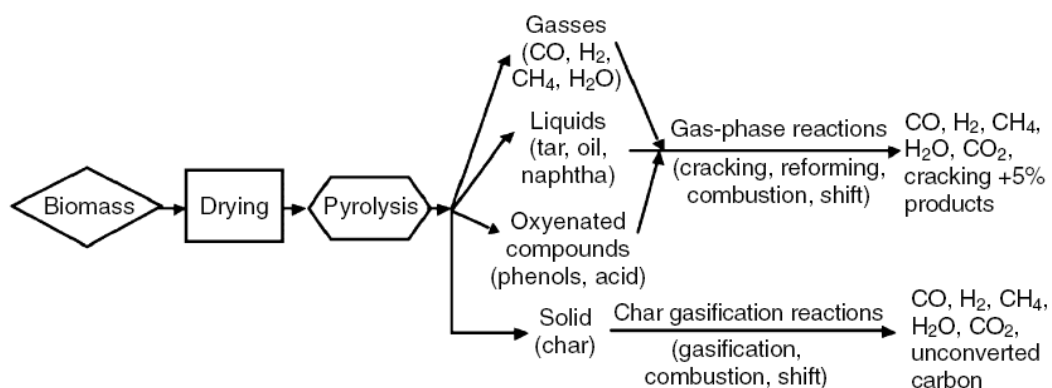


Figure 2.7 Potential paths for gasification (Basu, 2010b).

#### 1. Drying

Every kilogram of moisture content in the biomass requires a further 2260 kJ to vaporize water, and the energy is not recoverable. The final drying takes place after the feed enters the gasifier, where it receives water. Above 100°C, the loosely bound water that is in the biomass is irreversibly removed. As the temperature rises, the low molecular weight extractives start volatilizing. This process continues until a temperature of approximately 200°C is reached. The moisture content is affected in the gasification process, as the moisture content increase means that more energy is required for water evaporation reaction. For the production of a fuel gas with a

discreetly high heating value, the moisture content in biomass are 10-20% preferably prior to enter in the gasifier (Babu et al., 2004). The optimum moisture content in biomass was 10.82 wt% when gasified pine bark feed stock with downdraft reactor. The result was similar to (Hosseini et al., 2012; Ruiz et al., 2013) when the moisture fraction of the biomass entering was increased the exergy efficiency of biomass gasification process decreased.

## 2. Pyrolysis

Pyrolysis is a thermal decomposition processes that breakdown of larger hydrocarbon molecules of biomass into smaller gas molecules. This process occurs between 150 to 400°C, and results in the formation of char along with gases. The main gas components are H<sub>2</sub>O, CO<sub>2</sub>, H<sub>2</sub>, and hydrocarbons. The hydrocarbon fraction includes methane and organic compound (tar). For this process, one important product of pyrolysis is tar formed through condensation of the condensable vapor produced in the process. Being a sticky liquid, tar are creates a great deal of difficulty in industrial use of the gasification product. The breakdown of hydrocarbon fraction may be influenced by various parameters such as particle size, pressure, temperature, heating rate and residence time (Babu et al., 2004). In a slow pyrolysis type, the solid product moves toward the carbon corner of the diagram Figure 2.5, and more char is formed. In fast pyrolysis type, the process moves toward the C-H axis opposite the oxygen corner. The oxygen is largely reduced, and thus we expect more liquid hydrocarbon.

## 3. Combustion reaction

Most gasification reactions are endothermic. To provide the required heat of reaction as well as that required for heating, drying, pyrolysis, reduction, a certain amount of exothermic combustion reaction is allowed in a gasifier. The combustion reaction (R5) is the best in this regard as it gives the highest amount of heat 394 kJ/k.mol of carbon consumed. The carbon reaction (R4) produces the CO, but produces only 111 kJ/kmol of heat. The rate reaction of R4 is relatively slow. When carbon comes in contact with oxygen, both (R4) and (R5) can take place, but their

extent depends on the temperature zone. The combustion reactions are usually faster than gasification reaction under similar condition.

Table 2.2 Typical gasification reaction at 25°C (Higman et al., 2008a)

Reaction Type	Reaction	KJ/mol
Carbon Reactions (R)		
Boudouard (R1)	$C + CO_2 \rightleftharpoons 2CO$	+172
Water gas or steam (R2)		
	$C + H_2O \rightleftharpoons CO + H_2$	+131
Hydrogasification (R3)		
	$C + 2H_2 \rightleftharpoons CH_4$	-74.8
(R4)	$C + 0.5O_2 \rightarrow CO$	-111
Oxidation Reactions		
(R5)	$C + O_2 \rightarrow CO_2$	-394
(R6)	$CO + 0.5O_2 \rightarrow CO_2$	-284
(R7)	$CH_4 + 2O_2 \rightleftharpoons CO_2 + 2H_2O$	-803
(R8)	$H_2 + 0.5O_2 \rightarrow H_2O$	-242
Shift Reaction		
(R9)	$CO + H_2O \rightleftharpoons CO_2 + H_2$	-41.2
Methanation Reactions		
(R10)	$2CO + 2H_2 \rightarrow CH_4 + CO_2$	-247
(R11)	$CO + 3H_2 \rightleftharpoons CH_4 + H_2O$	-206
(R12)	$CO_2 + 4H_2 \rightarrow CH_4 + 2H_2O$	-165
Steam Reforming Reactions		
(R13)	$CH_4 + H_2O \rightleftharpoons CO + 3H_2$	+206
(R14)	$CH_4 + 0.5O_2 \rightarrow CO + 2H_2$	-36

#### 4. Reduction

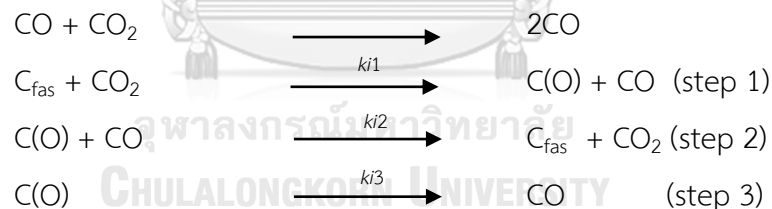
The gasification steps are followed in the pyrolysis involve reactions among the hydrocarbons in fuel, steam, carbon dioxide, oxygen, and hydrogen in the reactor. The char produced from pyrolysis of biomass is not necessarily pure carbon.



It contains a certain amount of hydrocarbon containing hydrogen and oxygen. Gasification of biomass char involves reactions between the char and the gasifying mediums. The gasifying agent like oxygen, carbon dioxide, and steam react with solid carbon to convert into lower molecular weight gases like carbon monoxide and hydrogen are shown in the table 2.2. Gasification reactions are generally endothermic, but some of them can be exothermic as well. For example, the reaction of carbon with oxygen and hydrogen ((R3), (R4), and (R5) in the table 2.2) are exothermic, whereas those with carbon dioxide and steam (R1 and R2) are endothermic.

- Boudouard reaction model

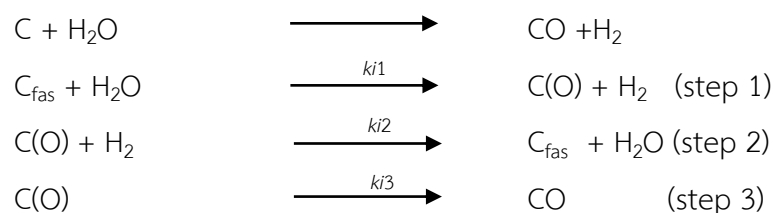
Boudouard reaction is known as the gasification of char in carbon dioxide. Blasi (2009) (Di Blasi, 2009) have been described the Boudouard reaction through the following steps. The first step,  $\text{CO}_2$  dissociates at a carbon-free active site ( $\text{C}_{\text{fas}}$ ), releasing carbon monoxide and forming a carbon-oxygen surface complex,  $\text{C}(\text{O})$ . This reaction can change in the opposite direction as well, forming a carbon active site and  $\text{CO}_2$  in the second step. In the third step, the carbon oxygen complex produces a molecule of  $\text{CO}$ .



where the  $k_i$  is the rate of the  $i$ th reaction, the rate of char gasification reaction to  $\text{CO}_2$  is insignificant below 1000K.

- Water Gas Reaction model

The gasification of char in steam, known as the water-gas reaction, its perhaps the most important gasification reaction.



The first step involves the dissociation of  $H_2O$  on free active site of carbon ( $C_{fas}$ ).  $H_2$  was released and formed hydrogen on a surface oxide complex of carbon. In the second and third steps, the surface oxide produces a new free active site and a molecule of  $CO$  (Di Blasi, 2009).

- Shift reaction model

The shift reaction is a necessary gas-phase reaction (R9). It increases the hydrogen distribution in the gasification product at the loss of carbon monoxide (Klass, 1998b). This is a pre-step in syngas production in the downstream of gasifier, which the ratio of hydrogen and carbon monoxide in the production gas is critical. The shift reaction is slightly exothermic, and its equilibrium yield proportion decreases with temperature. Depending upon temperature direction on products or reactants, but is not sensitive to pressure.

- Hydrogasification Reaction model

This reaction (R3) involves the gasification of char in a hydrogen environment, which leads to the production of methane. The reaction rate is slower than other reactions.

## 2.4 Gasifier type

Gasifiers types are classified on the basis of their gas and solid contacting mode. The broadly gasifiers are divided into three principal types: fixed bed, fluidized bed, and entrained flow. Each is further subdivided into specific types as shown in figure 2.7. One gasifier type is not necessarily suitable for the full range of gasifier capacities, there is an appropriate range of application for each. For example, the fixed bed type is used for smaller units (10 kWth–10 MWth); the fluidized-bed type is more appropriate for intermediate units (5 MWth–100 MWth); entrained-flow reactors are used for large-capacity units (>50 MWth). In Figure 2.9, the overlapped range of application for different types of gasifiers developed with data from (Maniatis, 2008). In entrained-flow and fluidized-bed gasifiers, the gasifying medium conveys the fuel particles through the reactor, but in a fixed-bed (sometimes called moving bed) gasifier the fuel is supported on a grate. The movement in the flow of biomass as it

passes through the reactor, though some authors refer to this type of reactor as fixed bed. Inexpensively fixed bed gasifiers can be built in small scale, which is one of their major attractions. For this reason, large numbers of small-scale fixed-bed biomass gasifiers are in use around the world. Both mixing and heat transfer within the fixed bed are rather poor, which makes it difficult to achieve uniform distribution of fuel, temperature, and gas composition across the cross-section of the gasifier. Fuel are prone to agglomerate during gasification. This is why fixed-bed gasifiers are not very effective for biomass fuels or coal with a high caking index in large-capacity units. There are three main types of fixed- or moving-bed gasifier: updraft, downdraft, and crossdraft.

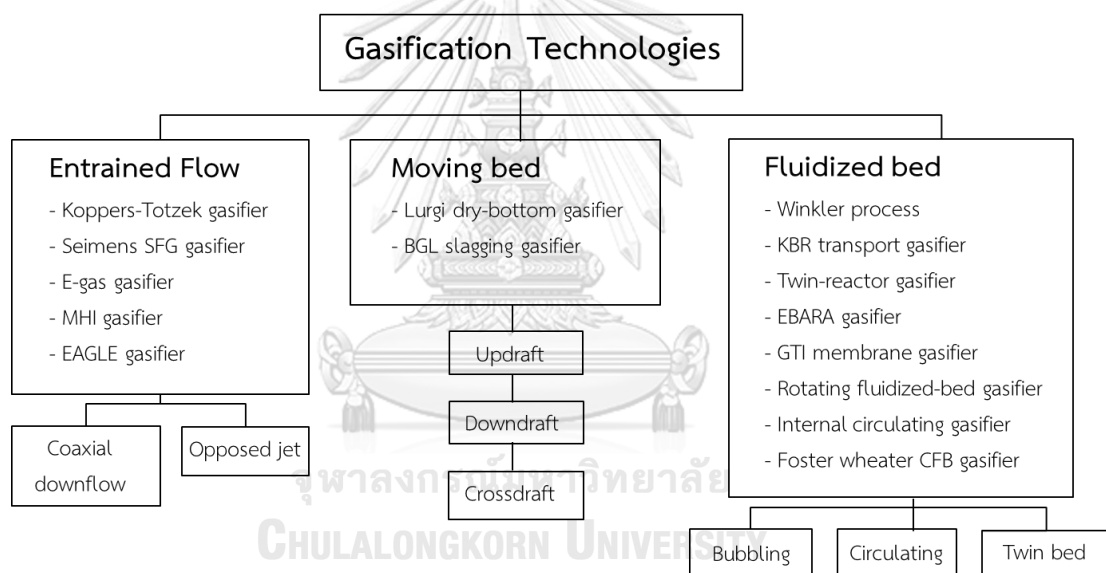


Figure 2.8 Gasification technologies and their commercial supplier (Basu, 2010c).

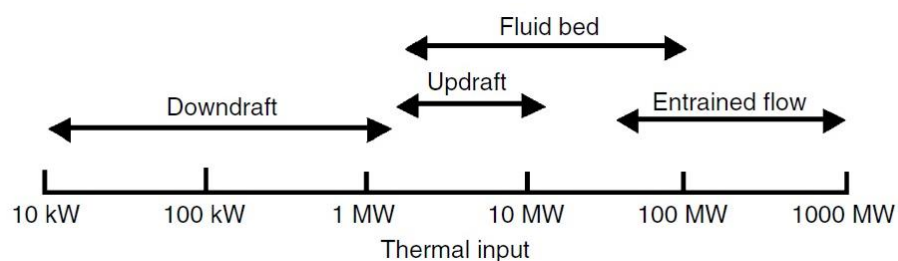


Figure 2.9 Range of applicability of biomass gasifier types (Basu, 2010c).

### 2.4.1 Updraft gasifier

The updraft gasifier is shown schematically in Figure 2.10 (a). Biomass is fed from the top and move downwards while the gasification agent is fed at the bottom and product gas moves upwards. At the top of the gasifier, the biomass is dried by the heat transferred from the bottom zone. In the pyrolysis zone, the hot gas pyrolyzes the biomass from drying zone into non condensable gases, condensable gases, and charcoal. In the reduction zone the charcoal thus formed reacts with rising  $\text{CO}_2$  and  $\text{H}_2\text{O}$  to make  $\text{CO}$  and  $\text{H}_2$ . Finally, the bottom of the reactor where the combustion reaction will take place at the hottest section of the gasifier. In this zone, the air incoming burns the charcoal to produce  $\text{CO}_2$  and heat. The combustion  $\text{CO}_2$  is exothermic, and the heat produced in the gas here is absorbed in the endothermic reduction and pyrolysis reactions above. Ash falls through the grate at the bottom and the hot gases pass upward with lower temperature resulting to the product gas contains large amount of tar. As a result of the low temperature of the gas flow out from gasifier with overall energy efficiency is high, but the low of tar content in the product gas. The biomass feeding has effect of the feed helps to produce a gas with low particulate content.

### 2.4.2 Downdraft gasifiers

Downdraft gasifiers have been successfully tested for machines operating because of the low tar content. The biomass is fed at the top and drops downwards in reactor, while the air is intake also from the top or one side and flow in the same direction with the products of the pyrolysis (Figure 2.10 (b)). The pyrolysis zone involves decomposition of dried biomass into low to high MW volatiles, tar and char. The product of pyrolysis and combustion drop downwards, air contacts the pyrolyzing biomass first, it contacts the char and supports a flame. As in the case of the match, the heat from the burning volatiles maintains the pyrolysis. Then the hot gas moves down, pass through the hot bed of char, where the reduction takes places. It is the principal mechanism appeared in downdraft gasifiers. The reduction zone increases the combustible gas component of the final gas product though decreasing the tar content. Downdraft gasifiers usually produce vapors that are less

than 1 % of the tars, the reason behind the almost exclusive use of downdraft gasifiers as an energy source for operating engines application. Moreover, the particulates content of gas production is high.

### 2.4.3 Cross draft gasifier

The crossdraft gasifier is shown in Figure 2.10 (c). Air flows at high velocity through a single nozzle from the sides, the gases being withdrawn from the opposite side of the consistent unit. A hot combustion zone forms around the entrance of the air feed and the pyrolysis and drying zones being formed higher up in the reactor. This produces very high temperatures in a very small volume and results in production of a low-tar gas, permitting rapid adjustment engine to load changes. The fuel and ash serve as insulation for the walls of the gasifier, permitting mild steel construction for all parts except the nozzles and grates, which may require refractory alloys or some cooling. Air-cooled or water-cooled nozzles are often required. The high temperatures reached require a low-ash fuel to prevent slagging (Kaupp 1984). The crossdraft gasifier is generally considered appropriate only for less tar in fuels product. Some success has been observed with unpyrolyzed biomass, but the nozzle-to-grate spacing is critical (Das 1986). Unscreened fuels that do not feed into the gasifier freely are prone to bridging and channeling, and the collapse of bridges fills the hearth zone with unpyrolyzed biomass, leading to momentarily high rates of tar production.

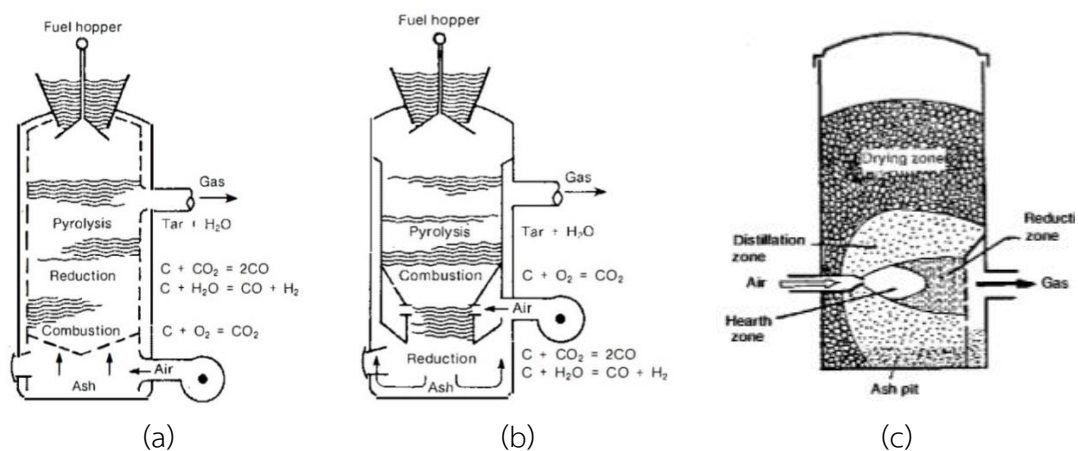
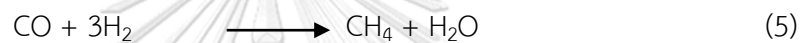
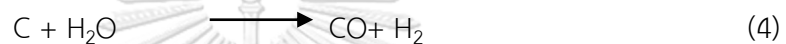
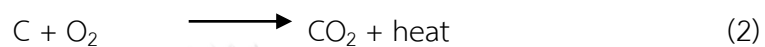


Figure 2.10 Schematics of (a) updraft (b) and (c) crossdraft gasifier (Basu, 2010b).

The char coal produced after completion of pyrolysis with updraft or downdraft gasification is 10% to 20% of the biomass. In an updraft gasifier, air entering at the grate bottom initially burns this char to release heat and CO<sub>2</sub> according to the exothermic reaction (2). Almost immediately, or even simultaneously, the CO<sub>2</sub> and any H<sub>2</sub>O present in the gasifier react with the char to release the CO and H<sub>2</sub> products by the following reactions (3-4).



The first reaction is named the Boudouard reaction, and the second is the water-gas reaction. The rate of the reaction has been studied by measuring the rate of disappearance of carbon, coal, or charcoal while passing CO<sub>2</sub> or H<sub>2</sub>O over the solid both of these reactions require heat (endothermic reactions). These reactions occur very rapidly at temperatures over 900°C, and their cooling effect on the gas temperature rising above this temperature. The reactions become sluggish and very little product forms at temperatures below 800°C. The CO and H<sub>2</sub> formed in the hot char zone can react below 900°C to form methane according to the reaction (R5).

Downdraft gasifiers can be used in IC-engine, which can be categorized as open and close top designs, respectively. The open top design configuration, see Figure 2.11 (a) has an open top, forcing air to move downwards throughout the gasifier with the aim of prevents hot spot formations. The homogeneous airflow also reduces inefficiencies in the thermo-chemical process taking place in the reactor, as well as a possibility of the formation of preferential channels and internal bridges. The stratified downdraft gasifier demonstrates high versatility and efficiency in operation with solid fuels of poly-dispersed nature, such as rice husk or small particle size and low-bulk density. The closed top gasifiers have two different

designs, a conventional downdraft with a straight cylindrical reactor as shown in Figure 2.11 (b) and one is a throat in the reactor core. In Figure 2.11 (c), it's called Imbert gasifier. The throat section design in the Imbert downdraft gasifier is to reduce the tar content by intense heat. The hot char and the pyrolysis product pass through the throat section, where most of cracking tar is cracked and char is gasified. In such gasifiers, air is introduced just on top of the throat and this creates a highly uniform temperature field and better mixing condition. About one-third of the way up from the bottom, there is a set of radially directed air nozzles that permit air to be drawn into the chips as they move down to be gasified. Typically, there are an odd number of nozzles so that the hot gases from one nozzle do not impinge on the opposite nozzle. The nozzles are attached to a distribution manifold that in turn is attached to the outer surface of the inner can. This manifold is connected through the outer can to a large air-entry port. One air nozzle is in line with this port, allowing the operator to ignite the charcoal bed through this nozzle.

Below the air nozzle zone places the gas-reduction zone, usually consisting of a classical Imbert hearth or in later years, of the "V" hearth. Most recently, the flat-plate hearth constriction (Figure 2.12) has been introduced. The latter two hearth designs accumulate a layer of retained ash to form a high-quality, self-repairing insulation. Improved insulation in the hearth results in lower tar production and a higher efficiency over a wider range of operating conditions. The nozzle spaces (Figure 2.12) allow some unpyrolyzed biomass pass through this zone. The hearth constriction then causes all gases to pass through the hot zone at the constriction, thus giving maximum mixing and minimum heat loss. The highest temperatures are reached in this section so the hearth constriction should be replaceable. If tarry gas is produced from this type of gasifier, common practice is to reduce the hearth constriction area until a low-tar gas is produced. The fine char-ash dust can eventually clog the charcoal bed and will reduce the gas flow unless the dust is removed. The charcoal is supported by a movable grate that can be shaken at intervals. Ash builds up below of the grate and can be removed in cleaning during process.

In practice, shorter residence times in the hot combustion zone and/or bridging and channeling problems increase the final tar content. Moreover the biomass fuel has to be uniformly sized in the range of 4-10 cm to realize regular flow, no blocking and channeling in the throat section providing enough room for the pyrolysis gases to flow downwards and allow heat transport from the throat zone upwards (Belgiorno et al., 2003; Olgun et al., 2011) (Kumar et al., 2009).

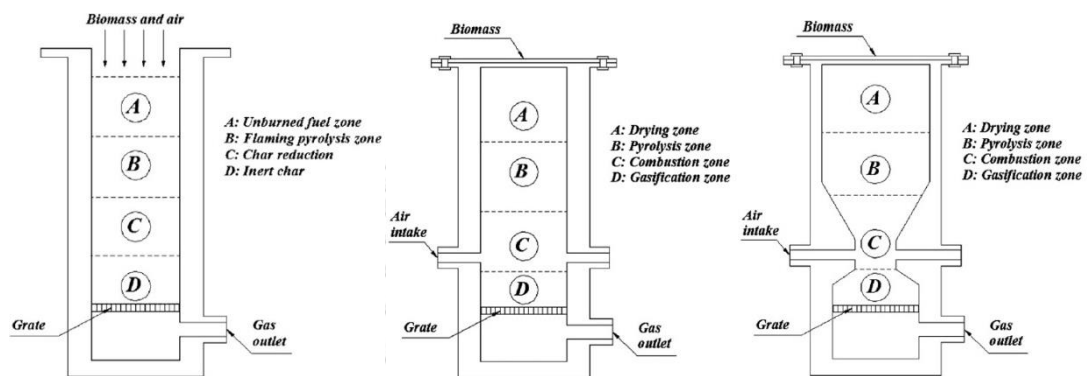


Figure 2.11 Downdraft gasifier with open top (a), conventional doendraft (b), Imbert gasifier (c) (Olgun et al., 2011).

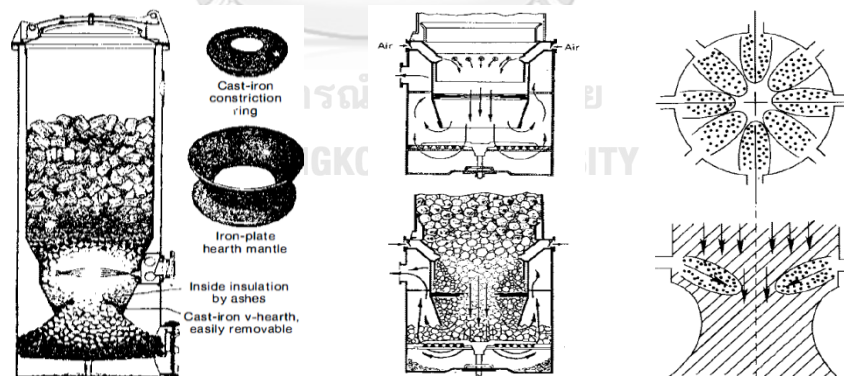


Figure 2.12 (a) V-heart Imbert gasifier, (b) Flat-plate hearth constriction, (c) The space between the nozzles (Klass, 1998b).

## 2.5 Gasification parameters

Gasification process is the conversion of biomass to a gaseous fuel by heating in a gasification medium such as air, oxygen or steam. This process converts the



intrinsic chemical energy of the carbon in the biomass into a combustible gas in two stages, unlike combustion where oxidation is substantially complete in one process.

### 2.5.1 Gasification parameters

#### 1. Equivalence ratio

The water gas, water gas shift, Boudouard and methane reactions provides the opportunity to calculate the product gas composition of a gasifier, but only in case this equilibrium can really be reached. Models can be used to calculate the gas composition as function of the temperature and/or the equivalence ratio (ER), which is the oxygen used relative to the amount required for complete combustion. This dimensionless parameter shows that curves of several parameters like chemical energy in the gas and the gas composition change significantly at ER = 0.25. A value of zero (left side) corresponds to pyrolysis while combustion is shown at the ER = 1.0. At ER = 0.25 all of char is converted into gas with giving the highest energy density of the gas; at lower values char is remaining and at higher values some gas is burned and the temperature will increase.

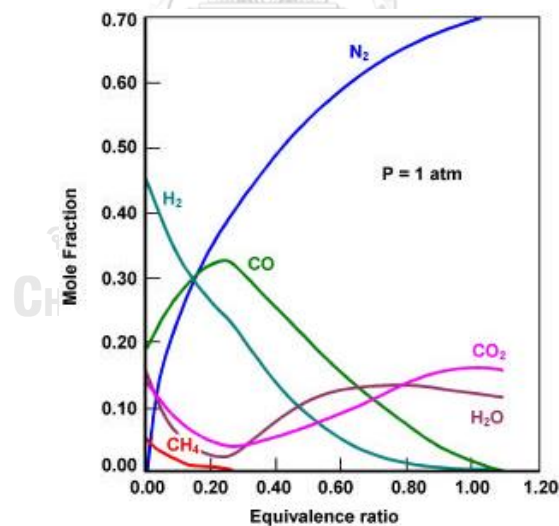


Figure 2.13 Equivalence ratio (Higman et al., 2008c).

#### 2. Superficial velocity and hearth load

The superficial velocity is one of the most important parameters defining the performance of a gasifier reactor, rate of gas production, content of gas energy, rate of fuels consumption, power output, and rate of tar-char production. The superficial velocity is calculated, which the gas flow rate ( $\text{m}^3/\text{s}$ ) divided by the cross section

area of reactor ( $m^2$ ). A low superficial velocity causes relatively slow pyrolysis conditions and results in high charcoal and a gas with high tar content. The hearth load for volume gas flow per unit of cross-section area is known as superficial gas velocity or space velocity. It has the unit of velocity. Maximum hearth load permits one to estimate the size of hearth that needed for various power engine or burner. The maximum hearth load is limited by many factors, such as the mechanical integrity of the char bed structure within the gasifier, degree of agitation, and the conversion time. High velocities do affect the char and fuel bed, causing instability. If char fragments become dislodged and airborne, they may plug the bed or channels. Therefore, a little agitation can effectively increase the maximum specific hearth load (Higman et al., 2008c; Klass, 1998b).

### 3. Turn-down ratio

For every gasifier is an optimum range of operating conditions corresponding to a certain turn-down ratio, i.e. The ratio under range of operation, which gas is produced of sufficient quality for its application. The turndown ratio is vital concept in sizing gasifiers, the ratio of the highest practical gas generation rate with low practical rate. For gasifiers the turn-down ratio is normally, although some technology developers claim higher values. Heat losses tend to be independent of throughput and at low loads become disproportionately high. A low specific hearth load may also cause tar formation problems. A high turndown ratio is less important for electric generators and irrigation pumps that constantly operate at full capacity.

### 4. Gas heating value

The gas heating value is usually expressed in either as Btu or  $MJ/Nm^3$ . A normal cubic meter is referring to the gas volume at 1 atmosphere and 25 °C. Higher heating value is the maximum energy released during complete oxidation of the fuel. This is including the thermal energy that can be recovered by condensing and cooling the product. The lower heating value as net energy released during oxidation of the fuel excluding the heat required for vaporization of the water in the fuel and the water produced from hydrogen combustion.

### 5. Gas flow rate and gas production

The gas flow rate can be calculated from the primary air flow. The nitrogen content in the producer gas is known, or measured by orifice plates, venturies, rotameters or pilot tubes. For calculate the gas flow in a  $\text{Nm}^3$  basis, the temperature and pressure need to be measured as well. The gas velocity in pipelines is generally about 15 m/sec to avoid blockage of entrained solids in the pipe lines. From the gas flow rate and fuel input, the gas production can be calculate per unit fuel input ( $\text{Nm}^3/\text{kg}$ ) or per energy produced ( $\text{Nm}^3/\text{kW}_e$ ). The gas flow rate and the gas heating value are important factors controlling the gasifier efficiency.

#### 6. Efficiency

Generally, the efficiency of gasification can be evaluated on cold-gas efficiency, hot-gas efficiency, or net gasification efficiency. Cold-gas efficiency is the chemical energy content of the producer gas was divided by the energy content of the biomass while the hot gas efficiency and heat energy content of producer gas were divided by the energy content of the biomass.

#### 7. Fuel consumption

The fuel consumption is needed to determine the overall gasifier efficiency. The fuel consumption can be measured by sizing hopper. The fuel consumption can be expressed on a unit mass per cross section diameter and time ( $\text{kg}/\text{m}^2 \cdot \text{h}$ )

#### 8. Tar and entrained particles

The amount of tar and entrained particles depends on the gasifier design and operating conditions, in particularly the load level (actual power output to the maximum rate).

### 2.6 Gas conditioning

Depending on the application, type of gasifier and fuel contaminants, a certain level of gas conditioning (cleaning/cooling system) is required. Cleaning part is particularly needed for combustion of producer gas in gas engines or gas turbines, and synthesis gas production. Wet and dry cleaning devices have been developed for wet gas cleaning, most of the impurities can be removed, but a contaminated waste water is produced which needs to be treated before disposal. Dry gas cleaning, usually only particulates are trapped. Cooling system is required for (i) combustion in

gas engines, (ii) when filters are applied with a maximum allowable temperature or (iii) when compressors are incorporated like with atmospheric IGCC. The most frequent impurities are liquid hydrocarbons (tar), dust (particulates), ammonia, sulfur, chloride, alkali compounds, etc. that need to be removed or converted. Dust is usually removed by cyclones and fabric filters. Ammonia, sulfur and chloride can be trapped by scrubbers or by using additives. Tar is the critical component to be handle.

### 2.6.1 Tar removal and conversion

Special gasifier designs have been developed for reducing tar concentration in the product gas, however a “tar-free” gasifier does not exist. Therefore, tar removal and conversion are required in most cases. The latter is preferred, because tar has a relatively high energy content. Different concepts developed to reduce the tar content include:

- Specific reactor designs: downdraft gasifiers with a V-shaped “throat” construction
- Staged gasification where the pyrolysis, gasification and/or combustion zones are separated
- Adding catalyst system in the reactor
- Separate the tar catalytic conversion in downstream gasifier reactor
- Physical removal with scrubbing, or absorption
- Recycling of tar into the gasifier reactor by physical removal

## 2.7 Catalytic Gasification

Gasification processes, tar is formed as by-product and may cause operation problem and also considered as loss of combustible materials. The formations of tar lead to process equipment failure by corrosion and deposit formation. The catalysts can remove tar from the product gas, especially if the downstream application or the installed equipment cannot tolerate it. Moreover, it can be reduced methane content in gas product, particularly when it used as syngas. The development of catalyst gasification is driven by the need for tar reforming, when the hot gas product passes over the catalyst particles, the tar or condensable hydrogen can be reformed

on the catalyst surface with either steam or carbon dioxide, thus producing additional hydrogen and carbon monoxide (Sutton et al., 2001). The reactions may be written in the simple form as below:

Steam reforming reaction

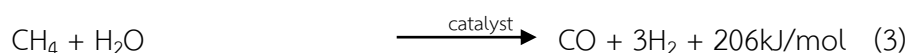


Carbon dioxide (or dry) reforming reaction

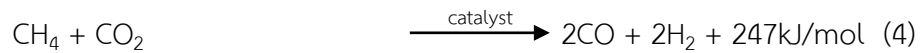


As one can see, instead of undesirable tar or soot, additional fuel gases through the catalyst tar-reforming reaction may be achieved via (1). Improving of both gas yield and the heating value of the product gas. The other options for tar removal is thermal cracking, but it requires a high temperature and produces soot, thus it cannot harness the lost energy in tar hydrocarbon. The second motivation for catalytic gasification is removal of methane from the product gas. For this either catalytic steam reforming or catalytic carbon dioxide reforming of methane may be applied. Reforming is very important for the production of syngas, which cannot tolerate methane and requires a precise ratio of CO and H<sub>2</sub> in the production gas. In steam reforming, methane reacts with steam in the temperature range of 700-1100°C in the presence of a metal based catalyst, thus it is reformed into CO and H<sub>2</sub> (J. Li et al., 2009). The steam reforming of methane reaction is widely used in hydrogen production from methane, for which nickel based catalysts are very effective. The carbon dioxide reforming (dry reforming of methane) is not widely used commercially as steam reforming, because it has the special attraction of reducing two greenhouse gases (CO<sub>2</sub> and CH<sub>4</sub>) in the reaction. It can be a good option for removal of CO<sub>2</sub> from the product gas. The reaction is highly endothermic. Nickel-based catalysts are also effective for the dry reforming reaction (Guan et al., 2009)

Steam reforming of methane



Dry reforming of methane



### 2.7.1 Catalyst Selection

Catalyst for reforming reactions is chosen with referable to their objective and particle usage. Some important catalyst selection criteria for tar removal of are as follows:

- Effective
- Resistant to deactivation by carbon fouling
- Easily regenerated
- Strong and resistant to attrition
- Inexpensive
- Thermal resistant

Catalyst can react in in-situ and post gasification reaction. The former may involve impregnating the catalyst in the biomass prior to gasification. It can be packed directly in the reactor, as the fluidized bed. Catalysts are placed in a secondary reactor downstream of the gasifier to convert the tar and methane formed in post-gasification. This has the additional advantage of being independent of gasifier operating condition. The reactor can be operated at temperatures optimum for the reforming reaction. The catalysts in biomass gasification are divided into three groups: earth metal, alkali metal, and nickel based. Alkali metal catalysts, potassium carbonate and sodium carbonate are important in biomass gasification as primary catalyst. Many biomass types have inherent potassium in their ash, so they can benefit from the catalytic action of the potassium with reduced tar production. However, potassium is notorious for agglomerating in fluidized beds, which offsets its catalyst benefit. For  $\text{K}_2\text{CO}_3$  is more effective than  $\text{Na}_2\text{CO}_3$ . Ni-based catalyst, nickel is highly effective as a reforming catalyst for reduction of tar as well as for adjustment of the  $\text{CO}/\text{H}_2$  ratio through the methane conversion. Earth metal catalysts, dolomite ( $\text{CaCO}_3 \cdot \text{MgCO}_3$ ) is very effective for disposal of tar, and it is inexpensive and widely available, obviating the need for catalyst regeneration. It can be used as primary

catalyst by mixing with the biomass or as a secondary catalyst in a reformer downstream

### 2.7.2 Catalyst

#### 1. Nickel

Ni catalysts have been investigated for gasification of biomass, since their comparative low price and high activity remove tar and increased hydrogen product (Sutton et al., 2001). Many commercial nickel catalysts are available in the market for reduction of tar as well as methane in the product gas. In addition to reducing the tar content, nickel catalyst improved the quality of the gaseous product in biomass gasification. It is economically and effectively attractive as both gasification and gas cleanup process occur in-situ, no downstream reactor or extra heating is required (Chan et al., 2014). Catalyst activity is influenced by temperature, residence time, particle size, and composition of the gas atmosphere. Steam-reforming nickel catalysts for heavy hydrocarbons are effect for reduction of tar while nickel catalysts for heavy hydrocarbons affect methane reduction. The carbon deposition and particle growth is a problem for nickel-reforming catalyst deactivation.

#### 2. Char

Char, a carbonaceous product of pyrolysis, also catalyzes tar reforming when used in the secondary reactor. Chars have been reported in an inexpensive catalyst type. Not only fair performance in tar removal, but also an excellent adsorbent. The char supported catalyst would low costs and be simply gasified to recover the energy the char without the need of expensive regenerate after deactivation (Shen et al., 2014a). The char supported could be easily produced carbonaceous product from the pyrolysis of biomass at slow heating rate, and spent catalyst could be consumed in gasification process directly (Shen et al., 2014a). And also catalyzes tar reforming when used in the secondary reactor.

#### 3. Dolomite

Dolomite ( $MgCO_3$ ,  $CaCO_3$ ) is relative inexpensive and is readily available. The used of dolomite as a catalyst in biomass gasification has attracted much attention (Devi et al., 2005), (Corella et al., 2005) because it is cheap disposable catalyst that

can reduce the tar content of the product gas from a gasifier significantly. It may be used as dry-mixed with the biomass, as a primary catalyst, and in a secondary downstream reactor. It is more active when calcined and used downstream in the post gasification secondary reactor at above 800°C. The reforming reactions of tar on a dolomite surface occur at higher rate with CO<sub>2</sub> reforming reaction than with steam reforming reaction. It can entirely convert the tar under proper condition but cannot convert methane for syngas production. Carbon deposition deactivates dolomite, which, being less expensive, may be discarded.

## 2.8 Biomass Gasification Models

The efficient operation of a biomass gasifier depends on a process of chemical reaction, such as pyrolysis, conversion of tar and hydrocarbon to gas (Puig-Arnau et al., 2010). A number of researchers consider the final product of chemical equilibrium model, while other considers the different process along the reactor. The purposes of model are to study the thermochemical processes through the biomass gasification and to evaluate the influence of input variable, such as moisture content, air fuel ratio, gas composition and the lower heating value. The models can be dispersed into kinetic rate, the thermodynamic equilibrium, or neural network models.

### 2.8.1 Kinetic rate models

Stoichiometric calculations can determine the reaction of products and describe the conversion during biomass gasification. Many of the chemical reactions discussed in the previous section proceed at a finite rate and to a finite extent. To extent a reaction progress is determined by its equilibrium state. Its kinetic rate, on the other hand, determines the fast rates of reaction products are formed and whether the reaction completes within the gasifier. Many researches have been focused on kinetic models of biomass gasification widely. Wang and Kioshitan (1993) mentioned the kinetic model based on mechanism of surface reactions in the reaction zone assuming a given residence time and temperature. Giltrap et al. (2003) established a model of the reduction zone of a downdraft gasifier to predict the composition of the producer gas under steady state. Chen's model was intended to



estimate the length of the gasification zone and the diameter of the reactor and studied the dependence of the reactor on operation parameters, i.e. input air temperature, material, moisture content, particle size, reactor simulation, and gasifier. Sharma (2008) presented a model for a downdraft gasifier which the reduction zone was modeled using a finite rate of reaction succeeding the chemical kinetics. The pyro-oxidation zone, previous to reduction zone was also modeled considering thermodynamic equilibrium. Babu, B.V. and P.N. Sheth (2006) improved Giltrap's model recommending an exponentially varying CRF to predict better simulation of the temperature profile in the reduction zone, the CRF value improved linearly and exponentially with the length of the reduction zone, The model was simulate with a finite difference method to predict the temperature and composition profiles.

#### 2.8.2 Thermodynamic equilibrium models

Thermodynamic equilibrium has been recommended to explain the complex biomass gasification process, design, optimization, simulation, and analysis of gasifier. At the equilibrium, a reacting system is at its most stable composition, a completed condition when the entropy of the system maximize whereas minimize of Gibbs free energy. Though, thermodynamic equilibrium may not be achieved, for the relatively low temperatures operation. The models based on thermodynamic equilibrium have been used widely, Zainal et al. (2002) established the biomass gasification process model on the stoichiometric thermodynamic equilibrium, which they predicted the production gas for different raw material. Jarunghammachote and Dutta (2007) improved model based on the equilibrium constant for predict the composition of gas from downdraft gasifier. They used coefficients correcting the equilibrium constant of the water gas shift and methane reaction that improve the model accuracy. Schuster et al. (2001) studied the equilibrium model for steam biomass gasification in a fluidized bed gasifier. Li et al. (2004) studied a stoichiometric equilibrium model to predict the gas composition, heating value, cold gas efficiency for biomass fluidized bed gasification. They resolved that real gasification process differ from chemical equilibrium. The chemical equilibrium is a good method when

simulating entrains flow gasifier in chemical process simulators providing the high temperature and residence time achieve at the throat section.

The ASPEN PLUS process simulator has been used by different investigators to simulate the gasification process. Nikoo and Mahinpey (2008) have developed ASPEN PLUS model and external FORTRAN subroutines for hydrodynamics and kinetics to simulate the gasification process. Ramzan (2011) have established steady state simulation model for gasification with ASPEN PLUS. They concluded that the model can be used as an analytical tool for optimization of the gasifier performance. The studies were carried out the influence based on the equivalence ratio, temperature, preheat, heating value. Keche Amba (2015) discovered the simulation of biomass gasification in downdraft gasifier for different biomass using ASPEN PLUS. This model is validated with data obtained from four biomass; babul wood, neem wood, mango wood, and bagasse. The model has predicted composition of H<sub>2</sub>, CO, and CO<sub>2</sub> while it has under predicted the CH<sub>4</sub>.

## 2.9 Literature review

According to literature review, a large number of researchers have attempted to work on the gasification with downdraft gasifier and upgrading the production gas with Ni catalyst. Dogru et al. (2002) studied gasification of hazelnut shells in pilot-scale downdraft gasifier. The objective is to direct use of the product gas in an Internal Combustion Engine to produce electric power. The quality of product gas is found to be dependent on the smooth flow of fuel and the uniformity of the pyrolysis. The optimum of the gasifier is 1.44-1.47 m<sup>3</sup>/kg of air fuel ratio with feed rate 4.06 - 4.48 kg/h. Furthermore, the GCV is 5 MJ/m<sup>3</sup> at a volumetric flow of 8-9 N m<sup>3</sup>/h. It was recommended that hazelnut shell easily gasified in a downdraft gasifier to produce good quality gas.

Sheth and Babu (2004) have investigated on producer gas generation from wood waste in a downdraft gasifier and examined the reliability of the results by carrying out material balance. Increasing the moisture content, biomass consumption rate inversely with an increase the air flow rate. The optimum equivalence ratio is

0.205 for the downdraft gasifier. The fraction of CO and H<sub>2</sub> shows increasing and decreasing trend opposite to N<sub>2</sub> and CO<sub>2</sub>.

Zainal et al. (2002) have investigated of a downdraft gasifier using wood chips and charcoal by varying the equivalence ratio from 0.259 to 0.46. The calorific value of the producer gas increases with equivalence ratio firstly, and then decreased with increased in equivalence ratio. The cold gas efficiency of the biomass gasifier is found to be about 80%, whereas the overall efficiency of the electrical power system is around 10-11%. The specific consumption of the biomass material is found at 2 kg/kWh. The performance of experimental in a complete gasifier IC engine plant were stated the difference of air fuel ratios system and woody with cubic shape.

Skoulou et al. (2008) studied the air-blown fixed bed gasification with olive kernels and tree cutting and compared the performance. They found that for both materials the amount of H<sub>2</sub> in the product gas increase with higher gasification temperature. The fraction of H<sub>2</sub> presented decreasing after increasing trend, where CO declined with an increasing ER. This revealed with the property of the biomass is an important factor the evolution of main gas composition.

Gai et al. (2012) studied the air gasification of corn straw with downdraft fixed gasifier. From the experiment, the variation of the concentrations of the sulfur and chlorine compounds in gaseous and ash are not a monotonic trend under different operations. The optimum value of ER is 0.28-0.32, LHV of 5.39 MJ/M<sup>3</sup>, 2.86 Nm<sup>3</sup>/kg of gas yield, efficiency of 73.61% and tar of 4.6 g/Nm<sup>3</sup>.

Olgun et al. (2011) designed and created the fixed bed downdraft gasifier system to be fed with agricultural and forestry residues. A throat has been combined into the design to achieve gasification with lower tar production. The experimental system consists of the downdraft gasifier and the gas cleaning unit including cyclone, scrubber and box of filter. The product gases are combusted in the flare built up as part of the gasifier system. The difference type of biomass, namely wood chips, barks, olive pomace and hazelnut shells are to be studied. The air to fuel ratio is

adjusted to produce gas with high heating value. The result revealed that the ER level changes depended on the downdraft gasifier system design and the physical chemical biomass properties.

Jain and Goss (2000) designed small core throat gasifier reactor having internal diameters of 15.2, 20.3, 24.4 and 34.3 cm for rice husk gasification. The gas quality, gas production rate, gasification efficiency, specific gasification rate, and equivalence ratio were measured of the four reactors. The optimum value of specific gasification rate is  $192.5 \text{ kg/hm}^2$  and equivalence ratio is 0.4. At this condition, the lower heating value of producer gas is  $4 \text{ MJ/m}^3$ , cold gas efficiency 65%, and the capacity range of 3-15 kW.

Bacaicoa et al. (2008) studied the gasification performance of high density polyethylene and wood mixtures. They found that the temperature increase with higher ratios of polyethylene in the wood feed. The experimental was carried out gasification of biomass only and mix biomass with 15%HDPE. The results showed that the gas compositions are 50%N<sub>2</sub>, 14%H<sub>2</sub>, 9-22% CO, and 7-17%CO<sub>2</sub> and its relatively high calorific value were appropriate for internal combustion engine generator consisting of a modified diesel engine combined with 25kv.

Erlich and Fransson (2011) examined the downdraft gasification of pellets of wood, palm-oil residues. The results showed that the gasification of wood pellets results in a richer producer gas while EFB pellets provide a poorer one with higher contents of non-combustion compounds. The linear relation between the air fuel ratio and the cold gas efficiency, higher air fuel ratios result in better efficiency.

Sharma et al. (2008) observed the production gas of gasified cashew nut shells with open core downdraft gasification. They found that calorific value and volumetric percentage of producer gas combustible constituents along with gasification efficiency increase with gas flow rate. The gasification efficiency was 70% by gas flow rate  $130 \text{ m}^2/\text{hr}$  and specific gasification rate of  $167 \text{ kg/hr.m}^2$ .

Lv et al. (2004) explored the potential of hydrogen production from biomass oxygen/steam gasification via a self-heated downdraft gasifier. The results discovered that compare to biomass air gasification, biomass oxygen/steam gasification can improve hydrogen yield depending on the volume of downdraft gasifier. The maximum LHV is  $11.11 \text{ MJ/Nm}^3$  with biomass oxygen/steam gasification. Over the ranges of operating conditions examined, the maximum hydrogen yield is  $45.16 \text{ g H}_2/\text{kg biomass}$ . For biomass oxygen/steam gasification, the  $\text{H}_2$  and CO is  $63.27\text{--}72.56\%$ , while the  $\text{H}_2$  and CO is to  $52.19\text{--}63.31\%$  for biomass air gasification. The  $\text{H}_2/\text{CO}$  ratio for biomass oxygen/steam gasification is  $0.70\text{--}0.90$ , which is lower than that of biomass air gasification ( $1.06\text{--}1.27$ ). The experimental and comparison results demonstrate that biomass oxygen/steam gasification in a downdraft gasifier is an effective, relatively low energy consumption technology for hydrogen-rich gas.

Perez et al. (2012) examined the effect of operating and design parameter on the gasification/combustion process of waste biomass in fixed bed downdraft reactors. They found the optimal gasification conditions through varying the air superficial velocity, biomass particle size and biomass moisture content. At the optimal gasification condition, the lower heating value of the producer gas was  $2965.6 \text{ kJ/Nm}^3$  and tar  $7.73 \text{ g/Nm}^3$  with air superficial velocity at  $0.06 \text{ m/s}$ , biomass particle size  $2 - 6 \text{ mm}$ , and moisture content  $10.62\%$ .

Wander et al. (2004) studied the potential of the sawdust with a fixed downdraft stratified and open top gasifier. The results found that the operational problems in the gasification of sawdust because of the bed mechanic characteristics. Hence, these residues need to condition before being processed in downdraft gasifier. Palletization is a proper option for biomass conditioning permitting production of stable dry fuels of uniform size from different biomass.

Wang et al. (2011, 2012) investigate char and char support nickel catalyst for secondary syngas cleanup. Ni-based catalysts were made by mechanically mixing NiO and char particles. Ni/coal-char and Ni/wood-char can convert  $97\%$  of tar in syngas at  $800^\circ\text{C}$ ,  $15\%$  NiO loading and  $0.3 \text{ sec}$  residence time. In addition, the catalyst granular

size was a factor for tar removal and syngas composition improvement, three Ni/char catalyst size were prepared with a mechanical mixing method. Tar removal efficiencies increased by the decreased of Ni/char granular size, which can be recognized to the higher active surface area from the smallest size. As the catalyst granular size was increased, the H<sub>2</sub> in the syngas was increased and the CO was significantly decreased.

Shen et al. (2014) studied tar conversion approach during biomass pyrolysis through in-situ dry reforming over biomass pyrolysis could be removed in the gasifier. The optimized conditions, the conversion efficiencies of tar can reach around 92.3% and 93% with Ni-Fe char and calcination of Ni char, respectively. The condensable tar could be catalytically transformed into small molecule gases resulting with the heating value increased of the product gas.

Zhang et al. (2013) also studied the iron supported on biomass char and iron supported on coal, char were used as hot gas cleaning catalysts at 800°C. The result showed that all catalysts decrease CO<sub>2</sub> and CH<sub>4</sub> concentrations and increase H<sub>2</sub> and CO concentration of product gas. The iron-containing species in char would favor the H<sub>2</sub>. Tar contents lower than 100 mg/Nm<sup>3</sup> using iron catalyst supported on biomass char or just biomass char.

Miao et al. (2010) studied the decomposition of acetic acid using porous dolomite pellets catalyst at 800°C. They found that 99.70% of acetic acid was decomposed and the porous dolomite pellets were much more effective than the natural dolomite particles.

Srinakrungsri et al. (Srinakrungsri et al., 2006) examined the performance of tar gasification in fixed-bed reactor with Ni/Al<sub>2</sub>O<sub>3</sub>, Ni/SiO<sub>2</sub>.Al<sub>2</sub>O<sub>3</sub>, Ni/dolomite catalyst. They demanded that Ni based on dolomite support catalyst is an effective catalyst for fixed bed gasification of tar cracking. The catalytic activity of toluene conversion decreased in the follower: Ni/Al<sub>2</sub>O<sub>3</sub> > Ni/SiO<sub>2</sub>.Al<sub>2</sub>O<sub>3</sub> > Ni/dolomite. However, Ni/dolomite catalyst was suitable for the longest duration test (7 hr) and the coke

formation was of following: Ni/dolomite < Ni/Al<sub>2</sub>O<sub>3</sub> < Ni/SiO<sub>2</sub>-Al<sub>2</sub>O<sub>3</sub>. The Ni/dolomite catalyst showed excellent activity for tar decomposition and anti-coking.

Guo et al. (Guo et al., 2014) studied the effect of design and operating parameters with corn straw feeding rate using a three air stage continuous downdraft gasifier. The results indicated that the three stage of air supply yield a high and uniform temperature in the oxidation and reduction zones. The combustion reactions were improved to release heat with increasing ER, which in turn led to higher temperature in the gasifier resulted higher rate of tar cracking. Biomass feeding rate at 7.5 kg/h and ER was 0.25-0.27, the product gas of the downdraft gasifier reaches a high condition with LHV 5400 kj/h and cold gas efficiency about 65%.



Table 2.3 Review of the biomass gasification with downdraft gasifier.

Research group	Biomass	Kg/h	T (°C)	CGC (%)	LHV (MJ/m <sup>3</sup> )	Remark
Dogru et al. (2002)	Hazelnut shells	5.4	1000	81	4.7	ER 0.276 • The quality product gas is found to be dependent on the smooth flow of fuel
Zainal et al. (2002)	wood, Charcoal	2		33	5.62	ER 0.388 • Gas production rate 1.08Nm <sup>3</sup> /kg
Lv et al. (2004)	pine sawdust	0.3-1	700-900	-	11.11	• Higher temperature contributed to more hydrogen production
Sharma (2009)	cashew nut shells	15	1100	70	4.2	• Gasification efficiency increased with increase in gas flow rate
Sheth and Babu (2009)	Wood furniture waste	2.59	900-1000	56	6.34	• ER 0.205, Gas production rate 1.62 Nm <sup>3</sup> /kg
Skoulou et al. (2008)	olive kernels, tree cutting	-	750-950	-	8.6-9.41	• H <sub>2</sub> in the product gas increase with higher temperature
Erlich et al. (2011)	Pellets of wood, palm oil	2-3.5	900-1200	63	4.1-5.4	• The linear relation between the air fuel ratio and the cold gas efficiency



Table 2.3 Review of the biomass gasification with downdraft gasifier (cont.).

Research group	Biomass	Kg/h	T (°C)	CGC (%)	LHV (MJ/m <sup>3</sup> )	Remark
Olgun et al. (2011)	wood chips and hazelnut shells	5.4	1000	81	5	<ul style="list-style-type: none"> <li>• ER 0.35</li> <li>• No operational problems tar blockage, agglomeration process break down</li> </ul>
Gai et al. (2012)	corn straw	8.3 - 9.9	1000 - 1100	73	5.39	<ul style="list-style-type: none"> <li>• Higher ER contributed to the increment of gas yield</li> <li>• The decrement of tar</li> </ul>
Perez et al. (2012)	Pine bark, sewage sludge	125	1300 - 1500	-	2.96	<ul style="list-style-type: none"> <li>• The optimal gasification conditions by varying the air superficial velocity</li> </ul>
Guo et al. (2014)	corn straw	7.5	900-1000	65	5.4-5.2	<ul style="list-style-type: none"> <li>• ER 0.25-0.27</li> <li>• Increasing biomass feeding rate led to higher biomass consumption rates, higher process temperatures</li> </ul>
Sornkade et al. (2013)	Cassava Rhizome	1.8	800	39-54	4.12	<ul style="list-style-type: none"> <li>• ER of 0.2-0.4</li> <li>• Drop tube (updraft)</li> </ul>

Table 2.3 Review of the biomass gasification with downdraft gasifier (cont.).

Research group	Biomass	Kg/h	T (°C)	CGC (%)	LHV <sup>3</sup> (MJ/m <sup>3</sup> )	Remark
Ngamchompoo and Triratanasirichai (2013)	Cassava Rhizome	-	900	65-69	5.11	<ul style="list-style-type: none"> <li>Temperature in all cases of the HTAG process were higher than in the air-steam gasification</li> </ul>

Table 2.4 Review of the biomass gasification with nickel Catalyst.

Research group	Type gasifier	Biomass	catalyst	Calcined (°C)	Remark
Wang et al. (2010)	second ary syngas cleanup	Sawdust waste	Ni/wood-Char, Ni/Coal-Char	800	<ul style="list-style-type: none"> <li>Removed 97% of tars</li> </ul>
Shen et al. (2014)	in-situ catalytic	Rice husk	Char, Ni-Fe/Char	600	<ul style="list-style-type: none"> <li>Catalysts remove tar effectively</li> <li>CO<sub>2</sub> reduced</li> <li>CO increased by dry reforming</li> </ul>
Zhang et al. (2013)	in-situ catalytic	Mallee wood	Fe/Char	600	<ul style="list-style-type: none"> <li>Decreased CO<sub>2</sub>, CH<sub>4</sub></li> <li>Increase H<sub>2</sub>, CO</li> </ul>
Srinakrungsri et al. (2006)	fixed-bed reactor	Tar (Toluene, naphthalene)	Ni/Al <sub>2</sub> O <sub>3</sub> , Ni/SiO <sub>2</sub> .Al <sub>2</sub> O <sub>3</sub> , Ni/dolomite	1200, 950, 750	<ul style="list-style-type: none"> <li>The Ni/dolomite catalyst showed excellent activity</li> <li>For tar decomposition and anti-coking</li> </ul>

Table 2.4 Review of the biomass gasification with nickel Catalyst (cont.).

Research group	Type gasifier	Biomass	catalyst	Calcined (°C)	Remark
Miao et al. (2010)	Tube reactor	acetic acid	Dolomite pellets	900	<ul style="list-style-type: none"> <li>• 99.70% of acetic acid decomposed</li> <li>• Size (3 mm-d ,4 mm-h)</li> </ul>
Wang et al. (2011)	lab-scale fixed bed	MSW	NiO on modified dolomite	900	<ul style="list-style-type: none"> <li>• The catalysts eliminate the tar</li> <li>• Increase the hydrogen yield</li> </ul>

Table 2.5 Review of biomass gasification models.

Research group	Biomass	Model	Remark
Jayah et al., 2003	Tea drying	Kinetic model	<ul style="list-style-type: none"> <li>• Kinetic model consists of two sub-models</li> <li>• The flaming pyrolysis</li> <li>• Gasification zone</li> </ul>
Tinanut et al. (2008)	-	Kinetic model	<ul style="list-style-type: none"> <li>• Developed gasifier</li> <li>• One-dimensional steady- state model</li> </ul>
Sharma (2011)	-	Kinetic model	<ul style="list-style-type: none"> <li>• Developed a one-dimensional steady- state model</li> <li>• To predict the performance of gasifier</li> <li>• Predict un-reacted char</li> <li>• Final gas composition</li> </ul>
Nikoo and Mahinpey et al. (2008)	pine	ASPEN PLUS	<ul style="list-style-type: none"> <li>• Developed ASPEN PLUS reactor</li> <li>• External FORTRAN subroutines for hydrodynamics</li> <li>• Kinetics</li> </ul>

Table 2.5 Review of biomass gasification models (cont.).

Research group	Biomass	Model	Remark
Ramzan et al. (2011)	FW, MSW, PW	ASPEN PLUS	<ul style="list-style-type: none"> <li>• Developed ASPEN PLUS</li> <li>• First stage (moisture content)</li> <li>• Second stage (volatile compound by FORTRAN)</li> <li>• Third stage (oxidation by Gibbs free energy)</li> </ul>
Kuo et al. (2014)	Bamboo and Torrefied Bamboo	ASPEN PLUS	<ul style="list-style-type: none"> <li>• Developed an ASPEN PLUS model</li> <li>• To evaluate the gasification potentials</li> </ul>



## CHAPTER 3

### Experimental Procedures

In this research work, the experimental procedure consists of four parts. The first part is characterization of the chemical and physical properties of biomass and the gasification of biomass are carried out in the Imbert downdraft gasifier with a throat section. The second part is tested and modified gasifier with the biomass. The third part involves the improvement of the gasification efficiency with metal catalyst on char and dolomite support and the final part is combined the gasifier with a small gas engine system for power generation and to predict product distribution from gasification using Advanced System for Process Engineering (ASPEN) as shown in figure 3.1.

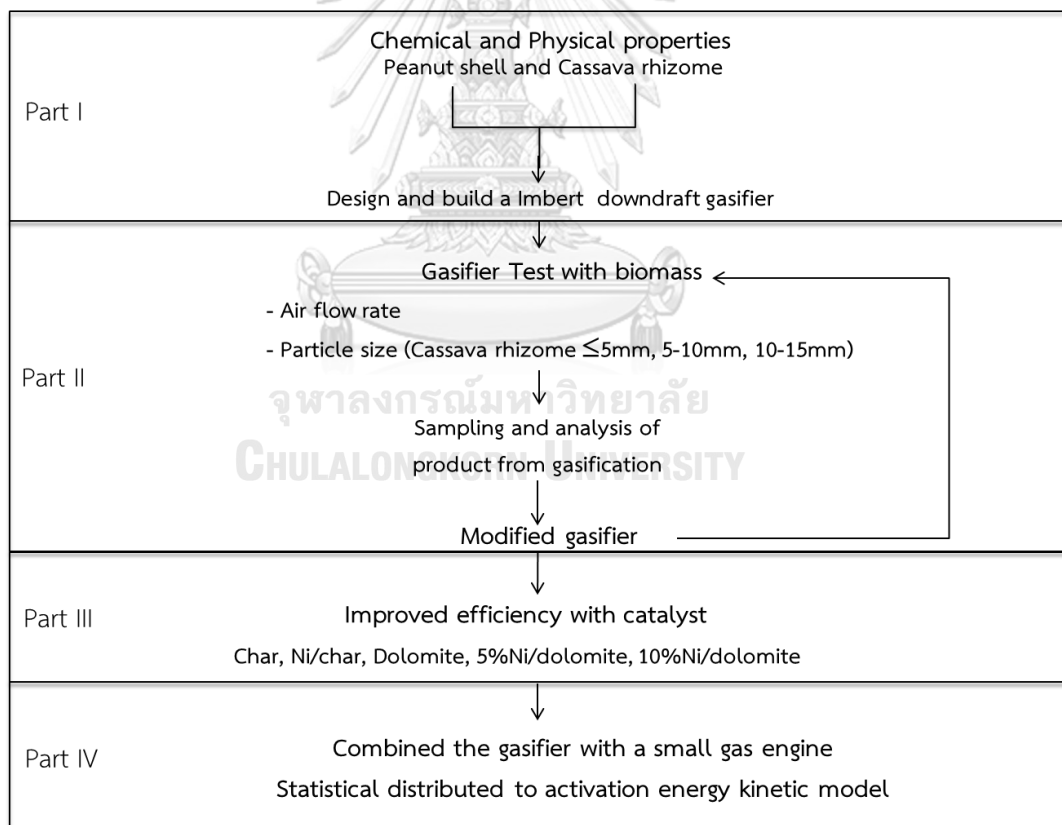


Figure 3.1 Experimental plan

### 3.1 Biomass Fuel Analysis and Experimental setup

#### 1. Proximate and ultimate analysis

Two types of analyses, proximate and ultimate, are useful for defining the fuel properties of a particular biomass feedstock. The proximate analysis of biomass on weight percentage basis was determined by following the standard method of ASTM-D5142-02. The ultimate analyses of carbon, hydrogen, sulfur, nitrogen, and oxygen of the biomass of the dry fuel on a weight percentage basis were carried out according to ASTM-D5373 using LECO CHNS-628 and LECO TruSpec Micro CHN/O as presented in Table 3.1 (ASTM standard methods for analysis of biomass).

#### 2. Chemical compositions

Thermochemical conversion of biomass greatly depends on the polymeric composition of biomass. The chemical compositions include ash, cellulose, hemicelluloses, lignin and extractives by TAPPI (T264), (T-203), (T-222).

#### 3. Heating value

The higher heating value of the fuel is determined by reacting the fuel with oxygen in a bomb calorimeter (LECO AC-350, ASTM) and measuring the heat released to a known quantity of water. The heat released during this procedure represents the maximum amount of energy that can be obtained from combusting the fuel and is a necessary value for calculating the efficiency of gasification. The high heating value (HHV) is measured in this test, since liquid water is produced; however, the low heating value (LHV) is more relevant to the amount of energy produced, and this can be calculated from the HHV value.

#### 4. Physical property

The bulk density is the weight of biomass packed loosely in a container divided by the occupied volume. Clearly, it is not an exact number, depending on the exact packing of the particles. The fuel shape and feeding characteristics determine whether it will be feasible to simply use gravity feeding techniques, or whether assistance, such as stirring and shaking, will be required. The angle of repose for a particular fuel type is generally measured by filling a large tube with the fuel, and then lifting the tube and allowing the fuel to form a pile. The angle of repose is

the angle from the horizontal to the sides of the pile. The basic feed characteristic is more easily judged from the dugout angle of repose, the steepest angle (measured from the horizontal) formed by the sides of a pile of fuel when material is removed from the bottom of the pile. Angles approaching or exceeding 90° are a good indication of the tendency of the fuel to bridge or tunnel in the gasifier.

Table 3.1 ASTM standard methods for analysis of biomass

Analysis	Methods
Proximate Analysis	ASTM-D5142-02
Ultimate Analysis	ASTM-D5373
Lower Heating Value	E711
Chemical composition	TAPPI (T264), (T-203), (T-222) for wood pulp

### 3.1.1 Biomass Preparation

#### 1. Cassava Rhizome

Cassava rhizome is a part of the neck between trunks and tuberous roots, which become the residue from cassava plantations. According to the recent survey in Thailand, approximately 7 million acres of cassava plantation could yield 25 million tons of cassava roots (<http://www.tapiocaonline.com>). Usually, the current practice of cassava rhizome residue management is open burning, which releases not only the greenhouse gases but also other pollutions as well as loss of energy. Usually, the current practice of cassava rhizome residue management is open burning, which releases not only the greenhouse gases but also other pollutions as well as loss of energy. Therefore, utilization of cassava rhizome as energy source by gasification will resolve this environmental problem while generating useful fuel gas products. The cassava rhizome used in the experiments is biomass residues from cassava plantations procured from Nakornsawan province in Thailand. The biomass was dried in air for 24 hour to reduce the moisture content. The particle sizes of cassava rhizome after chipping is in the range of 5-15 mm are shown in figure 3.2-3.3.

## 2. Peanut shell waste

Peanut plantation is a common agricultural in Asia. Nevertheless, worldwide peanut production was 40.18 million tons, of which 50,000 tons were produced in Thailand (USDA). Although these residues have high heating value, peanut shell wastes are usually burned by combustion process, not gasification process which is a more efficient process. Their high heating value and low moisture content are appropriate with gasification process. The peanut shell waste used in the experiments is biomass wastes generated from Lampang province in Thailand, shown in Figure 3.4.



Figure 3.2 Grinding Machine



(a)  $\leq 5$  mm

(b) 5-10mm

(c) 10-15 mm

Figure 3.3 The particle sizes of cassava rhizome.



Figure 3.4 The peanut shell waste.



### 3.1.2 Experimental setup

The experimental system set-up consists of a downdraft reactor, feeding system by auger motor and control with fuel level sensor, air supply system, swirl burner, and the clean-up system consists of cyclone, packed bed filter of char coal, and two condensers. The schematic of a modular downdraft gasifier system is illustrated in Figure 3.5. The height of the reactor is 610 mm and reduction zone is 200 mm. The diameter of the drying zone is 203 mm, the throat is 77 mm. The catalyst bed of 305 mm of diameter and 100 mm height was placed after cyclone. The auger motor feed coupled with drying hopper utilizes output production gas to dry incoming raw materials, while at the same time cooling down the exhausts gas. Air was supplied into the gasifier from the center air distribution nozzle, which was controlled by an ejector venturi. Flow rate of air inlet and product gas were determined by measuring pressure drop across respective orifice plates with U-tube manometers using water as the manometric fluid. The pressure drop between the throat section and the top end of the packed bed filter was also measured using a manometer. Temperature profiles along the reactor were measured by installation of thermocouples at 4 points along the center of reactor length which are drying (T1) at 250 mm, pyrolysis (T2) at 350 mm, oxidation (T3) at 457 mm, and reduction (T4) at 660 mm from the top of reactor, respectively. Product gas is cleaned in two steps, cyclone and two packed bed filters of char coal, before passing the air supply and finally flares burn.

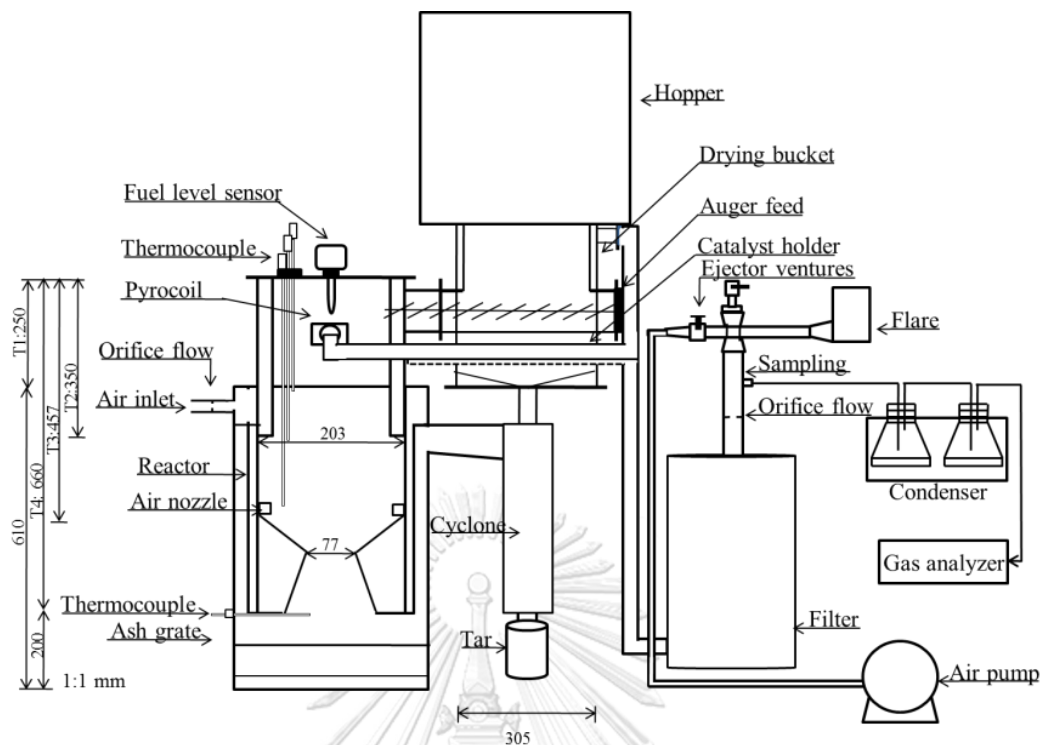


Figure 3.5 Schematic of a modular downdraft gasifier system used in the experiment.

### 3.2 Gasifier test and modified

During the startup of experiment, the ejector venturi was open to pull air supplied from air pump into the reactor. The solid fuel (hot charcoal) igniter was ignited into reduction zone of gasifier above the grate. Feeding of biomass into the gasifier was carried out through the hopper. The temperature profiles were measured by K-type thermocouples at each location. During the test, the temperature of four thermal conversion zones of the reactor was continuously recorded with data logger every 1 min. The produced gas from the reactor entered the following filter bed and cooling units. Gas samples were drawn by peristaltic pump into a small clean up unit for gas composition analysis using portable analyzer (Gasboard-3100p) which is based on NDIR to measure the gas concentration of CO, CO<sub>2</sub>, CH<sub>4</sub>, and C<sub>n</sub>H<sub>m</sub> and based on TCD (MEMS) to simultaneously measure the gas concentration of H<sub>2</sub>. In addition, condensate of tar, char and ash were concurrently measured.

### 3.2.1 Characteristics of gas

Gas samples were drawn by peristaltic pump into a small clean up unit for gas composition analysis using portable analyzer (Gasboard-3100p) (Figure 3.6) which is based on NDIR to measure the gas concentration of CO, CO<sub>2</sub>, CH<sub>4</sub>, and C<sub>n</sub>H<sub>m</sub> and based on TCD (MEMS) to simultaneously measure the gas concentration of H<sub>2</sub>. In addition, condensate of tar, char and ash were concurrently measured.



Figure 3.6 Portable analyzer (Gasboard-3100p).

### 3.2.2 Characteristics of char and tar

Char obtained after experiment was analyzed in order to observe the change in solid material properties. The ultimate analysis of char was determined using the same methods as for the raw materials. Tar content from experiment was analyzed by gas chromatography - mass spectrometry (GC-MS QP2010, Shimadzu). The GC column was a fused silica column (DB1701) with 60 m length, 0.25 mm inner diameter and 0.25  $\mu$ m film thicknesses. The GC oven temperature profile was programmed to increase from 50 to 300°C at 5°C/min with a hold time of 1 min at 45°C and of 10 min at 280°C.

### 3.2.3 Modifier with the thermal integration unit

The main reactor was coupled with the thermal integration unit to provide heat recovery. This is a gas circulating heat exchanger, used to return hot flue gas exits the gasifier to drying and pyrolysis zone of the reactor as shown in Figure 3.7.



Figure 3.7 The thermal integration unit.

### 3.2.4 The effect of gasification parameter

The experiment was to investigate the effect of air flow rate at 1.2-3.05 m<sup>3</sup>/hr and the particle sizes of cassava rhizome  $\leq 5$  mm, 5-10 mm, and 10-15 mm on gas production performance of biomass gasification. The performance of gasification was evaluated in term of attainable zone temperature, producer gas composition, conversion, gasification efficiency, air superficial velocity, biomass consumption rate, and specific gasification rate.

## 3.3 Improvement of the gasification efficiency with metal catalyst

### 3.3.1 Catalyst Preparation

#### 1. Ni on char support

The char support was prepared by slow pyrolysis of cassava rhizome (particle size 15 mm) using the tube reactor, it can be seen in Figure 3.8. The temperature of pyrolysis was 600°C in the N<sub>2</sub> atmosphere 2 l/min then hold at the final temperature 600°C 1 hr. The Ni/char catalysts was prepared by the impregnation method using Ni(NO<sub>3</sub>)<sub>2</sub>·6H<sub>2</sub>O (Merck, Ltd). The char support was doped with 5%Ni at 80°C for 3 hour. After impregnation, the catalyst was drying for 24 hour at 105°C and calcined in N<sub>2</sub> at 800°C for 2 hour as illustrated in Figure 3.9.

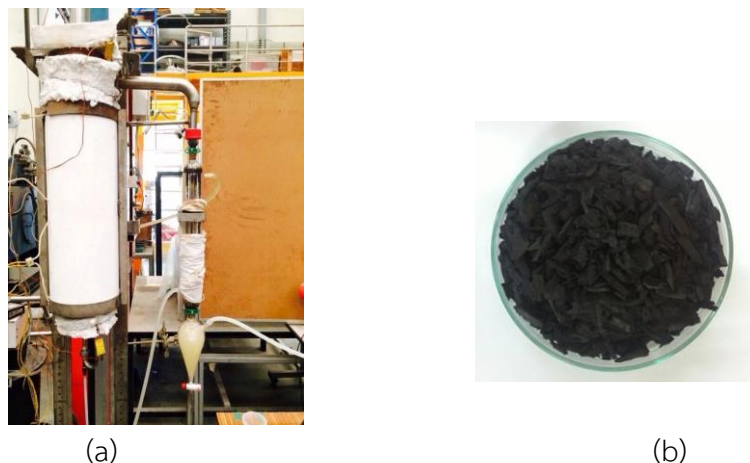


Figure 3.8 Char support was prepared by slow pyrolysis of cassava rhizome (b) Char support.



Figure 3.9 Ni/char catalyst was prepared by the impregnation method (a) char support (b) impregnation with  $\text{Ni}(\text{NO}_3)_2 \cdot 6\text{H}_2\text{O}$  (c) drying (d) calcination.

## 2. Ni on dolomite pellet support

The dolomite pellet support was prepared by extrusion dolomite powder ( $\text{MgCO}_3 \cdot \text{CaCO}_3$  mixed with 10% kaolin powder, 12% organic binder, and 10% distilled water) and extruded through the die with 6.50 mm of outside diameter. In Figure 3.10, the dough was then formed into cylindrical shape by extruder (FM-30-1, Miyazaki Iron Work). The green samples were drying in room temperature for overnight. The dolomite rod used support to prepare catalyst, 10 mm in length and 6.50 mm of outside diameter was obtained. The dolomite pellets were sintered at  $1200^\circ\text{C}$  for 3 hours. The dolomite pellet support catalyst was prepared with  $\text{Ni}(\text{NO}_3)_2 \cdot 6\text{H}_2\text{O}$  (Merck, Ltd) by the impregnation method that is similar with Ni/char catalysts in Figure 3.11. The dolomite support was doped with 5%Ni at  $80^\circ\text{C}$  for 3 hr.

After impregnation, the catalyst was drying for 24 hr at 105°C and calcined in ambient air at 700°C for 2 hr.

In the experiment, the catalytic holder of 305 mm in diameter and 100 mm in height was attached after cyclone as shown in Figure 3.12. Effect of addition of 5%Ni/char and 5%Ni/dolomite pellet catalyst module for secondary syngas cleanup on gasification efficiency was also examined.

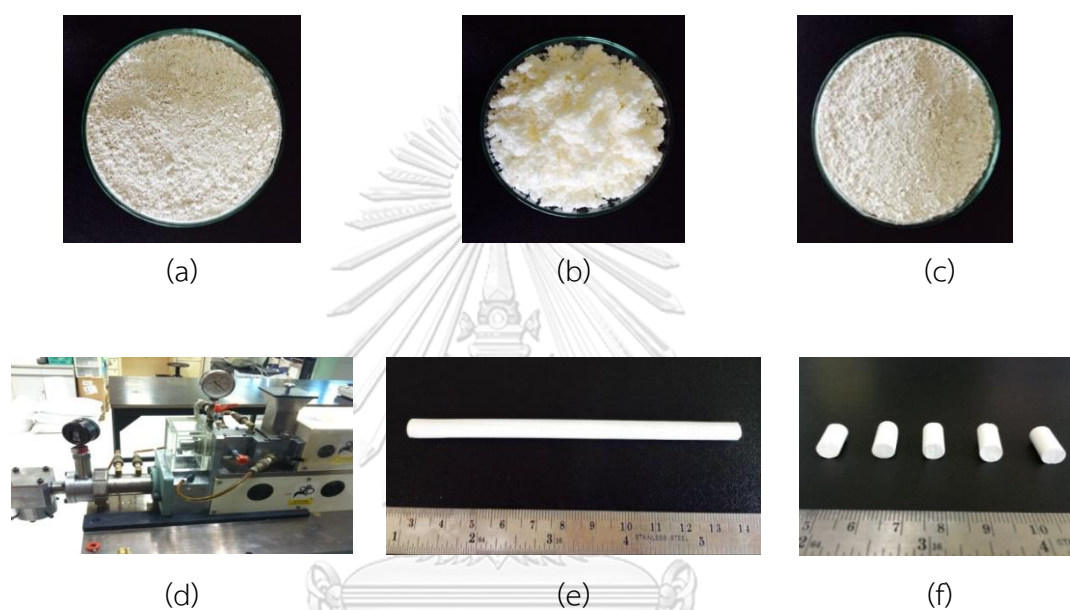


Figure 3.10 (a) dolomite power (b) organic binder (c) kaolin power (d) extruder (e) and (f) extrusion dolomite.

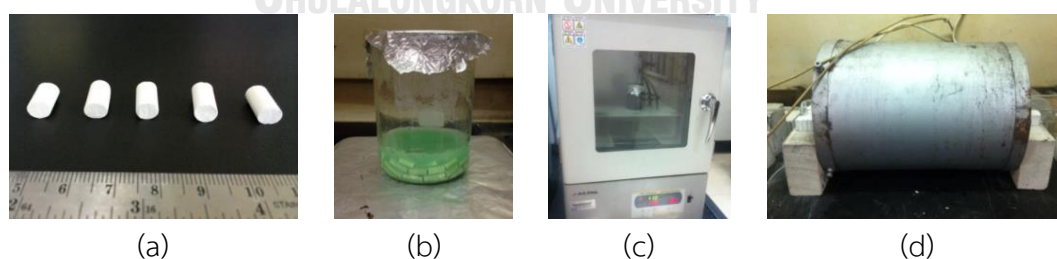


Figure 3.11 Ni/dolomite pellet catalyst was prepared by the impregnation method (a) dolomite support (b) impregnation with  $\text{Ni}(\text{NO}_3)_2 \cdot 6\text{H}_2\text{O}$  (c) drying (d) calcination.





Figure 3.12 The catalyst holder.

### 3.3.2 Characterization of catalyst

The support and catalyst were characterized by X-ray diffraction (Rigaku, Japan) to confirm phase of active catalyst. The surface area and pore volume of catalyst were analyzed by nitrogen adsorption and desorption using Autosorb-1 (Quantachrome instruments). The surface area of catalysts and the catalyst distribution on support material were investigated by scanning electron microscopy (Hitachi, Japan). In addition energy dispersive x-ray analysis (EDX) was determined the actual amount of available active of metal.

## 3.4 Power generation and predict product distribution from gasification unit.

### 3.4.1 Power generation

The fuel gas produced from the gasification unit was combined with a small gas engine (base on LPG fuel) system for power generation.

The gas clean-up system consists of cyclone and two packed bed filter of char coal. The producer gas after cleaning process can directly be supplied to the engine. The schematic diagram of the downdraft gasifier combined with power generation is shown in Fig 3.12. The specifications of gas engine/generator are given in Table 3.2.

Table 3.2 Specification of gas engine/generator

Engine	Model	Sm 2500 lpg
	Type	4 - stoke
	Number of Cylinders	1
	Displacement	196 cc
	Engine speed	1500 rpm
	Starting system	Recoil/Electric
	Max. Power Output	6.5 hp
	Noise level	62 dB
	Generator	Ac Max. Output
Ac Con. Output		2.0 kW
Voltage		220 V
Frequency		50 Hz
Nominal power		2.0 kW
DC Voltage/Amp		12/8.3

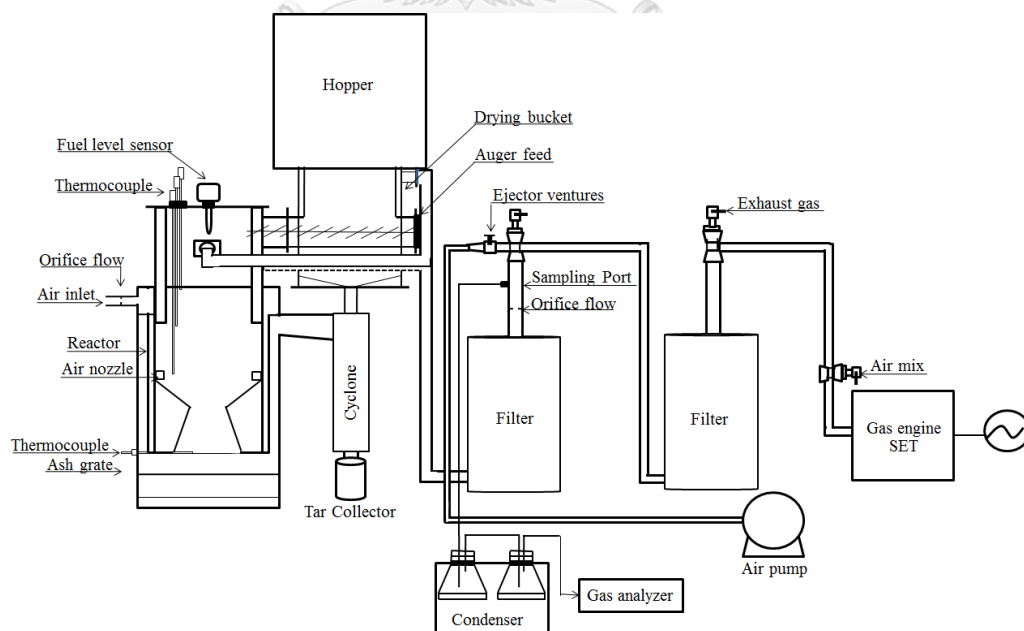


Figure 3.13 Schematic diagram of the downdraft gasifier combined with power generation system.





Figure 3.14 gas engine/generator system

#### 3.4.2 Predict product distribution from gasification unit.

Advanced System for Process Engineering (ASPEN) is a software package that gives a complete integrated solution to chemical process and reactors. Aspen Plus can be used to model many processes involving solids. Solids process modeling in Aspen Plus supports rigorous descriptions of solids processing steps. The simulations of biomass gasification process were based on mass energy balance and chemical equilibrium among all processes. This model uses unit operation blocks, which are the models of specific process operations. The user places these blocks on a flow sheet, specifying material, and energy streams. An extensive built-in physical properties database is used for the simulation calculations.

## CHAPTER 4

### The Characteristic of Biomass and Catalyst

#### 4.1 Characteristic of biomass

##### 4.1.1 The cassava rhizome

The cassava rhizome is the biomass residues from cassava plantations procured from Nakornsawan province, Thailand. The biomass was dried in ambient air for 24 hours to reduce the moisture content. The size of cassava rhizome after chipping is in the range of 5-15 mm for the experiment. The physical and component properties of the cassava rhizome are presented in Table 4.1. The proximate and ultimate analysis of the dried cassava rhizome on weight percentage basis was determined by standard methods as shown in Table 3.1. The proximate analysis of cassava rhizome showed high volatile matter and low moisture content. The ultimate analysis results revealed important fractions represented by carbon (39.80%) and hydrogen (5.03%). The heating value of cassava rhizome is 15.10 MJ/kg. Generally, this raw material has high carbon and volatile matter and low moisture content which is appropriate for thermochemical conversion through gasification process. In addition, the results of biomass component indicated higher cellulose than lignin. Accordingly, the cellulose component in biomass is mainly responsible for the releasing and conversion of volatile matter as gas, whereas lignin components are the main contributor to char (Dangzhen Lv, 2010).

##### 4.1.2 The peanut shell waste

The peanut shell waste used in the experiments is biomass wastes produced from Lampang province, Thailand. The biomass was dried in ambient air for 24 hours similar to cassava rhizome sample to reduce the moisture content. The result of physical and component properties are shown in Table 4.2. It can be observed that this biomass contained higher volatile and carbon whereas low nitrogen and sulfur with the heating value of 16 MJ/kg. The moisture content of biomass was 9.52%. Generally, the limitation of moisture content of biomass for operating a downdraft

gasifier is considered to be no more than 30-40% (Dogru et al., 2002). Therefore the biomass sample is suitable for this type of thermal conversion with low environmental pollution prospect.

Table 4.1 Characteristic of cassava rhizome

Proximate Analysis (wt.%)		Ultimate Analysis (wt.%)	
Moisture	10.28	Carbon	39.80
Ash	8.62	Hydrogen	5.03
Volatile organic content	72.30	Nitrogen	1.38
Fixed carbon	9.40	Sulfur	0.15
L HV, (MJ/Kg)	15.10	Oxygen	37.50
		Other*	16.14
Physical Properties			
Bulk density (kg/m <sup>3</sup> )	145 (5 mm), 140 (10 mm), 132 (15 mm)		
Component Analysis (wt.%)			
Cellulose	35.39		
Hemi cellulose	24.21		
Lignin	30.73		
Extractives	9.67		

\*Other by difference จุฬาลงกรณ์มหาวิทยาลัย

CHULALONGKORN UNIVERSITY

Table 4.2 Characteristic of peanut shell

Proximate Analysis (wt.%)		Ultimate Analysis (wt.%)	
Moisture	9.52	Carbon	40.34
Ash	17.92	Hydrogen	6.35
Volatile organic content	65.78	Nitrogen	0.79
Fixed carbon	2.78	Sulfur	0.29
LHV, (MJ/Kg)	16.47	Oxygen	35.47
		Other*	16.76
Physical Properties			
Bulk density (kg/m <sup>3</sup> )	60		
Component Analysis (wt.%)			
Cellulose	27.81		
Hemi cellulose	26.38		
Lignin	36.91		
Extractives	8.9		

\*Other by difference

## 4.2 Characterization of catalyst

### 4.2.1 Ni/Char catalyst

The char obtained from the pyrolysis experiment was characterized using XRD patterns as presented in Figure 4.1. The char exhibited intensified peaks at  $2\theta = 28^\circ$  and  $29.50^\circ$ , corresponding to carbon. For calcined 5%Ni/char, the intensified peaks at  $2\theta = 44^\circ$  and  $52^\circ$ , corresponding to Ni. The TGA and DTG curves of 5% Ni/char is presented in Figure 4.2. The measurement was carried out with heating rate of  $10^\circ\text{C}/\text{min}$  from  $30$  to  $950^\circ\text{C}$  under  $60\text{ ml}/\text{min}$  of  $\text{O}_2$  and  $\text{N}_2$ . Peaks at  $80$ - $160^\circ\text{C}$  were attributed to the desorption of adsorbed water and the crystalline structure of water. The residue of volatile in char support was found to decompose between  $350^\circ\text{C}$  and  $700^\circ\text{C}$ . The surface area of char and catalysts were investigated by SEM in Figure 4.3. The char support from pyrolysis at  $600^\circ\text{C}$  has high porous surface structure as a result of the removal of volatile materials. The sizes of porous 5%Ni/char after calcined are

extend with thinner walls and characterized as a honeycomb-shaped. The actual amount of available active of 5%Ni metal as measured by energy dispersive x-ray analysis (EDX) was 5.28%Ni. The surface area and pore volume of catalyst analyzed by nitrogen adsorption and desorption were calculated along with the Langmuir surface area method. The char support obtained at the pyrolysis temperature of 600°C has surface area of 37.9 m<sup>2</sup>/g whereas those of 5%Ni/char and 5%Ni/char after calcined are 66.8 m<sup>2</sup>/g and 79 m<sup>2</sup>/g, respectively. Total pore volume of 0.0827 ml/g and average pore diameter of 63.9 Å are in good agreement with the result obtained by SEM. The 5%Ni/char after calcination resulted in relatively high surface area of porous carbonaceous material which is suitable to be applied as catalyst or adsorbent.

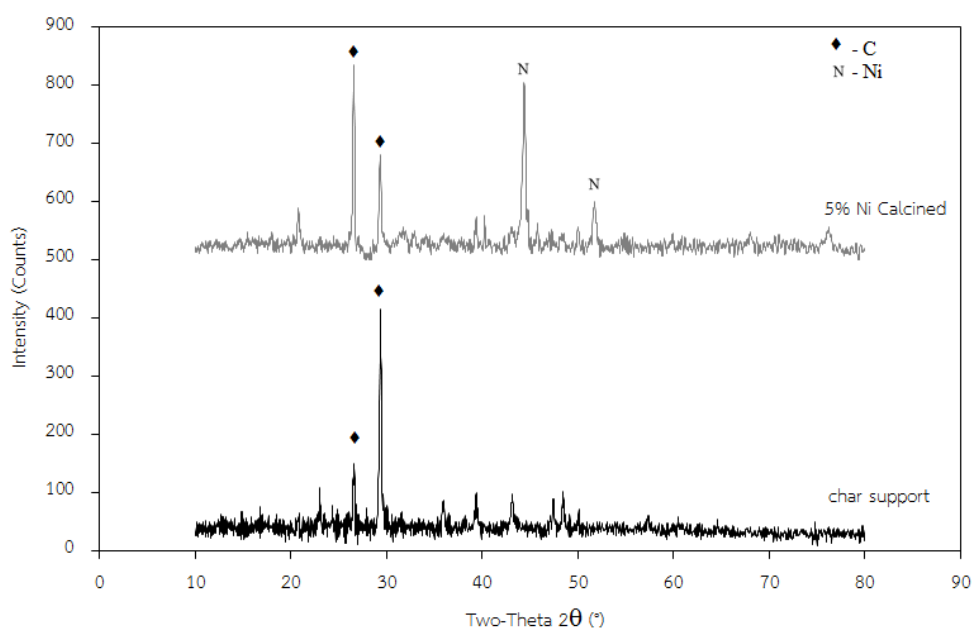


Figure 4.1 X-Ray diffraction of char support and calcined 5%Ni/char.

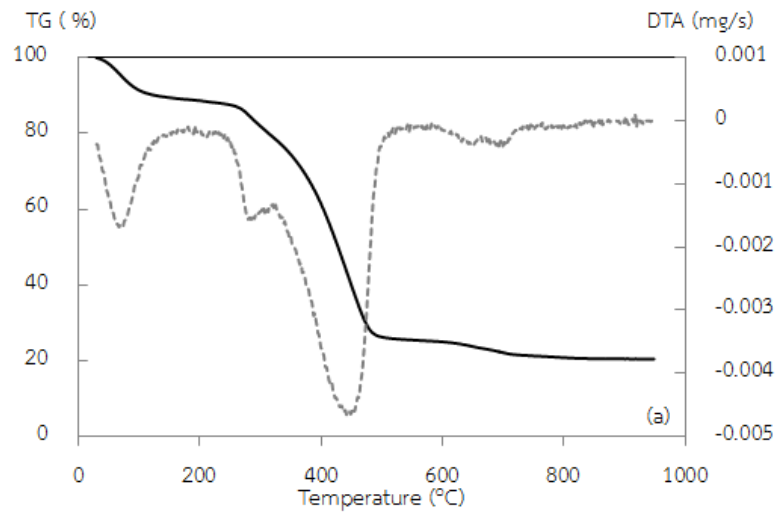


Figure 4. 2 TGA results of (a) 5%Ni/char (b) calcined 5%Ni/char

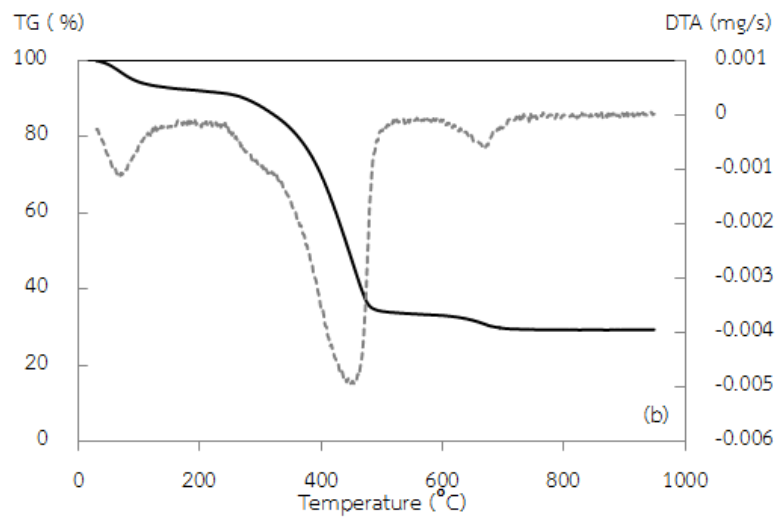


Figure 4.2 TGA results of (a) 5%Ni/char (b) calcined 5%Ni/char

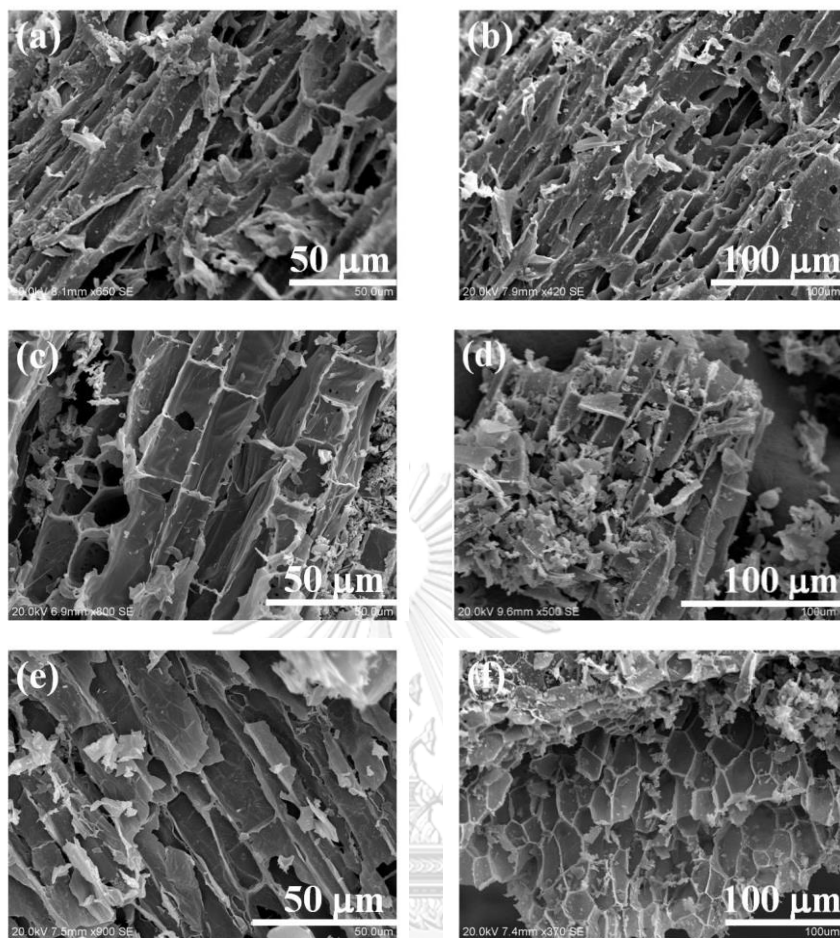


Figure 4.3 SEM of (a, b) char support, (c, d) 5%Ni/char and (e, f) calcined 5%Ni/char.

#### 4.2.2 Ni/dolomite Catalyst

The XRD patterns of the dolomite pellet support and catalyst are presented in Figure 4.4. The dolomite pellet support exhibited intensity peaks at  $2\theta = 43^\circ$ ,  $62^\circ$ , and  $78^\circ$ , corresponding to MgO, whereas  $32^\circ$  and  $34^\circ$  corresponding to CaO. The presence of NiO was confirmed in 5% Ni/dolomite at  $2\theta = 37^\circ$ ,  $43.5^\circ$ , and  $63^\circ$ . The TGA and DTG curves of calcined dolomite and calcined Ni/dolomite are presented in Figure 4.5. The peak at 80-200°C was attributed to desorption of adsorbed water and crystalline structure of water. The dolomite was found to decompose between 450°C and 800°C. Then  $\text{CO}_2$  was released leaving CaO and MgO phases, which was confirmed by XRD analysis (Wang, T. J., 2005). The morphology of fresh catalysts was explored by SEM analysis and the results are shown in Figure 4.6. During dolomite

calcination, Mg in  $\text{CaMg}(\text{CO}_3)_2$  moved to the surface and released  $\text{CO}_2$  gas leading to the external and internal growth of MgO and the internal growth of  $\text{CaCO}_3$ , respectively. As a result of this phenomenon, the surface of calcined dolomite was of higher porosity than raw dolomite. The specific surface area was increased from 3.97 to 13.81  $\text{m}^2/\text{g}$ , which, in turn, upgraded the metal active site capacity. Furthermore, large pore spaces and rough grains of Ni on the surface of dolomite were the characteristics of calcined 5%Ni/dolomite catalyst. The EDX analysis exhibited that the Ni loading was 6.28% on the surface of dolomite pellet support. The surface area of 5% Ni/dolomite was 56.09  $\text{m}^2/\text{g}$  and total pore volume was 0.0850 ml/g. Though, the surface area and total pore volume of 5%Ni/dolomite was reduced to 17.59  $\text{m}^2/\text{g}$  and 0.0499 ml/g after calcination. This decreased surface area was probably because of the covered pore spaces and then sintering on the dolomite support during the calcination process (Figure 4.6).

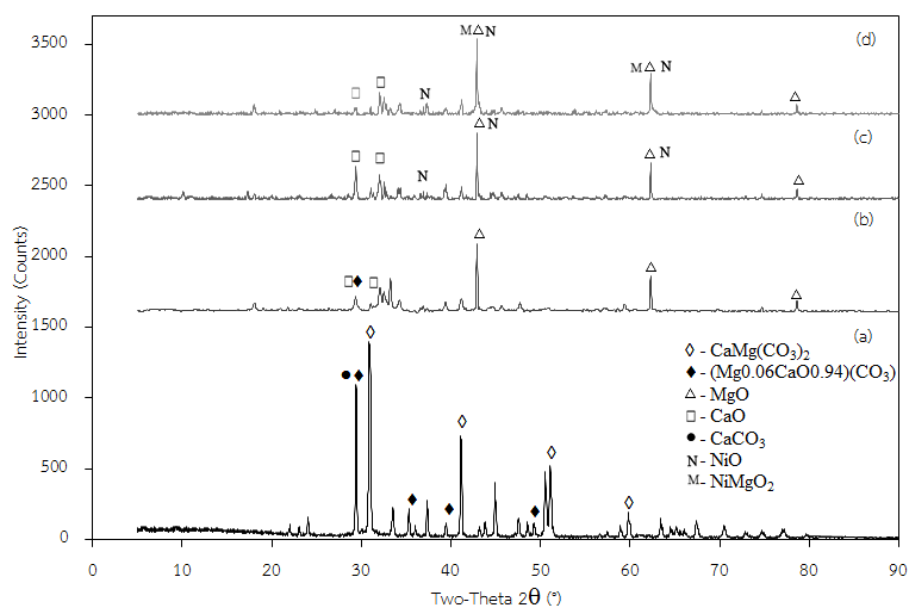


Figure 4.4 XRD of the fresh catalyst; (a) dolomite (b) calcined dolomite (c) 5%Ni/dolomite and (d) calcined 5%Ni/dolomite.



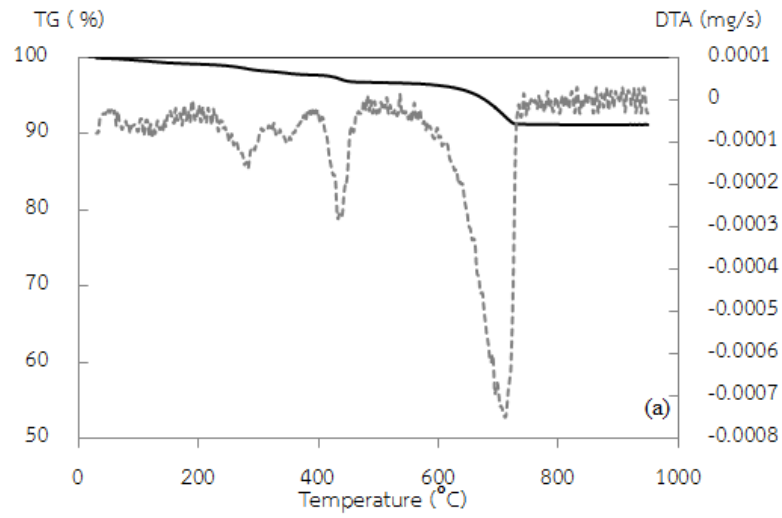


Figure 4.5 TGA thermogram of (a) calcined dolomite (b) calcined 5%Ni/dolomite

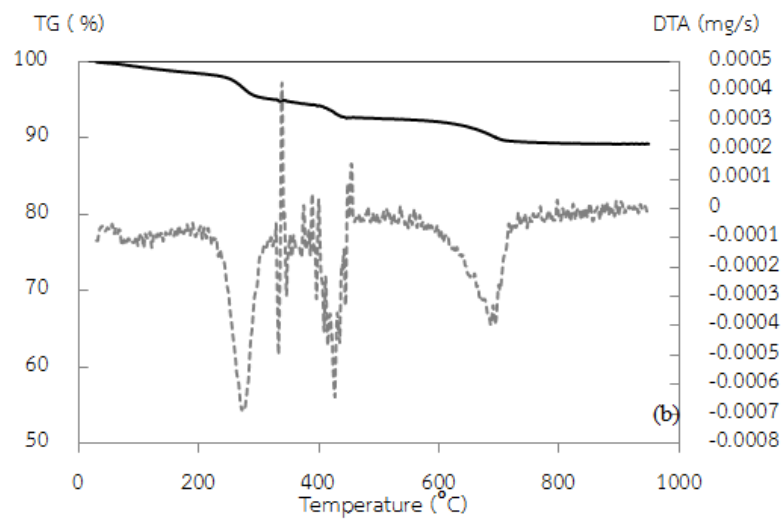


Figure 4.5 TGA thermogram of (a) calcined dolomite (b) calcined 5%Ni/dolomite

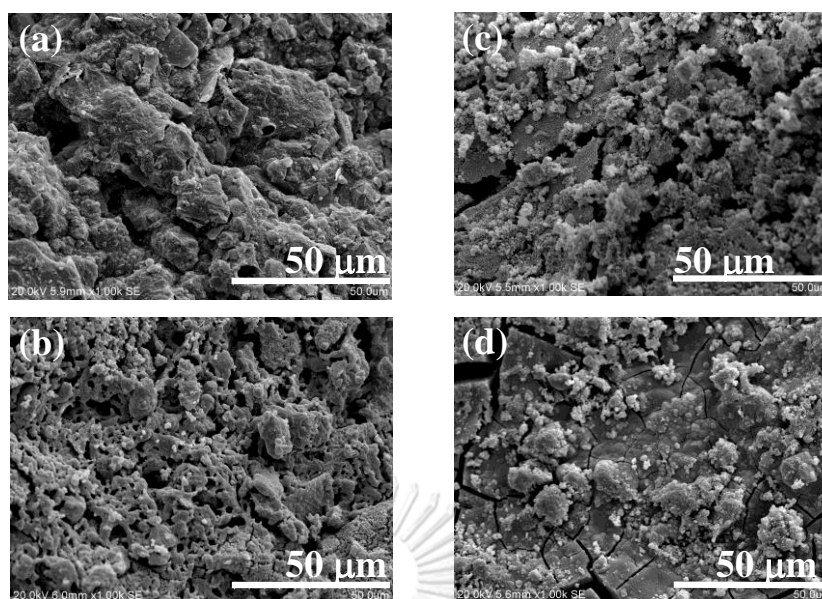


Figure 4.6 SEM of (a) dolomite (b) calcined dolomite (c) 5%Ni/dolomite

### 4.3 Characteristic of spent catalyst

#### 4.3.1 Ni/char catalyst

The characteristics of catalyst after experiment were determined to study carbon deposit and structure. Figure 4.7 showed TGA and DTG analysis to investigate the rate of mass loss which is an indication of reactivity of catalysts under investigation. First step was the loss of water of crystallization (30-150°C), decomposition of the condensed volatiles (350-550°C), and lastly, the decomposition of carbon (650-750°C). This result exhibited similar trend for both catalysts. After gasification process with char and 5% Ni/char catalyst, the volatiles, condensable, and primary vapors covered on catalysts surface. Their SEM images are shown in Figure 4.8. From this result, the catalysts displayed resistant to high temperature and hence, regeneration capability would be further investigated.

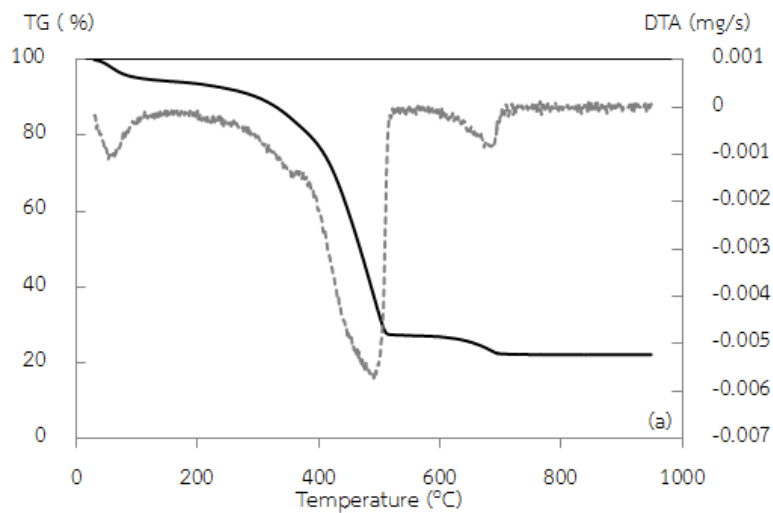


Figure 4.7 TGA of (a) spent char and (b) spent 5%Ni/char

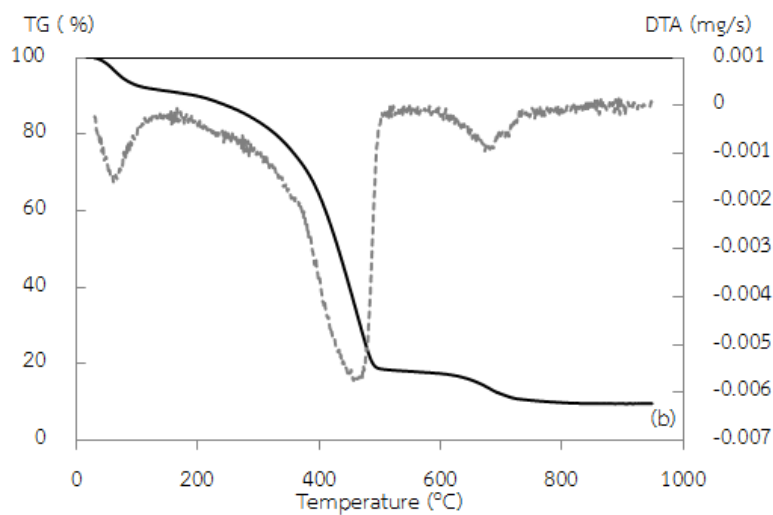


Figure 4.7 TGA of (a) spent char and (b) spent 5%Ni/char

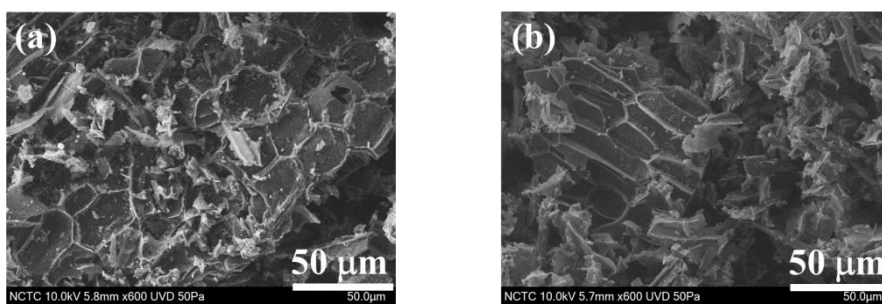


Figure 4.8 SEM of (a) spent char and (b) spent 5%Ni/char

### 4.3.2 Ni/dolomite catalyst

The corresponding TGA profile of used catalysts exhibited three distinct weight-loss steps as shown in Figure 4.9. First step was the loss of water of crystallization (25-230°C), decomposition of the condensed and volatiles (350-550°C), and the decomposition of carbon (600-800°C). The decomposition of condensed and volatile from dolomite support was higher than that of 5%Ni/dolomite catalyst. These results correlated with the SEM image shown in the previous section. After gasification with dolomite and 5% Ni/dolomite, volatiles and condensable primary vapors covered on each of reacted catalysts surface. Their SEM images are shown in Figure 4.10 (a) and (b), respectively. Both dolomite pellet and 5%Ni/dolomite surface displayed the coating of condensable vapors. From this result, the support and catalyst exhibited resistant to high temperature in which the catalyst life time and regeneration capability would be further investigated.

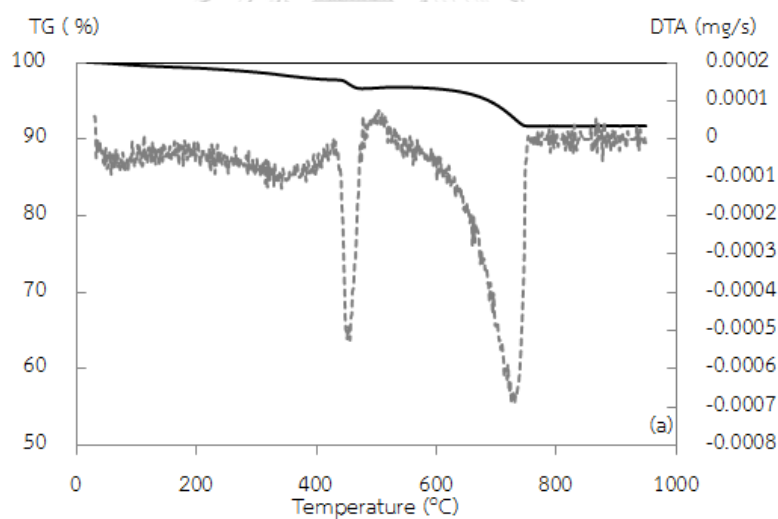


Figure 4.9 TGA of (a) spent dolomite pellet and (b) spent 5%Ni/dolomite.

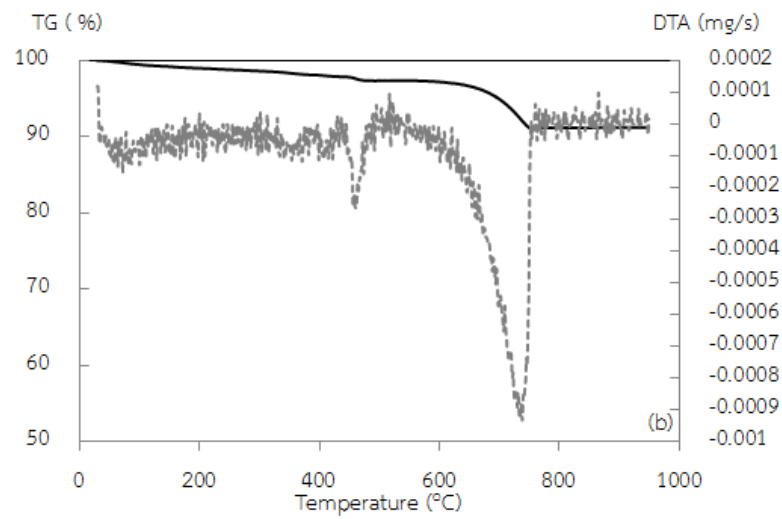


Figure 4.9 TGA of (a) spent dolomite pellet and (b) spent 5%Ni/dolomite.

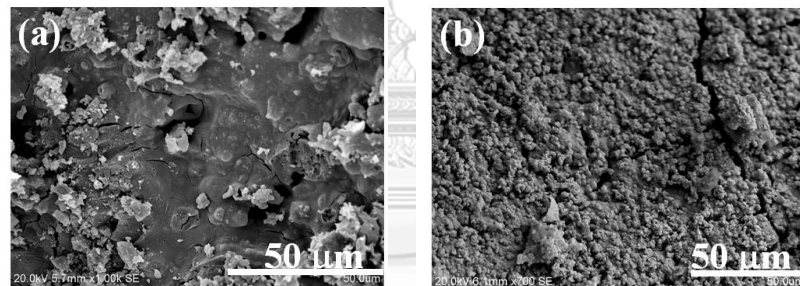


Figure 4.10 SEM of (a) spent dolomite pellet and (b) spent 5% Ni/dolomite.

## CHAPTER 5

### Biomass Gasification with a Downdraft Gasifier

#### 5.1 Gasification performance of downdraft gasifier with peanut shell waste

##### 5.1.1 The system performance and effect of heat recovery unit.

The peanut shell waste was fed at the rate of  $\sim 3$  kg/hr with  $1.62 \text{ m}^3/\text{hr}$  air flow inlet in a continuous operation. The temperature distributions along the gasifier for the non-catalytic case with addition of heat thermal integration unit are shown in Figures 5.1 and 5.2. In the drying zone, moisture was released as water vapor by the heat from the oxidation zone. After 20-30 minutes, the temperatures at drying and pyrolysis zones were slightly increased. The temperature of oxidation zone was between 800 to 900°C. Generally, the oxidation temperature of downdraft gasifier is about 800 to 1400°C (Basu, 2010b). The generated heat from this zone was transferred to upper and lower zones which promoted and sustained reactions in the gasifier. The temperature at the reduction zone was about 600 to 700°C. Products from pyrolysis and combustion zones were converted and reformed to produce synthesis gas at this reduction zone. From Figure 5.2, the temperature of drying and pyrolysis zones increased more rapidly than those of system without heat thermal integration unit. The temperature of oxidation zone was around 800 to 1000°C which depends upon the air flow rate inlet and the heat released from the biomass combustion.

In case of the experiment without heat thermal integration unit at  $1.62 \text{ m}^3/\text{hr}$  air flow rate, the hydrogen and carbon conversions were 32.17% and 49.92%, respectively, and increased to 40.42% and 52.48%, correspondingly, for the case of heat thermal integration unit addition (Figure 5.3). As a result, the carbon conversion to CO, CO<sub>2</sub>, and CH<sub>4</sub> and hydrogen conversion to H<sub>2</sub>, CH<sub>4</sub> were increased (Table 5.1). The heat exchanger returns heat from the exhaust gas to heat recover section at drying and pyrolysis zone of reactor, resulting in more efficient drying process and pyrolysis reaction.

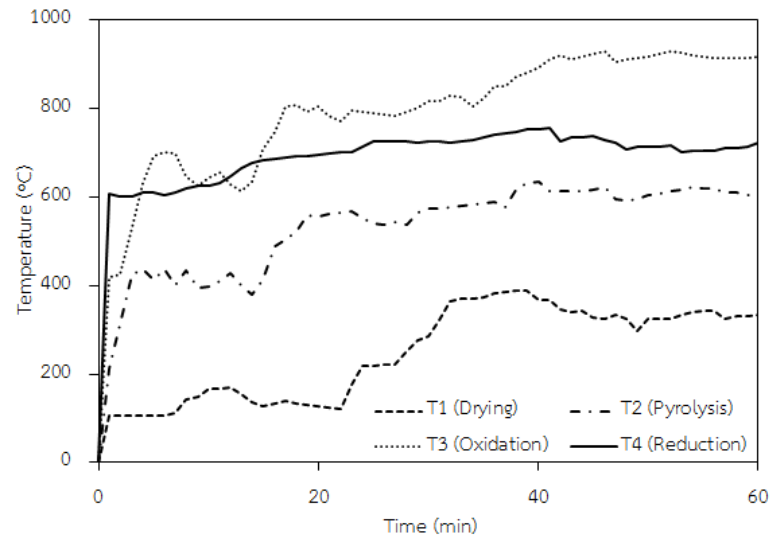


Figure 5.1 Temperature distribution within gasifier w/o thermal integration unit.

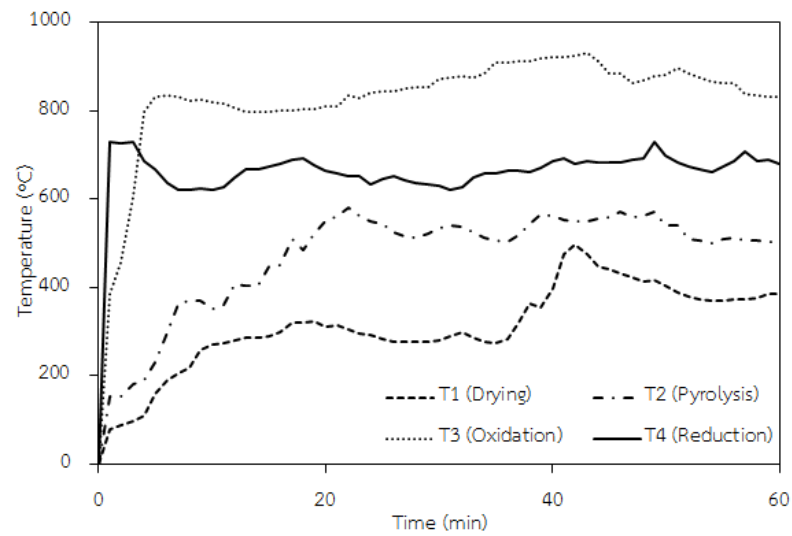


Figure 5.2 Temperature distribution within gasifier with heat thermal integration unit.

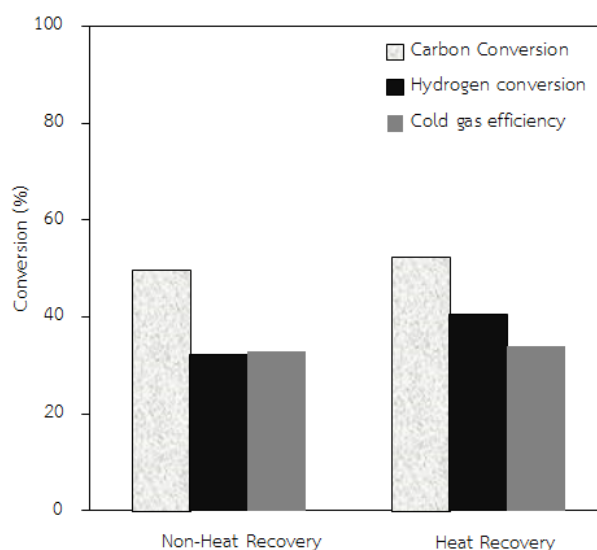


Figure 5.3 Effect of heat recovery addition on conversion and cold gas efficiency.

Table 5.1 Effects of heat thermal integration unit addition (1.62 m<sup>3</sup>/hr air flow rate)

	Carbon Conversion (%)			Hydrogen Conversion (%)		LHV (MJ/m <sup>3</sup> )	Cold gas Efficiency (%)
	CO	CO <sub>2</sub>	CH <sub>4</sub>	H <sub>2</sub>	CH <sub>4</sub>		
Heat recovery	21.76	23.81	6.91	23.89	16.53	3.79	34.08
Non-Heat recovery	19.27	25.75	4.91	20.53	11.64	3.66	32.90

### 5.1.2 The effect of air flow rate

In this experiment, the air flow rate can be controlled but the equivalence ratio cannot be directly manipulated because the biomass consumption rates mainly depend on the reaction rate at the combustion zone. The range of air flow rate for the experiment vary from 1.62 to 3.54 m<sup>3</sup>/hr which correspond to superficial gas velocity of 26.44 to 57.77 m/hr, respectively, yielding equivalence ratio (ER) of around 0.11 to 0.23. The effects of air flow rate on conversion are shown in Figures



5.4 and 5.5. At low air flow rate, the formation of CO<sub>2</sub>, tar and char was greater than that of higher air flow rate. This is probably a result of lower temperature at oxidation zone leading to lesser cracking and reforming reactions of products from drying and pyrolysis zones. The rate of reversed reaction of the reversible water gas shift reaction is slower than the rate of forward reaction at the low air flow rate (Gai et al., 2012). When increased air flow rate from 1.62 to 3.06 m<sup>3</sup>/hr, the hydrogen conversion to H<sub>2</sub> and carbon conversion to CO increased while the carbon conversion to CO<sub>2</sub> decreased for both conditions because the water shift reaction can also take place and produces more H<sub>2</sub> and CO in the product gas. In addition, the carbonaceous residues and combustible species will be oxidized in the oxidation zone through Boudouard reaction and water gas reaction. After increased air flow rate up to 3.54 m<sup>3</sup>/hr, the conversion was slightly decreased under both conditions. From these results, the highest carbon conversions to CO<sub>2</sub>, CO and CH<sub>4</sub> were 35.94%, 44.03%, and 7.14%, respectively and hydrogen to H<sub>2</sub> and CH<sub>4</sub> were 40.18% and 17.03%, respectively. Increase air flow rate means higher equivalence ratio and more oxygen for oxidization reactions. The results agree with Dogru et al. (2002) , Gai et al. (2012) , Zainal et al. (2002), and P. Lv et al. (2007).

The data on biomass consumption, specific gasification rate, specific gas production rate, cold gas efficiency and lower heating of produce gas are summarized in Table 5.2. With increasing air flow rate to the gasifier, specific gasification rate, specific gas production rate, and cold gas efficiency increased linearly. However, the cold gas efficiency was declining at 3.54 m<sup>3</sup>/hr air flow due to the decrease in lower heating values of producer gas. The increasing trend of gas lower heating value with air flow rate might be due to deviation from the turn down ratio of gasifier (Singh et al., 2006). The turndown ratio is a vital concept in sizing gasifiers which is the ratio of the highest practical gas generation rate with low practical rate (low turndown ratio will be generated tar). Also at greater air flow rate, biomass consumption rate increased which also accounted for the increase in efficiency. Increase the air flow rate leads to higher increase oxygen to oxidize and greater amount of biomass being combusted (Basu, 2013b). The results of air flow rate on biomass consumption rate and H<sub>2</sub>/CO ratio are given in Figure. 7. The range

of  $H_2/CO$  ratio was 1.0 to 1.2, suggesting that the produced gas can be used in power applications.

Mass balance calculation is a preferred method to check the consistency of the experiment and collected data. Total mass inputs include biomass and air, while total mass outputs include total gas product, liquid (tar and water), and solid (char and ash). Therefore, the favored indicator to determine any possible experimental discrepancies in the mass balance closure which is the percentage ratio of the total product output mass to that of the total raw material input. Due to nature of a relatively large-scale setup and variety of multi-phase reactant and product involved in this experiment, 100% closure is challenge, however most of the trials resulted in acceptable closures of within the 80–98%. Sheth et al. (2010) discovered that the average mass balance closure is found to be 94% from waste wood gasification using downdraft gasifier. Ouadi et al. (2013) reported the mass balance and closure from paper industry waste gasification using fixed bed downdraft gasifier were in the range of 86-130%. They described that the closures outside this margin were largely due to the instrumental error.

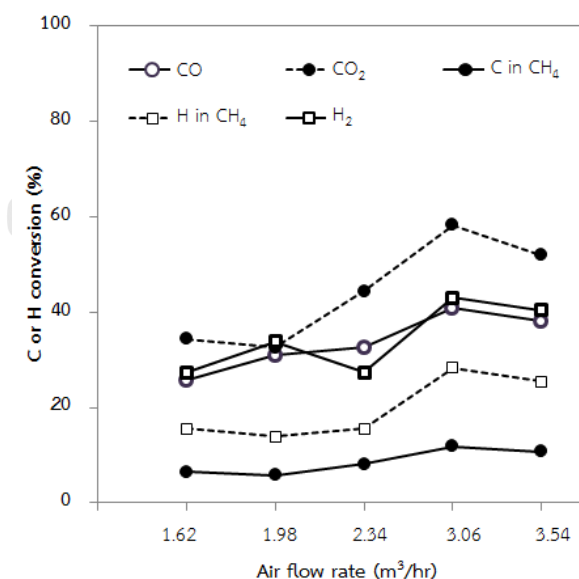


Figure 5.4 Effect of air flow rate on conversion without heat thermal integration unit.

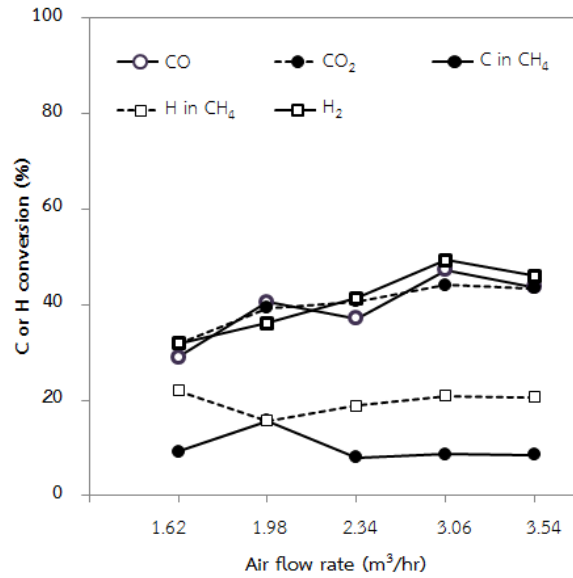


Figure 5.5 Effect of air flow rate on conversion with heat thermal integration unit.

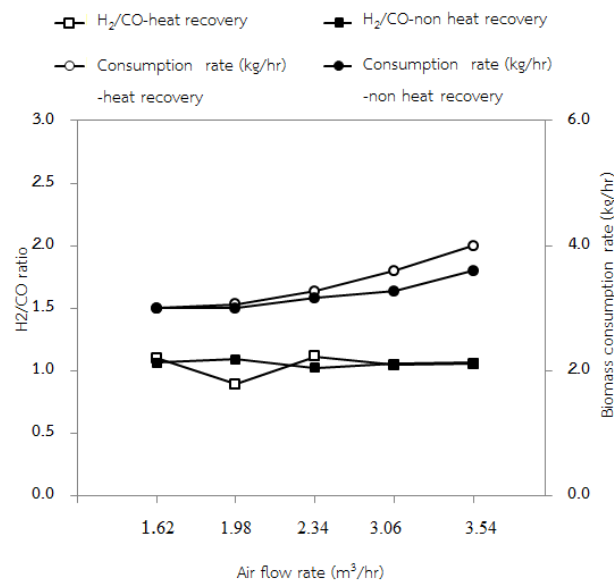


Figure 5.6 Effect of air flow rate on H<sub>2</sub>/CO and biomass consumption rate.

Table 5.2 Effects of air flow rate on biomass consumption and cold gas efficiency.

	Gas flow rate (m <sup>3</sup> /hr)	Biomass consumption rate (kg/hr)	Specific fuel		Cold gas efficiency (%)	LHV (MJ/m <sup>3</sup> )
			Specific gasification rate (kg/hr.m <sup>2</sup> )	gas production rate (m <sup>3</sup> /hr.m <sup>2</sup> )		
Non-Heat Integratio n	1.62	3.00	48.96	23.53	32.90	3.66
	1.98	3.00	48.96	35.55	34.68	3.82
	2.34	3.16	51.53	39.50	48.41	3.43
	3.06	3.27	53.41	42.31	53.59	3.91
	3.54	3.60	58.75	44.13	54.39	3.57
Heat Integratio n	1.62	3.00	48.96	19.05	34.08	3.79
	1.98	3.06	49.93	23.58	38.11	4.23
	2.34	3.27	53.41	30.38	47.28	3.47
	3.06	3.60	58.75	41.55	56.10	3.92
	3.54	4.00	65.27	42.45	53.33	3.49

Table 5.3 The mass input, mass output and the mass balance closures from peanut shell gasification.

Size	Total input			Total out put			Mass balance closure (%)
	Air flow rate (m <sup>3</sup> /hr)	Biomass consumption rate (kg/hr)	Producer gas flow rate (m <sup>3</sup> /hr)	Producer gas flow rate (kg/hr)	solid product (kg/hr)	liquid product (kg/hr)	
Non- Heat Integration	1.62	3.00	4.10	3.69	0.87	0.12	95.90
	1.98	3.00	5.04	4.54	0.59	0.04	97.47
	2.34	3.16	5.83	5.25	0.43	0.10	98.18
	3.06	3.27	6.13	5.52	0.26	0.04	85.10
	3.54	3.60	7.13	6.42	0.26	0.02	86.70

Table 5.3 The mass input, mass output and the mass balance closures from peanut shell gasification (Cont.).

Size	Total input			Total out put			Mass balance closure (%)
	Air flow rate (m <sup>3</sup> /hr)	Biomass consumption rate (kg/hr)	Producer gas flow rate (m <sup>3</sup> /hr)	Producer gas flow rate (kg/hr)	solid product (kg/hr)	liquid product (kg/hr)	
	1.62	3.00	4.10	3.69	0.54	0.08	88.41
	1.98	3.06	5.04	4.54	0.37	0.02	91.75
Heat Integration	2.34	3.27	5.83	5.25	0.36	0.07	94.72
	3.06	3.60	6.13	5.52	0.22	0.05	80.75
	3.54	4.00	7.13	6.42	0.17	0.02	81.30

### 5.1.3 The effect of Ni/char catalyst addition

The quality of product gas from peanut shell gasification was expected to be improved in this presence of char and 5%Ni/char catalysts. In the experiment, 300 g of catalyst was placed in the catalyst module (secondary reactor). The temperature of catalyst module was kept at 500°C by using heating tape. The peanut shell was fed at around 3-4 kg/hr. The inlet air flow rate of 1.62 m<sup>3</sup>/hr. Figure 5.7 showed the gas composition obtained from experiments with char, 5%Ni/char and activated carbon. In general, addition of char and 5%Ni/char catalysts have positive effect on gas composition. The concentration of H<sub>2</sub> and CO was increased with both catalysts. The result indicated that CO<sub>2</sub> reacted with carbon in char by dry reforming reaction over the catalyst resulting in higher CO. The concentration of CH<sub>4</sub> was reduced as pyrolysis product and tar are effectively cracked by catalytic thermochemical reforming. Furthermore tar can be adsorbed on particles of char and react over the active sites of Ni catalyst. Interestingly, the gas composition obtained from char and 5%Ni/char catalyst displayed no significant difference in term of conversions, as shown in Table 5.2.

Comparison of the results from using 5%Ni/char and activated carbon (commercial grade) indicated that the CO concentration was increased while CO<sub>2</sub>

decreased, probably through the promoting of the Boudouard reaction. Whereas  $H_2$  concentration decreased and CO increased, this might be attributed to the gas shift reaction. Moreover, the concentration of  $CH_4$  was reduced more than the cases of using char and 5%Ni/char catalysts, possibly from the fact that activated carbon has much larger surface area to react with the hydrocarbon to produced synthesis gas.

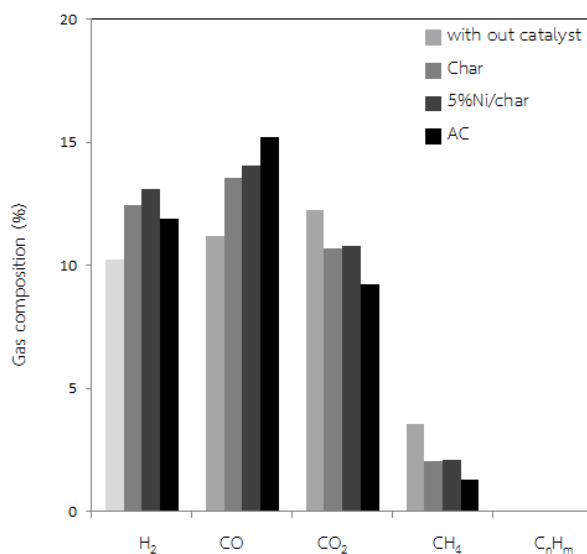
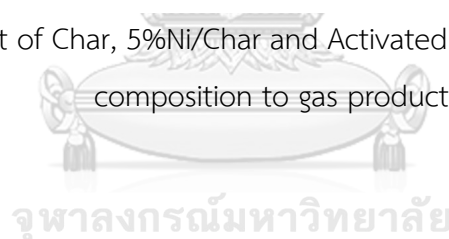


Figure 5.7 Effect of Char, 5%Ni/Char and Activated carbon catalysts on gas composition to gas products.



จุฬาลงกรณ์มหาวิทยาลัย  
CHULALONGKORN UNIVERSITY

#### 5.1.4 The effect of Ni/dolomite catalyst

The experiment was performed with addition of dolomite and Ni/dolomite catalysts using two different metals loadings of 5 and 10%wt, respectively. The catalyst was placed in a separate catalyst module. The peanut shell feed rate was around 3-4 kg/hr at inlet air flow rate of  $1.62 \text{ m}^3/\text{hr}$ . Figure 5.8 displayed effect of dolomite quantity (300 g and 600 g) on the gas yields. The gas composition from gasification using dolomite (300 g) as catalyst was 12.02%CO, 9.74% $CO_2$ , 9.25% $H_2$ , 1.74% $CH_4$ , and 0.05%  $C_nH_m$ . When dolomite loading was increased to 600 g, the gas composition was 12.12%CO, 11.49% $CO_2$ , 10.37% $H_2$ , 1.55% $CH_4$ , and 0.04% $C_nH_m$ . Higher catalyst loading led to greater gas species yields except for  $CH_4$  and  $C_nH_m$ . The result indicated that the surface area of dolomite after calcined improves the volatiles and

hydrocarbon cracking as well as steam reforming reactions. Carbon and hydrogen conversions were 85.36% and 54.90% (300 g) and 91.68% and 58.77% (600 g), respectively, as shown in Table 5.4.

Figure 5.9 showed the gas product concentration with 5%Ni/dolomite and 10%Ni/dolomite catalysts. The average concentration of produced gas was measured to be H<sub>2</sub> 8.76%, CO 11.78%, CO<sub>2</sub> 10.70% and CH<sub>4</sub> 2.19% for a case of 5%Ni/dolomite (300 g). Here, carbon and hydrogen conversions were 98.08% and 59.95%, respectively. It was observed that the conversion to synthesis gas for the case of 5%Ni/dolomite increased with active site of Ni. The concentration of H<sub>2</sub> and CO<sub>2</sub> was slightly increased to 9.11% and 11.08%, respectively, with 600 g of 5%Ni/dolomite. However, carbon and hydrogen conversions were slightly decreased to 97.44% and 57.86%, respectively with 600 g loading 5%Ni/dolomite..

To evaluate the effect of Ni loading on dolomite support, the Ni loading was increased from 5% to 10%wt. (based on 300 g of 5%Ni/dolomite and 10% Ni/dolomite) in the experiments. The comparison of 5%Ni/dolomite with 10%Ni/dolomite catalysts revealed that H<sub>2</sub> concentration of the later was higher. On the contrary, the carbon and hydrogen conversion of 10%Ni/dolomite was less than runs with 5%Ni/dolomite. This probably caused by lower surface area of 10%Ni/dolomite than that of 5%Ni/dolomite. Lower of surface area of 10%wt is maybe due to the Ni block some pores on the dolomite support effect to decreased active site of the catalyst. The conversion performance was as follows: 5%Ni/dolomite > 10%Ni/dolomite > dolomite > w/o catalyst based on 300 g of catalyst. Interestingly, increasing the amount of dolomite and 5%Ni/dolomite from 300 g to 600 g did not show the highest activity even though it contains higher catalyst loading. The experimental results indicated that 5%Ni/dolomite exhibited the suitable reaction condition for synthesis gas production.

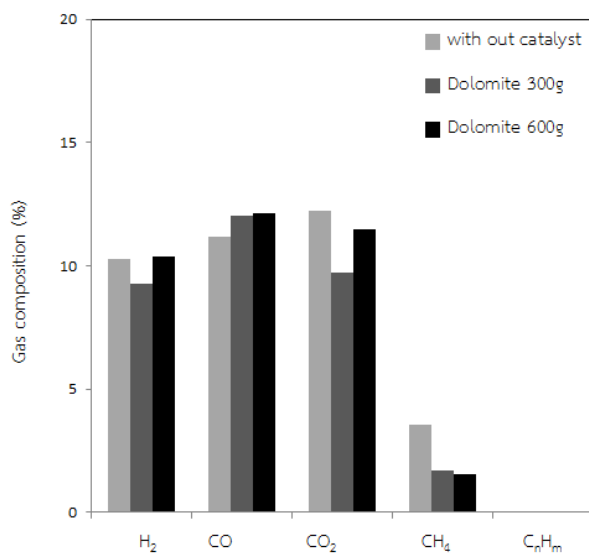


Figure 5.8 Effect of dolomite catalyst on gas composition.

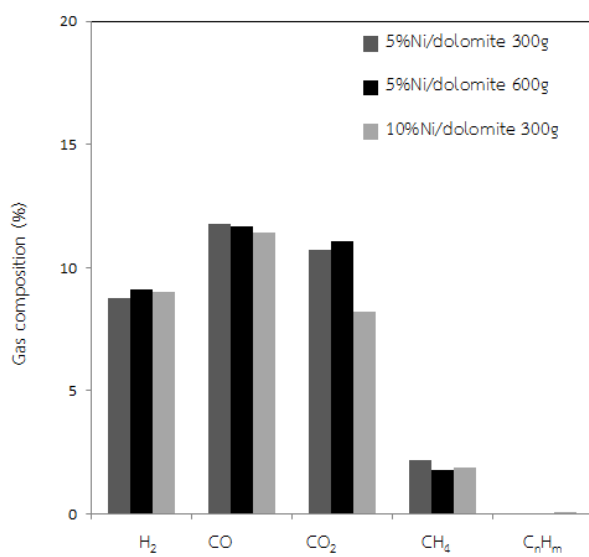


Figure 5.9 Effect of 5%Ni/dolomite and 10%Ni/dolomite catalyst on gas composition.



Table 5.4 Effect of catalyst on carbon and hydrogen conversions.

Catalyst	Carbon conversion			Hydrogen conversion			
	CO	CO <sub>2</sub>	CH <sub>4</sub>	C	H <sub>2</sub>	CH <sub>4</sub>	H
w/o	29.01	31.74	9.22	69.97	31.85	22.04	53.89
Char (300g)	33.55	26.45	5.08	65.08	38.75	12.75	51.50
5%/Ni/Char (300g)	34.80	26.71	5.29	66.80	40.74	13.28	54.02
Activated carbon (300g)	48.26	29.28	4.06	81.61	44.82	9.66	54.48
Dolomite (300g)	43.64	35.37	6.35	85.36	39.85	15.05	54.90
Dolomite (600g)	44.00	41.72	5.95	91.68	44.65	14.12	58.77
5% Ni/dolomite (300g)	46.76	42.47	8.85	98.08	39.72	20.24	59.96
5% Ni/dolomite (600g)	46.25	43.97	7.22	97.44	41.31	16.50	57.81
10% Ni/dolomite (300g)	45.43	32.51	7.45	85.39	40.82	17.03	57.86

## 5.2 Gasification performance of downdraft gasifier with Cassava rhizome

### 5.2.1 The system performance and effect of heat recovery unit.

The cassava rhizome (size 10-15 mm) was fed approximately 3-4 kg/hr in a continuous operation with average air flow inlet of 1.98 m<sup>3</sup>/hr. Figures 5.10 and 5.11 showed the temperature distributions along of the gasifier w/o and with heat thermal integration unit. During system startup, the temperature at each zone increased, and then became stable after 10-20 min. The temperature of drying and pyrolysis was around 100-200°C and 200-400°C, respectively. Temperature in the drying and pyrolysis stages is relatively low because the input energy mainly transmitted by radiative heat transfer between solid and gas phase from oxidation zone (Tinaut et al., 2008). The temperature of the throat section (oxidation zone) was varies around 700 to 800°C and that of reduction zone was stable at around 600°C.

The heat thermal integration unit was used to return hot gas exiting from the reactor to heat recover section (at drying and pyrolysis zone of the reactor). This can improve the heating performance and resulting in set point temperature being reached in short time and facilitated stability of each temperature zone. The result was compared with non-heat thermal integration unit as shown in Figure 5.10. During

system startup, longer time was needed for temperature of drying and pyrolysis zone to reach set points though the final temperature was not stable for the case of non-heat integration unit. The oxidation zone temperature depends upon the heat released due to the biomass combustion and air flow rate. For this reason, the gasifier has thermal inertia, hence temperature will not be raised to a high temperature until the thermal inertia is overpower (P. Lv et al., 2007). The average gas composition was about 12.83%CO, 11.88%CO<sub>2</sub>, 12.63%H<sub>2</sub>, 2.13%CH<sub>4</sub>. The conversion data for cases of both non-heat and heat thermal integration units are given in Figure 5.12. For non-heat thermal integration unit, carbon conversion to CO, CO<sub>2</sub> and CH<sub>4</sub> were, 25.37%, 50.92%, and 8.64%, respectively and hydrogen conversion to H<sub>2</sub>, CH<sub>4</sub> were 43.01% and 22.78%, respectively with lower heating value of 3.37 MJ/m<sup>3</sup>. For heat thermal integration unit, carbon conversion to CO, CO<sub>2</sub> and CH<sub>4</sub>, were increased to 26.85%, 39.21%, and 8.23%, respectively and hydrogen conversion to H<sub>2</sub>, CH<sub>4</sub> were greater at 42.00% and 21.79%, respectively with lower heating value of 3.06 MJ/m<sup>3</sup> (Table 5.3).

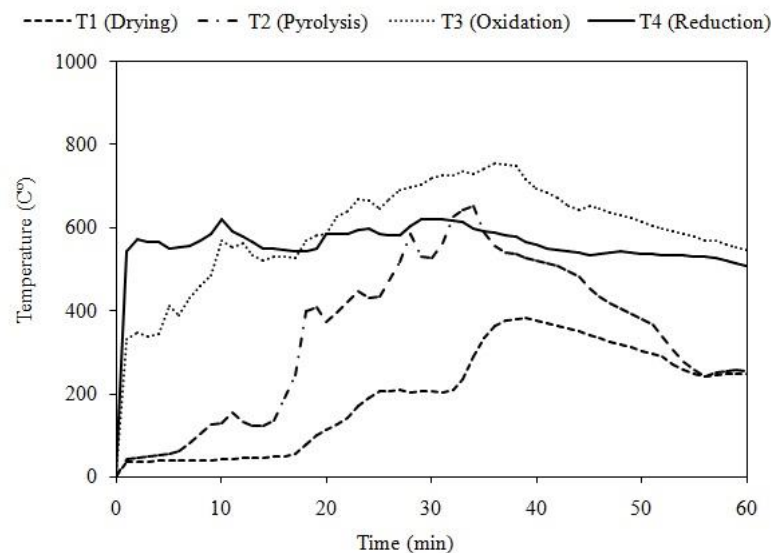


Figure 5.10 Temperature distribution within gasifier w/o thermal integration unit.

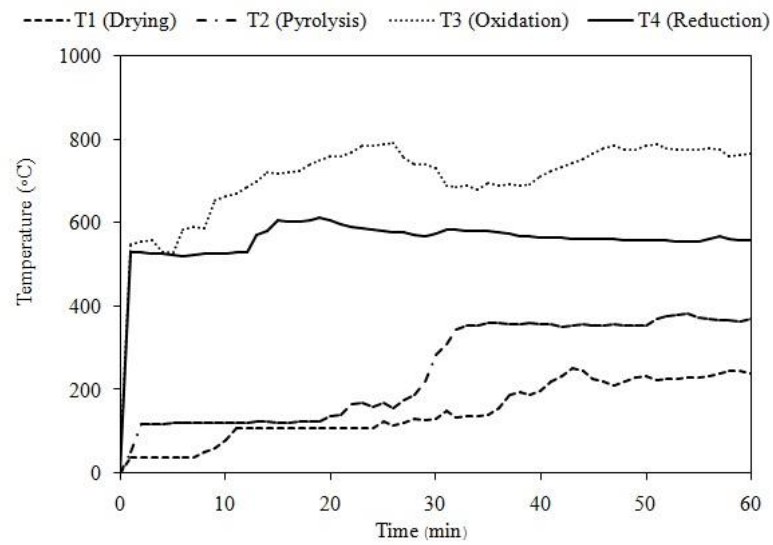


Figure 5.11 Temperature distribution within gasifier with heat thermal integration unit.

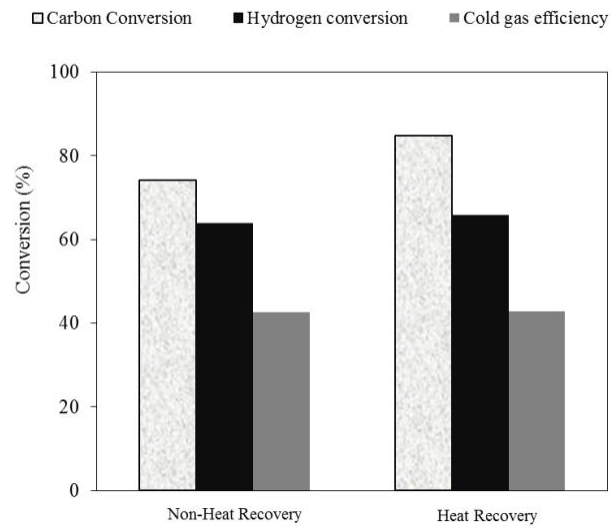


Figure 5.12 Effect of heat recovery addition on conversion and cold gas efficiency.

Table 5.5 Effects of heat thermal integration unit with 1.98 m<sup>3</sup>/hr

	Carbon Conversion (%)			Hydrogen Conversion (%)		LHV (MJ/m <sup>3</sup> )	Cold gas Efficiency (%)
	CO	CO <sub>2</sub>	CH <sub>4</sub>	H <sub>2</sub>	CH <sub>4</sub>		
	Heat recovery	26.85	39.21	8.23	42.00		
Non-Heat recovery	25.37	50.92	8.64	43.01	22.78	3.37	42.81

### 5.2.2 The effect of air flow rate

In this experiment, the rate of inlet air flow can be directly controlled but not the case for the equivalence ratio since the biomass consumption rates depend on the reaction rate in the reactor. The inlet air flow rate varies from 1.98 to 3.54 m<sup>3</sup>/hr and superficial gas velocity was 32.31 to 49.93 m/hr., which comparable to equivalence ratio (ER) of 0.13 to 0.29. Figure 5.13 showed the effect of air flow rate on carbon and hydrogen conversions. At low air flow rate, the concentration of CO<sub>2</sub>, tar and char was greater than that of higher flow rate. This is maybe due to lower temperature at combustion zone which led to lesser cracking and reforming reactions of products from the pyrolysis zone. When improved inlet air flow rate from 1.98 to 2.50 m<sup>3</sup>/hr, the hydrogen conversion to H<sub>2</sub> and carbon conversion to CO increased whereas the carbon conversion to CO<sub>2</sub> decreased. Furthermore, more heat to the gasification process also enhanced tar destruction and hence, better product gas quality. Increasing the air flow rate resulted in higher temperature at oxidation zone which led to higher rate of reaction at drying, pyrolysis and reduction zones. Moreover it could be due to the carbon in char reaction with CO<sub>2</sub> and steam which resulted in higher CO/CO<sub>2</sub> ratios. The CO/CO<sub>2</sub> ratio thermodynamically favored increased with temperature (Franco et al., 2003). When increased air flow rate up to 3.06 m<sup>3</sup>/hr, the conversion was slightly decreased since more N<sub>2</sub> was supplied into the oxidation zone. This also resulted in diluted gases product and deteriorated energy content in gas. The optimum air flow rate to fuel ratio was achieved for 2.50

$\text{m}^3/\text{hr}$  at 3.84 kg/hr of cassava rhizome (5-10 mm). It is recommended that the gasifier should be operated within these ranges to produce high quality produced gas. At this condition, the carbon conversions to  $\text{CO}_2$ ,  $\text{CO}$  and  $\text{CH}_4$  were 36.72%, 46.22% and 9.44%, respectively and hydrogen conversions to  $\text{H}_2$  and  $\text{CH}_4$  were 41.10% and 24.81%, respectively. Furthermore, the lower heating value of  $4.46 \text{ MJ}/\text{m}^3$  and the cold gas efficiency of 54.86% were obtained as illustration in Table 5.6. The air flow rate significantly effects to the gasifier performance as it regulates the biomass consumption rate (Table 5.6). As the air flow rate increased, the oxidation reaction increased by more oxygen availability and the heat transfer from the oxidation reaction promoted the endothermic gasification reactions (Pérez et al., 2012). The oxidation temperature depends on the heat released via the biomass combustion and air flow rate which provides more oxygen to oxidize material in the gasifier (Sheth et al., 2009). When the air flow rate increased, the biomass consumption rate increased resulting in greater specific gasification rate which also accounted for the increase in gasification efficiency (Hernández et al., 2010). Singh et al. (2006) examined cashew nut shell gasification using down draft gasifier, their results suggested that the producer gas lower heating value and gas yields of its combustible constituents and gasification efficiency increased at air flow rate. The results agree with Dogru et al. (2002) Zainal et al. (2002) and Pratik and Babu (2009) Martinez et al. (2012).

The experimental results could then be compared with other studies on gasification of the cassava rhizome. Sornkade et al. (Sornkade et al., 2013) explored the conversion of cassava rhizome using an updraft fixed bed gasifier at  $800^\circ\text{C}$ , ER of 0.2-0.4 without catalyst. They found that the cold gas efficiencies were 38.43-53.97%. Ngamchompoo and Triratanasirichai. (2013) described the quality improvement of producer gas from cassava rhizome gasification with downdraft gasifier. They claimed the maximum cold gas efficiency of 65%, which was slightly lower than the cold gas efficiency of typical air-steam gasification (69%).

### 5.2.3 The effect of biomass particle size

In this experiment, the effect of cassava rhizome particle size  $\leq 5$ , 5-10, and 10-15 mm while air flow rate varied from 1.98 to 3.06 m<sup>3</sup>/hr was studied with increase inlet air flow rate from 1.98 to 2.34 m<sup>3</sup>/hr. The biomass consumption rate is directly relational to the air flow rate and superficial gas velocity while it was conversely proportional to the particle size of biomass (Table 5.6). From results obtained, the conversion to H<sub>2</sub> and CO increase with particle size, while the conversion to CH<sub>4</sub> and CO<sub>2</sub> decrease. The hydrogen conversion to H<sub>2</sub> and carbon conversion to CO increased for all particle sizes while carbon conversion to CO<sub>2</sub> and CH<sub>4</sub> and hydrogen conversion to CH<sub>4</sub> slightly declined via dry reforming reaction. As gas species pass over the hot char and charcoal in the reduction zone, the exothermic water shift reaction can also take place and produce H<sub>2</sub> and CO at this zone. Additionally carbon in char was reformed with CO<sub>2</sub> to produce CO through Boudouard reaction. At the air flow rate of 2.50 m<sup>3</sup>/hr, the highest conversions for both carbon and hydrogen were 92.39% and 65.92%, respectively, using particle size of 5-10 mm as shown in Figure 5.14. The carbon and hydrogen conversions were then slightly decreased to 86.85% and 61.07%, respectively, with particle size of 10-15 mm as shown in Figure 5.15. The conversion to CO, H<sub>2</sub> and CH<sub>4</sub> increased by increasing the particle size of biomass and air flow rate, which can be described by the high temperature favored high conversion rate.

The smaller cassava rhizome particles tend to block the air void age, leading to high pressure drop in side the reactor and the exothermic reaction at burning zone (McKendry, 2002a). Larger particle of cassava rhizome would take longer time to burn and react; therefore the reforming and cracking reactions of volatile products were improved. Moreover, the moisture content in biomass would encourage water gas and shift reactions, thus leading to the upgrading of the producer gas quality. However the conversion of largest particles (10-15 mm) was slightly decreased which could be explained by mass and heat transfer resistance of the surface area. Lv et al. (2004) state that the larger particles of biomass contains greater heat transfer resistance, the actual temperature inside biomass is lower, which leads to devolatilization process. Similar to Hernandez et al. (2010) who say that the small

particles are exposed to greater heat transfer as the external of surface area to mass ratio is higher. These results suggested that the optimum cassava rhizome particle size for this modular gasification system burning cassava rhizome is 5-10 mm. The mass balances closures from cassava rhizome gasification with varied air flow rate and particle size are presented in Table 5.7. The results indicate that the mass balances closures are within 70–96%.

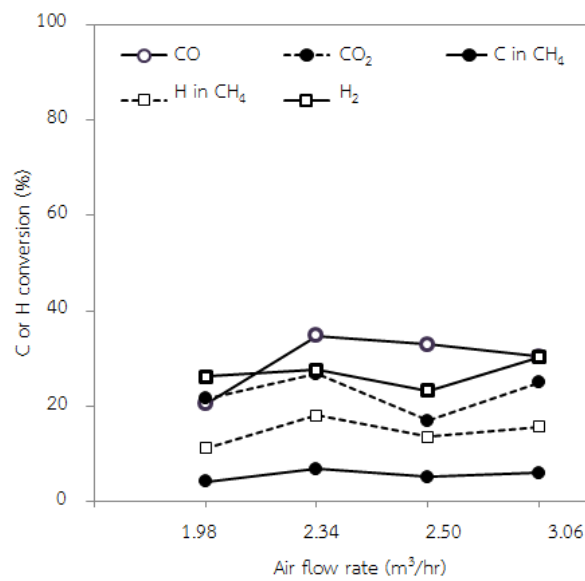


Figure 5.13 Effect of air flow rate on conversion of cassava rhizome ( $\leq 5$  mm).

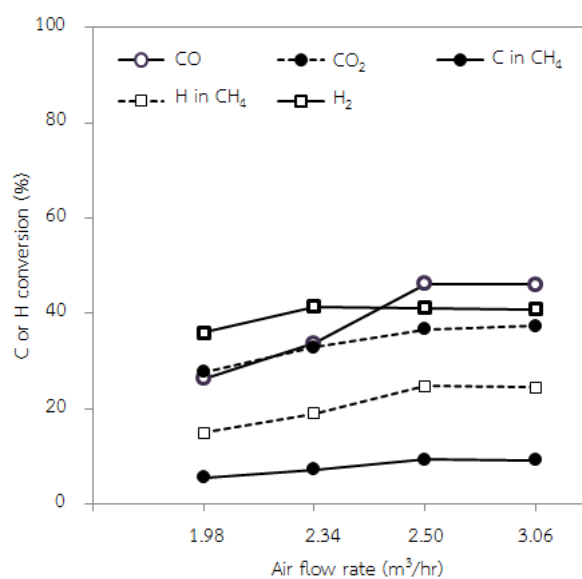


Figure 5.14 Effect of air flow rate on conversion of cassava rhizome (5-10 mm).

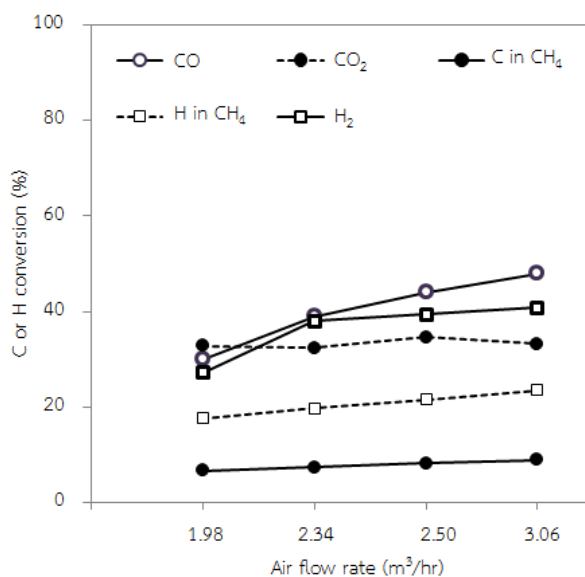


Figure 5.15 Effect of air flow rate on conversion of cassava rhizome (10-15 mm).

Table 5.6 Effects of air flow rate on biomass consumption and cold gas efficiency.

Size (mm)	Gas flow rate (m³/hr)	Biomass		Specific fuel gas production rate (m³/hr·m²)	Cold gas efficiency (%)	LHV (MJ/m³)
		consumption rate (kg/hr)	Specific gasification rate (kg/hr·m²)			
≤5	1.98	4.54	75.61	21.67	27.05	4.55
	2.34	4.43	73.81	29.66	39.36	4.51
	2.50	6.20	103.33	37.24	34.45	4.52
	3.06	6.00	100.00	38.39	36.81	4.03
5-10	1.98	3.50	58.33	22.38	36.20	4.66
	2.34	3.60	60.00	28.10	44.68	4.16
	2.50	3.84	64.00	36.03	54.86	4.46
	3.06	4.50	75.00	43.76	56.54	4.64
10-15	1.98	2.84	47.27	17.36	36.43	3.80
	2.34	3.71	61.90	27.80	51.15	4.19
	2.50	3.86	64.29	34.20	55.02	4.23
	3.06	4.43	73.75	42.02	43.01	4.39



Table 5.7 The mass input, mass output and the mass balance closures from cassava rhizome gasification.

Size (mm)	Air flow rate (m <sup>3</sup> /hr)	Total input			Total out put			Mass balance closure (%)
		Biomass consumption rate (kg/hr)	Producer gas flow rate (m <sup>3</sup> /h)	Producer gas flow rate (kg/h)	Char produced (kg/h)	liquid (kg/hr)		
≤5	1.98	4.54	4.10	3.69	0.73	0.10	70.52	
	2.34	4.43	5.83	5.25	1.02	0.07	88.61	
	2.50	6.20	6.13	5.52	1.24	0.13	70.49	
	3.06	6.00	7.13	6.42	0.93	0.10	73.64	
5-10	1.98	3.50	4.10	3.69	0.50	0.12	80.13	
	2.34	3.60	5.83	5.25	0.78	0.10	96.85	
	2.50	3.84	6.13	5.52	0.85	0.05	86.70	
	3.06	4.50	7.13	6.42	0.60	0.09	82.39	
10-15	1.98	2.84	4.10	3.69	0.40	0.05	87.81	
	2.34	3.71	5.83	5.25	0.51	0.04	90.18	
	2.50	3.86	6.13	5.52	0.49	0.10	82.23	
	3.06	4.43	7.13	6.42	0.49	0.09	81.81	

#### 5.2.4 The effect of Ni/char catalyst

To study the effect of Ni/char catalyst, cassava rhizome particle (10 mm) was fed in a continuous operation during gasification with secondary catalytic reactor attached. In these runs, 300 g of 5%Ni/char catalyst was placed on the catalyst reactor. The selected inlet air flow rate was 1.98 m<sup>3</sup>/hr, because this condition presented high tar and hydrocarbon gas in product. Figure 5.16 showed the gas composition with and without catalyst. It can be observed that CO and H<sub>2</sub> productions were improved whereas the CO<sub>2</sub> production reduced when used with 5%Ni/char catalyst. The result suggested that CO<sub>2</sub> reacted with carbon in char via dry

reforming reaction over 5%Ni/char catalyst resulting in the enhance of CO. The CH<sub>4</sub> production decreased because tar is cracked and reacted to smaller gas molecules. Also tar can be adsorbed on char particles and react over the active sites of Ni catalyst. The carbon and hydrogen conversions increased to 65.22% and 55.69%, respectively when the catalyst was used (Figure 5.17). Abu El-Rub et al. (2008) discovered that the adsorbed of tars and carbon in cokes formed can be catalytically converted to CO and H<sub>2</sub> by steam and dry reforming reactions. Additionally the carbon in char can easily reacts with oxygen and be oxidized into CO (Shen et al., 2014b). Comparing with the activated carbon, the carbon conversions to CO<sub>2</sub>, CO and CH<sub>4</sub> were 30.97%, 40.31%, and 5.75%, respectively and hydrogen to H<sub>2</sub> and CH<sub>4</sub> were 40.21% and 15.08%, respectively. From these results, the carbon conversion was increased as a result of the active site of activated carbon.

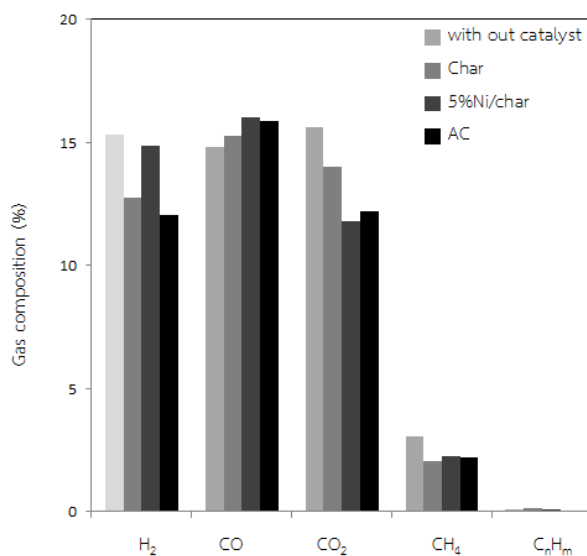


Figure 5.16 Effect of 5%Ni/char catalyst on gas composition from cassava rhizome gasification.

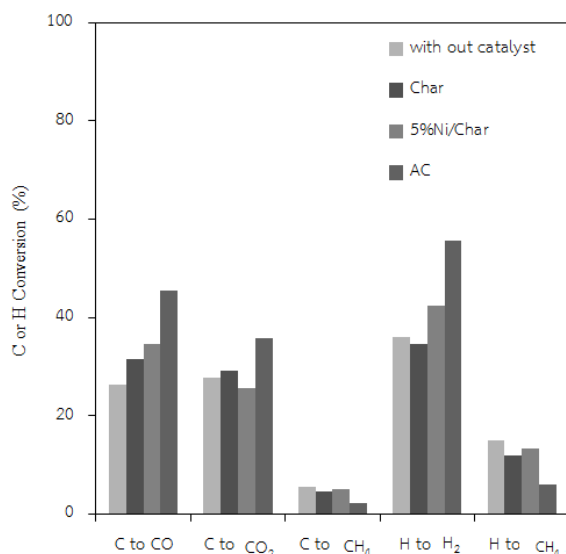


Figure 5.17 Effect of 5%Ni/char catalyst on C and H conversions from cassava rhizome gasification.

#### 5.2.5 The effect of Ni/dolomite catalyst

Figure 5.18 showed the gas compositions obtained by gasification with dolomite support and 5%Ni/dolomite addition. The gas composition from cassava rhizome gasification using dolomite 300 g was 14.19%CO, 11.21%CO<sub>2</sub>, 14.02%H<sub>2</sub>, 2.12%CH<sub>4</sub>, and 0.11%C<sub>n</sub>H<sub>m</sub> and when increased dolomite to 600g, the gas composition was 14.07%CO, 13.96%CO<sub>2</sub>, 10.92%H<sub>2</sub>, 2.14%CH<sub>4</sub>, and 0.04%C<sub>n</sub>H<sub>m</sub>. The concentration of CO<sub>2</sub> increased, probably due to its released from CaO and MgO phases in dolomite. The carbon conversion increased from 76.33% to 83.79% with increased loading of dolomite from 300 to 600g. The dolomite support not only promoted the catalytic reaction but also protected sintering of catalyst. Moreover, it can help relief pressure drop in reactor and eliminate the loss of the catalyst as fly ash. This result was similar to Waheed et al. (2016) who studied the effect of Ni/dolomite on rice husks by dry reforming reaction. They found that dry reforming reactions with 10% Ni/dolomite can increase H<sub>2</sub>/CO<sub>2</sub> ratio. In addition, the porous property of dolomite support might help cracking and reforming of tar (Gao et al., 2012).

In the presence of 5%Ni/dolomite catalyst, the influence of 300 g and 600 g of 5%Ni/dolomite loading was investigated. In Figures 5.18-5.19, it might be noticed that the concentration of CO and H<sub>2</sub> were greater whereas the CH<sub>4</sub> reduced with higher catalyst loading. The H<sub>2</sub>/CH<sub>4</sub> and CO/CO<sub>2</sub> ratio were increased with 5%Ni/dolomite catalyst, demonstrating the effectiveness of steam reforming of CH<sub>4</sub> and char reaction with CO<sub>2</sub> via Boudouard reaction. The carbon and hydrogen conversions also enhanced with increased catalyst loading to 600 g. For 600 g of 5%Ni/dolomite loading, the result showed that the highest conversions were 55.70% and 6.07% for hydrogen conversion to H<sub>2</sub>, CH<sub>4</sub> and carbon conversion to CO<sub>2</sub>, CO and CH<sub>4</sub>, were 35.90%, 45.57% and 2.32% respectively.

The product with 5%Ni/dolomite catalyst improved the cracking of tar to form higher gas generation. The hydrogen yields through the use of catalyst were significantly increased when compared with dolomite support. The H<sub>2</sub> yield with 5%Ni/dolomite catalyst was improved to 23.95 g H<sub>2</sub>/kg biomass. The catalyst reaction was driven for tar reforming, when the product gas passed over the catalyst, then the tar and condensable hydrocarbons could be reformed on the active site of catalyst surface with steam and carbon dioxide, hence producing hydrogen and carbon monoxide. Li et al. (2008) argued that the Ni catalyst might extend gas residence times in the reactor which would promote water-gas reaction and cracking of tar and hydrocarbon after the vapor passed through the layer of catalyst. Miao et al. (2010) also explained the reaction on catalyst surface in which the gas product and hydrocarbon vapor diffused on the external surface and internal pore of catalyst and then the cracking process ensued at those sites.

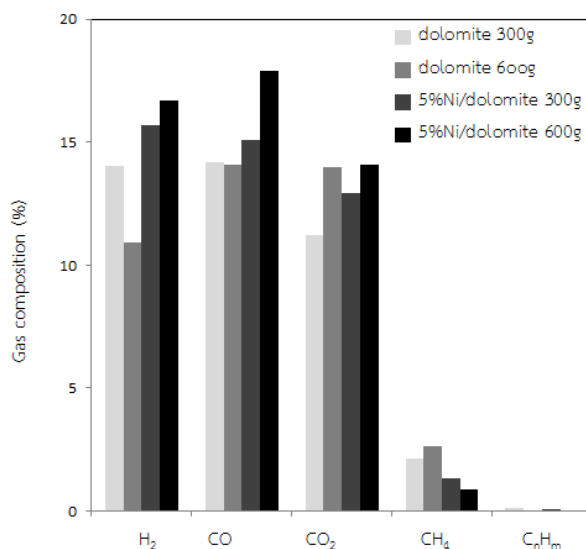


Figure 5.18 Effect of 5%Ni/dolomite catalyst on gas composition from cassava rhizome gasification.

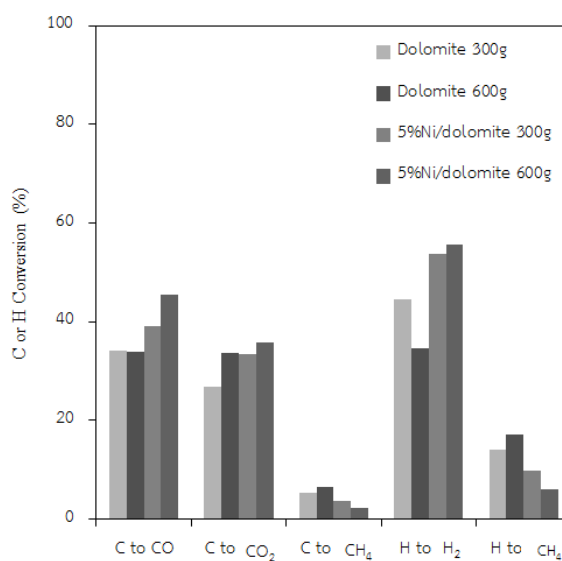


Figure 5.19 Effect of 5%Ni/dolomite catalyst on C and H conversions from cassava rhizome gasification.

### 5.3 Characteristic of char and tar from gasification

The ultimate analyses of char produced from the peanut shell and cassava rhizome gasification after each test are presented in appendix which would be used to determine elemental contents in the char residue. The carbon content at low air

flow rate inlet was more than that at high air flow rate. The decomposition of char increased with air flow rate because more char can be converted to gas through thermal cracking, Boudouard, and other oxidation reactions.

Tar condensate formation during each experimental was also measured. However, any tars downstream of the charcoal filter and pipe lines were not determined. Generally, the tar production was relatively small and reliably collection was challenging. The collected tars were in the range of 0.3-4% as shown in Table 5.3 and Table 5.7. Normally some tars by products are present in the produced gas from gasification process. The main components of tars are heavy hydrocarbon compounds, containing aromatic compounds and other oxygen-containing hydrocarbons (Olgun et al., 2011). The functional groups present in the tar from pipe line are shown in appendix. The compounds present in the tar were identified by comparing the mass spectra chromatogram obtained with that of standard chromatogram. It was found that tars comprise around 40 compounds with carbon chain of C<sub>6</sub>-C<sub>20</sub>. The most prominent peaks are 1-heptadecene, 1-nonadecene, phenol, and anthracene which can be utilized as chemical feedstock or further steam reforming with catalyst to produce synthesis gas.

#### 5.4 Power gas generation

Figures 5.20 and 5.21 showed the gas composition from peanut shell and cassava rhizome gasification. The gas composition from peanut shell gasification, the gas composition was 14.55%CO, 8.48%CO<sub>2</sub>, 7.45%H<sub>2</sub>, 3.05%CH<sub>4</sub>, and 0.12%C<sub>n</sub>H<sub>m</sub> with air flow rate of 2.34 m<sup>3</sup>/hr. The lower heating value of producer gas was 3.79 MJ/m<sup>3</sup> and the carbon and hydrogen conversions were 79.56% and 52.18%, respectively. In case of cassava rhizome (5-10 mm) was 15.37%CO, 10.12%CO<sub>2</sub>, 10.92%H<sub>2</sub>, 2.80%CH<sub>4</sub>, and 0.18%C<sub>n</sub>H<sub>m</sub> with air flow rate of 2.50 m<sup>3</sup>/hr. The lower heating value of producer gas was 4.19 MJ/m<sup>3</sup> and the carbon and hydrogen conversions were 85.31% and 66.85%, respectively. Generally, the minimum lower heating value required in the gas engine application should be around 3.5-4.0 MJ/m<sup>3</sup> (Basu, 2010d). From the

experimental results, power generation may proceed when supplying 3-4 kg/hr of peanut shell or cassava rhizome.

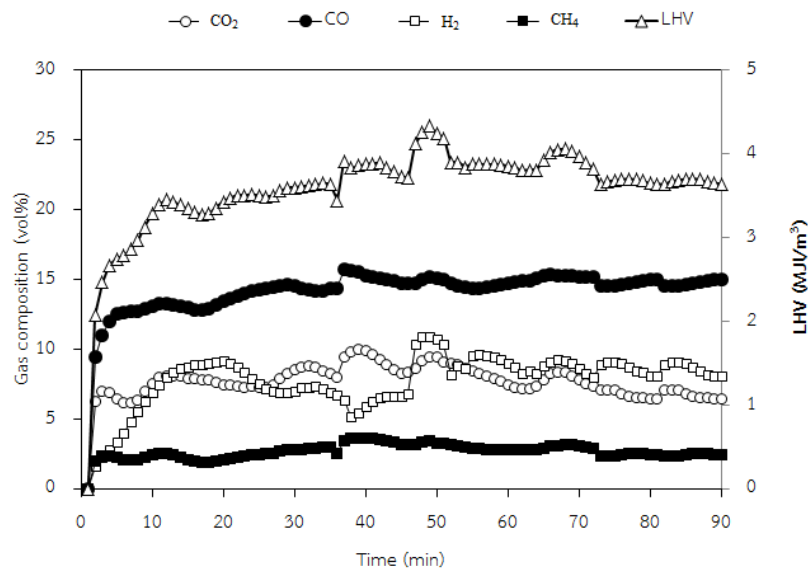


Figure 5.20 Composition of gas produced from peanut shell gasification.

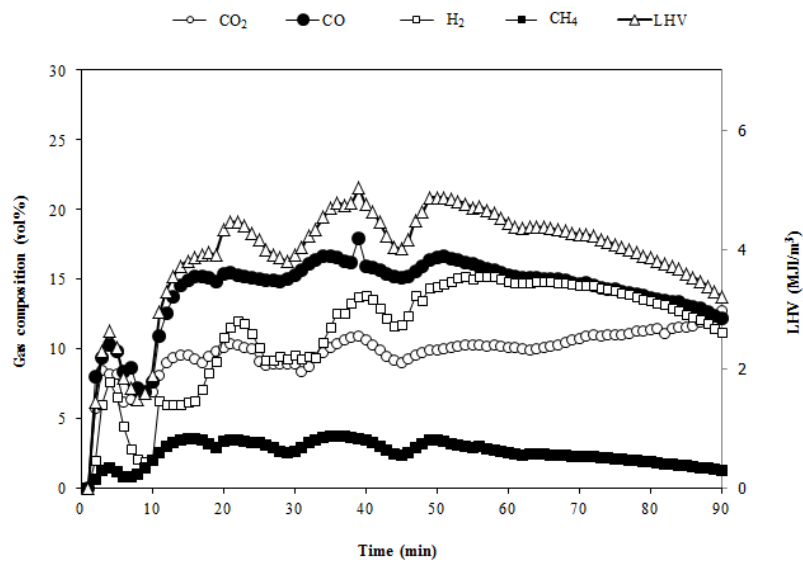


Figure 5.21 Composition of gas produced from cassava rhizome gasification.

Power generation using producer gas from peanut shell and cassava rhizome gasification was carried out in a reciprocating internal combustion engine originally designed for Liquefied Petroleum Gas (LPG) fuel. The specification of gas engine and

generator are shown in Table 3.2. Compared to LPG fuel when the efficiency is about 16.88%, if producer gas is used, the efficiency then decreased to 11.03% and 11.29% for cases of peanut shell and cassava rhizome gasification, respectively (at maximum load, Figures 5.22-5.24). The cold gas efficiency of the gasification system was 53.66% and 54.92% for peanut shell and cassava rhizome feedstock, respectively. During the experiment, the generated electricity output was approximately 0.32-0.48 kW at 220-110V. Generally, the gasification provided producer gas with enough flow to the gas engine. The producer gas consumption of engine was around 1.8-2.4 m<sup>3</sup>/hr, whereas the producer gas flow from gasifier was close to 5.83 m<sup>3</sup>/hr. The specific consumption was mainly influenced by the energetic potential of fuel as a function of required power. The specific fuel consumption of biomass (SFC) at high load with peanut shell was 3.98 kg/kWh and 3.25 kg/kWh with cassava rhizome. The efficiency for the overall system would be the sum of the gas efficiency of gasifier and the efficiency of the power generation. Here, the overall efficiency of system from peanut shell and cassava rhizome was 11.84% and 12.12%, respectively.

However, the global efficiency dropped on the conversion of the producer gas into electricity, mainly due to low thermal efficiency of reciprocating internal combustion engines and calorific value of gas. The result was similar to Boloy et al. (2011) who performed downdraft gasification couple to engine generator and reported that at the maximum load, the thermal and electricity generation efficiency was 13.5% and 12.8%, respectively. Marculescu et al. (2016) found that the global efficiency of engine generator was 24.24% with natural gas and the efficiency then decreased to 18.2% with synthesis gas. Li Chaves et al. (2016) studied the small scale electricity generation by gasification of wood residue to engine generator, the overall efficiency of the engine generator system was lower (4.5-17%). The thermal efficiency of ICE and quality of producer gas strongly dictate the overall energy generation efficiency.



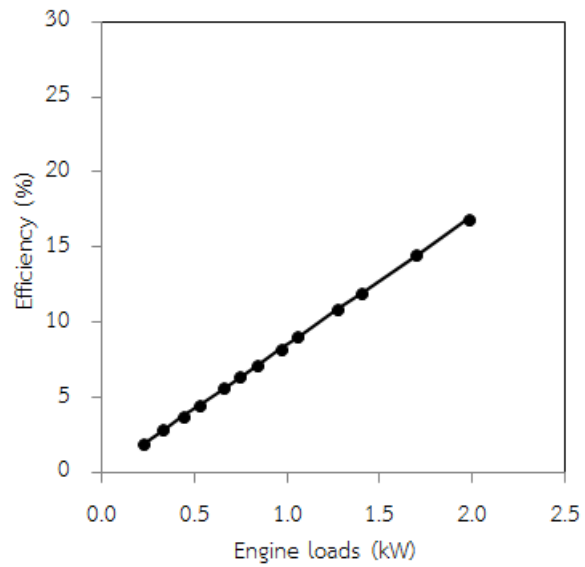


Figure 5.22 The efficiency of the engine generator using LPG fuel.

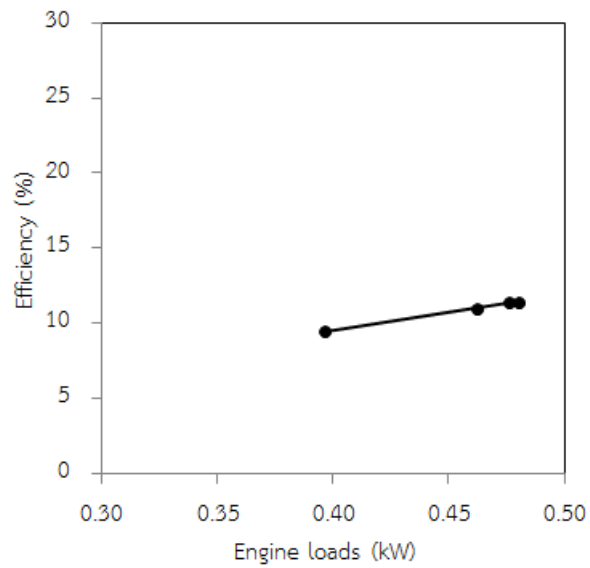


Figure 5.23 The efficiency of the engine generator using producer gas from cassava rhizome gasification.

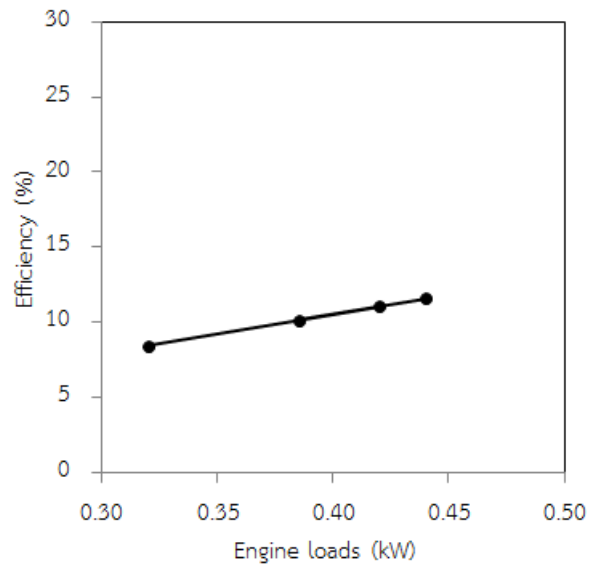


Figure 5.24 The efficiency of the engine generator using producer gas from peanut shell gasification.

## 5.5 ASPEN MODEL

### 5.5.1 Simulation Assumptions

The Aspen plus simulation flowchart of biomass gasification is shown in Figure 5.25. The following assumptions were considered in modeling the biomass gasification process.

- The gasification processes are isothermal and in steady state.
- The chemical reactions take place at an equilibrium state.
- The production gas is a mixture of CO, CO<sub>2</sub>, CH<sub>4</sub>, H<sub>2</sub>, N<sub>2</sub>, and H<sub>2</sub>O and follows the idea gas law.
- The sulfur content in the biomass and the formation of air pollutions are negligible.
- Tars are assumed to be negligible in the producer gas.
- Char contains only carbon and ash is inert.

### 5.5.2 Gasification model description

The overall gasification process consists of a number of steps: drying, decomposition, combustion and gasification. Feed is specified as a non-conventional component in Aspen Plus and defined in the simulation model by using the ultimate and proximate analysis. This simulation is developed under the assumption that the residence time is long enough to allow the chemical reactions to reach an equilibrium state. Peng-Robinson method is recommended for gas-processing, refinery and petrochemical applications. In this study, biomass was defined as non-conventional components from the perspectives of ultimate and proximate analysis (Table 5.8-5.9). Ashes were also defined as a non-conventional component. A number of Aspen Plus reactors were used to develop the model. The main processes were simulated by four reactors in Aspen plus: RStoic, RYield, RGibbs and Requilibrium (Table 5.8). The block DRYREACT was used to drying process by Rstoic reactor (FORTRAN code). Then the devolatilization process was decomposed in the block DECOMP by RYield reactor. The biomass was transformed from non-conventional component (from ultimate analysis) to conventional (elements C, H, N, O, S etc.) by FORTRAN code. Then the combustion and gasification process was performed in the block BURN and REQU, which in chemical equilibrium based on Gibbs free energy and phase equilibrium stoichiometric. The product gas was cooled and separated in COOLER and SEPARATE block. To validate the simulation result, experimental data from gasification of peanut shell waste and cassava rhizome with downdraft gasifier were used.

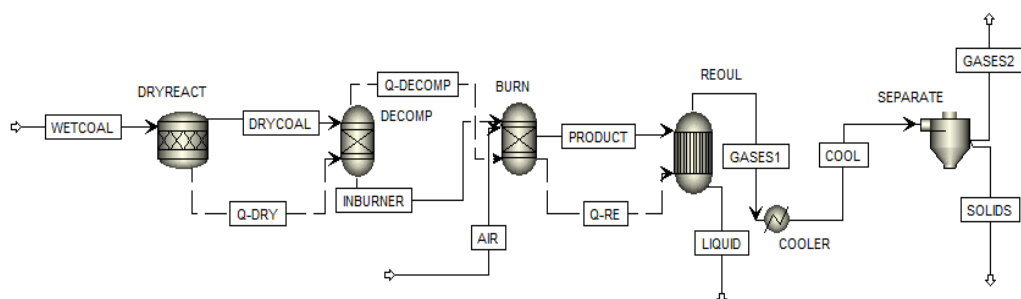


Figure 5.25 Flow chart of biomass gasification simulation using Aspen Plus.

Table 5.8 The simulation of operation condition gasification parameter.

Items	Parameter	
Method	Peng-Robinson	
Stream	MCINCPD	
Nonconventional properties	Enthalpy	HCOALGEN
	Density	DCOALIGT
Ambient condition	30°C and 1 atm	
Gasifier	700-900°C	
Air input	1.62-3.50m <sup>3</sup> /hr	
Biomass	peanut shell and cassava rhizome	

Table 5.9 Description of the unit operation of the blocks in the simulation.

Block	Model	Description	Purpose
DRYREAC	RStoic	Reduction of biomass moisture content (FORTRAN)	Drying of biomass
DECOMP	RYield	Conversion of non-conventional feed to conventional components (FORTRAN)	Decomposition of biomass according to its proximate and ultimate analyses
BURN	RGibbs	Chemical equilibrium based on Gibbs free energy	Combustion of biomass
REQUL	REquil	Chemical and phase equilibrium based on stoichiometric calculation	Gasification of biomass
COOLER	Heater	Cooling of product gas	
SSPLIT	SSplit	Separation of solid from product gas	

In the simulation study, the effect of biomass and air flow rate on gas composition has been investigated. The producer gas composition results obtained

from experimental data and predicted gas composition with peanut shell at 3.05 m<sup>3</sup>/hr air flow rate are shown in Figure 5.26. The predicted results of peanut shell were close to results from experiment data with the exception of CH<sub>4</sub>. The predicted results of H<sub>2</sub>, CO and CO<sub>2</sub> in the producer gas are in good agreement with the experiment data. The results from experiments and simulations for gas composition with varied air flow rate input are shown in Table 5.10. This result displays similar trend with 3.05 m<sup>3</sup>/hr air flow rate. The model under over-predicted CH<sub>4</sub> to the experiment data which may be due to the chemical equilibrium in the model promoted methanation reactions. This result is similar to Nikoo and Mahinpey (2008) who say that the result of CH<sub>4</sub> from simulation likely to overestimate. However, most results from simulation maintain acceptable degree of deviation in most cases. Kuo et al. (2014) reported that the measured CH<sub>4</sub> cannot be explained based on purely thermodynamic equilibrium.

From the simulation results with cassava rhizome it was found that the gas compositions of cassava rhizome particle size 5-10 mm were close to the experimental result with the exception of cassava rhizome particle size 1-5 and 10-15 mm as shown in Figure 5.27-5.29 and Table 5.11-5.13. This may be due to the effect of particle size distribution and mass transfer resistance in the model. In this result, the gas composition from cassava rhizome particle size 5-10 mm at 2.50 m<sup>3</sup>/hr showed reasonable agreement with the experimental data for all components with the exception of CH<sub>4</sub>. The H<sub>2</sub> from experimental data are lower than predicted results because in reality all chemical equilibrium reactions cannot be reached within turnover time inside the reactor. The predicted gas composition from simulation model of peanut shell waste is closer to experimental result than that of cassava rhizome. The developed model is able to simulate the performance of the gasifier and predicted results are in good agreement to the experimental results.

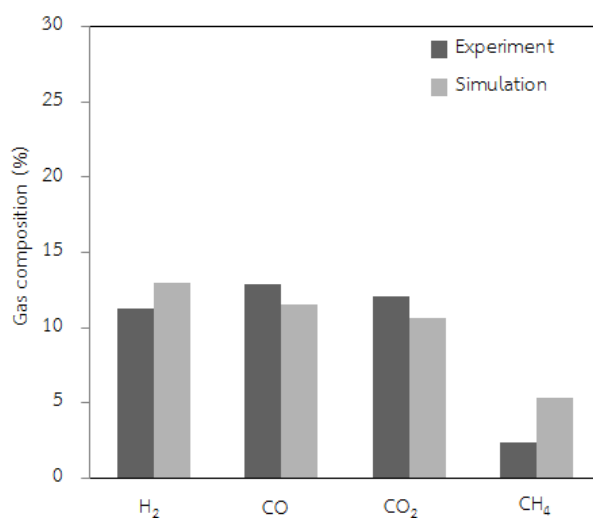


Figure 5.26 Comparison of gas composition from peanut shell gasification: experimental & simulation.

Table 5.10 The gas composition from peanut shell gasification: experimental & simulation.

Air flow rate (m <sup>3</sup> /hr)	Gas composition (%)				Solid (kg/hr)
	Experimental				
	H <sub>2</sub>	CO	CO <sub>2</sub>	CH <sub>4</sub>	
1.62	10.26	11.17	12.22	3.55	0.54
1.98	11.98	15.92	15.42	2.60	0.13
2.34	10.76	11.34	12.42	2.45	0.33
3.06	11.32	12.92	12.07	2.40	0.18
3.54	10.56	11.95	11.90	2.36	0.13
	Simulation				
1.62	13.02	13.72	13.70	9.33	0.16
1.98	12.44	11.26	12.26	8.11	0.16
2.34	11.54	10.86	11.88	8.15	0.17
3.06	13.00	11.55	10.37	5.53	0.19
3.54	13.22	11.45	10.58	5.48	0.22

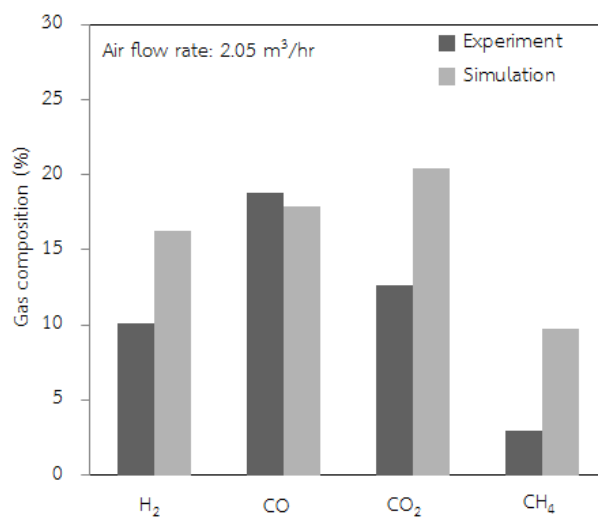


Figure 5.27 Comparison of gas composition from cassava rhizome (1-5 mm) gasification: experimental & simulation.

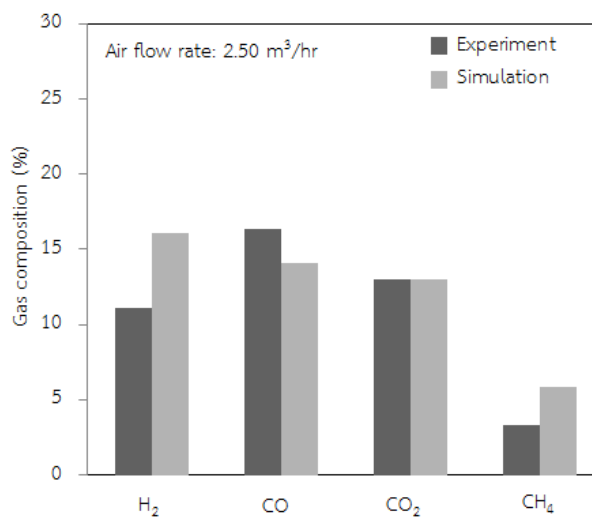


Figure 5.28 Comparison of gas composition from cassava rhizome (5-10 mm) gasification: experimental & simulation.

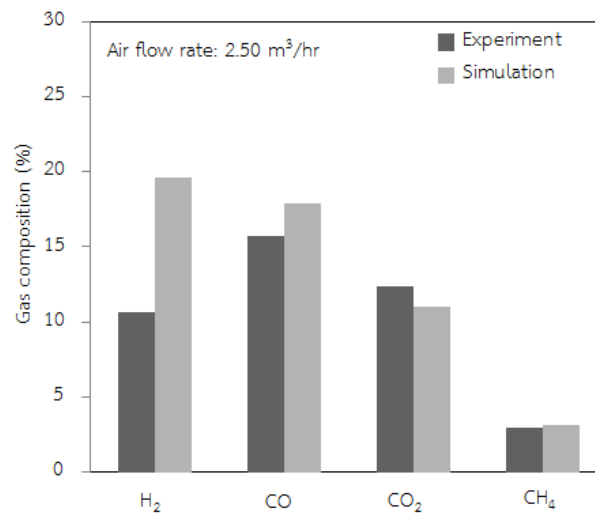


Figure 5.29 Comparison of gas composition from cassava rhizome (10-15 mm) gasification: experimental & simulation.

Table 5.11 The gas composition from cassava rhizome (1-5 mm) gasification: experimental & simulation.

Air flow rate (m <sup>3</sup> /hr)	Gas composition (%)				Solid (kg/hr)
	Experimental				
	H <sub>2</sub>	CO	CO <sub>2</sub>	CH <sub>4</sub>	
1.98	14.41	14.77	15.66	3.05	0.73
2.34	10.38	17.23	13.27	3.4	0.84
2.50	10.11	18.82	12.66	2.95	0.96
3.06	10.97	14.49	11.92	2.83	0.93
	Simulation				
1.98	15.67	15.67	21.89	10.37	0.19
2.34	16.01	15.07	17.90	8.48	0.18
2.50	16.23	17.86	20.45	9.74	0.26
3.06	13.83	15.21	17.42	8.30	0.25



Table 5.12 The gas composition from cassava rhizome (5-10 mm) gasification: experimental & simulation.

Air flow rate (m <sup>3</sup> /hr)	Gas composition (%)				Solid (kg/hr)
	Experimental				
	H <sub>2</sub>	CO	CO <sub>2</sub>	CH <sub>4</sub>	
1.98	15.31	14.82	15.62	3.07	0.50
2.34	12.79	13.69	15.62	2.84	0.78
2.50	11.08	16.39	13.02	3.18	0.85
3.06	11.11	17.82	11.80	3.19	0.60
Simulation					
1.98	15.90	14.98	16.36	8.30	0.15
2.34	14.32	15.83	13.00	6.78	0.16
2.50	16.07	14.12	12.99	5.84	0.16
3.06	16.18	14.10	13.14	4.98	0.17

Table 5.13 The gas composition from cassava rhizome (10-15 mm) gasification: experimental & simulation.

Air flow rate (m <sup>3</sup> /hr)	Gas composition (%)				Solid (kg/hr)
	Experimental				
	H <sub>2</sub>	CO	CO <sub>2</sub>	CH <sub>4</sub>	
1.98	9.37	13.54	14.81	3.02	0.40
2.34	11.14	15.07	12.54	2.88	0.51
2.50	10.67	15.68	12.35	2.93	0.49
3.06	10.91	16.91	11.70	3.14	0.49
Simulation					
1.98	14.06	11.52	15.67	5.07	0.12
2.34	17.90	15.83	14.51	4.14	0.15
2.50	19.64	17.86	11.04	3.57	0.16
3.06	19.22	17.28	11.20	3.04	0.18

## CHAPTER 6

### Conclusions and Future work recommendations

The aim of this study is to investigate the effects of air flow rate, biomass particles size, addition of thermal integration unit and catalyst unit on biomass gasification efficiency of peanut shell and cassava rhizome using modular downdraft gasifier. The produced gas was also fed to a small gas engine system for power generation. In addition, a steady state simulation for biomass gasifier to predict the gas composition using ASPEN PLUS was performed.

The heat thermal integration unit returns product gases to heat recover section which improves the temperature stability of the reactor and quality of producer gas. As a result, the carbon conversion increased up to 3-10% at low air flow rate. Increasing air flow rate to the reactor, led to a higher temperature at combustion zone where the reactions are exothermic and heat is transferred to the pyrolysis zone and reduction zones. The quality of product gas is found to be depending on inlet of air flow rate and temperature at the oxidation zone with both raw materials. For peanut shell gasification with the modified modular gasifier, the optimum conversion without catalyst for carbon conversion and hydrogen conversion were 87.10% and 57.21%, respectively at 3.06 m<sup>3</sup>/hr air flow. The lower heating value and cold gas efficiency were 3.95 MJ/m<sup>3</sup> and 56.10%, respectively. In case of cassava rhizome, carbon and hydrogen conversion were 92.36%, and 65.92%, respectively with particle size of 5-10 mm at 2.5 m<sup>3</sup>/hr air flow. The lower heating value and cold gas efficiency were 4.46 MJ/m<sup>3</sup> and 54.86%, respectively. The smaller cassava rhizome particle sizes tend to block the air void, leading to high pressure drop in the reactor, whereas the larger particles possess greater heat transfer resistance.

In order to improve gasification efficiency, catalyst unit was coupled to the main reactor. Char and 5%Ni/char catalyst are active to cracking and reforming production gas into synthesis gas. The gas composition obtained from char and 5%Ni/char catalyst displayed no significant difference in term of conversions.

Dolomite catalyst can be employed as both the filter of the tar and also enhanced catalytic cracking reactions. Using synthesized 5%Ni/dolomite catalyst also leads to high carbon and hydrogen conversions. Increasing the amount of dolomite and 5%Ni/dolomite from 300 g to 600 g did not show the superior activity even though it contains higher catalyst loading. Moreover, the 5%Ni/dolomite catalyst showed good resistant to high temperature from biomass gasification.

On conversion of the producer gas into electricity, the global efficiencies were to 11.03% (peanut shell waste) and 11.29% (cassava rhizome) comparing with 16.88% when using LPG. The efficiency of gasifier-cogeneration system from cassava rhizome and peanut shell was 11.84% and 12.12%, respectively, mainly due to low thermal efficiency of reciprocating internal combustion engines and partly to the calorific value of gas. Although, the technology is a promising alternative to supply electricity from biomass gasification, especially in places where electrical distribution network is not yet available.

A model was developed for the gasification of biomass with downdraft-fixed bed gasifier using the ASPEN PLUS simulator. The predicted results of peanut shell were close to experimental data with the exception of  $\text{CH}_4$ . The predicted gas composition from simulation of peanut shell is closer to experimental result than that of cassava rhizome. This may be due to the effect of particle size distribution and mass transfer resistance in the model. The developed model is able to simulate the performance of the gasifier and predicted results are in good prediction.

#### **Future work recommendations**

- Modification the ash grates removal with a motorized design for continuous operation should be carried out.
- Improvement of the air intake system from the gasification system to power generation should be made.
- The effect of biomass particle size distribution on the ASPEN PLUS model for simulating the performance of the gasifier should be examined.

## REFERENCES

- Abu El-Rub, Z., Bramer, E. A., & Brem, G. (2008). Experimental comparison of biomass chars with other catalysts for tar reduction. *Fuel*, 87(10–11), 2243-2252.
- Babu, B. V., & Chaurasia, A. S. (2004). Heat transfer and kinetics in the pyrolysis of shrinking biomass particle. *Chemical Engineering Science*, 59(10), 1999-2012.
- Babu, B. V., & Sheth, P. N. (2006). Modeling and simulation of reduction zone of downdraft biomass gasifier: Effect of char reactivity factor. *Energy Conversion and Management*, 47(15–16), 2602-2611.
- Basu, P. (2010a). Chapter 2 - Biomass Characteristics. In P. Basu (Ed.), *Biomass Gasification and Pyrolysis* (pp. 27-63). Boston: Academic Press.
- Basu, P. (2010b). Chapter 5 - Gasification Theory and Modeling of Gasifiers. In P. Basu (Ed.), *Biomass Gasification and Pyrolysis* (pp. 117-165). Boston: Academic Press.
- Basu, P. (2010c). Chapter 6 - Design of Biomass Gasifiers. In P. Basu (Ed.), *Biomass Gasification and Pyrolysis* (pp. 167-228). Boston: Academic Press.
- Basu, P. (2010d). Chapter 9 - Production of Synthetic Fuels and Chemicals from Biomass. In P. Basu (Ed.), *Biomass Gasification and Pyrolysis* (pp. 301-323). Boston: Academic Press.
- Basu, P. (2013a). Chapter 3 - Biomass Characteristics. In P. Basu (Ed.), *Biomass Gasification, Pyrolysis and Torrefaction (Second Edition)* (pp. 47-86). Boston: Academic Press.
- Basu, P. (2013b). Chapter 7 - Gasification Theory. In P. Basu (Ed.), *Biomass Gasification, Pyrolysis and Torrefaction (Second Edition)* (pp. 199-248). Boston: Academic Press.
- Belgiorno, V., De Feo, G., Della Rocca, C., & Napoli, R. M. A. (2003). Energy from gasification of solid wastes. *Waste Management*, 23(1), 1-15.
- Boloy, R. A. M., Silveira, J. L., Tuna, C. E., Coronado, C. R., & Antunes, J. S. (2011). Ecological impacts from syngas burning in internal combustion engine:

- Technical and economic aspects. *Renewable and Sustainable Energy Reviews*, 15(9), 5194-5201.
- Bulushev, D. A., & Ross, J. R. H. (2011). Catalysis for conversion of biomass to fuels via pyrolysis and gasification: A review. *Catalysis Today*, 171(1), 1-13.
- Chan, F. L., & Tanksale, A. (2014). Review of recent developments in Ni-based catalysts for biomass gasification. *Renewable and Sustainable Energy Reviews*, 38(0), 428-438.
- Chaves, L. I., da Silva, M. J., de Souza, S. N. M., Secco, D., Rosa, H. A., Nogueira, C. E. C., & Frigo, E. P. (2016). Small-scale power generation analysis: Downdraft gasifier coupled to engine generator set. *Renewable and Sustainable Energy Reviews*, 58(Supplement C), 491-498.
- Corella, J., & Sanz, A. (2005). Modeling circulating fluidized bed biomass gasifiers. A pseudo-rigorous model for stationary state. *Fuel Processing Technology*, 86(9), 1021-1053.
- Demirbaş, A. (2001). Biomass resource facilities and biomass conversion processing for fuels and chemicals. *Energy Conversion and Management*, 42(11), 1357-1378.
- Devi, L., Craje, M., Thüne, P., Ptasinski, K. J., & Janssen, F. J. J. G. (2005). Olivine as tar removal catalyst for biomass gasifiers: Catalyst characterization. *Applied Catalysis A: General*, 294(1), 68-79.
- Di Blasi, C. (2009). Combustion and gasification rates of lignocellulosic chars. *Progress in Energy and Combustion Science*, 35(2), 121-140.
- Dogru, M., Howarth, C. R., Akay, G., Keskinler, B., & Malik, A. A. (2002). Gasification of hazelnut shells in a downdraft gasifier. *Energy*, 27(5), 415-427.
- Erlich, C., & Fransson, T. H. (2011). Downdraft gasification of pellets made of wood, palm-oil residues respective bagasse: Experimental study. *Applied Energy*, 88(3), 899-908.
- Franco, C., Pinto, F., Gulyurtlu, I., & Cabrita, I. (2003). The study of reactions influencing the biomass steam gasification process ☆. *Fuel*, 82(7), 835-842.
- Gai, C., & Dong, Y. (2012). Experimental study on non-woody biomass gasification in a downdraft gasifier. *International Journal of Hydrogen Energy*, 37(6), 4935-4944.

- Gao, N., Li, A., Quan, C., Qu, Y., & Mao, L. (2012). Characteristics of hydrogen-rich gas production of biomass gasification with porous ceramic reforming. *International Journal of Hydrogen Energy*, *37*(12), 9610-9618.
- García-Bacaicoa, P., Mastral, J. F., Ceamanos, J., Berruero, C., & Serrano, S. (2008). Gasification of biomass/high density polyethylene mixtures in a downdraft gasifier. *Bioresource Technology*, *99*(13), 5485-5491.
- Giltrap, D. L., McKibbin, R., & Barnes, G. R. G. (2003). A steady state model of gas-char reactions in a downdraft biomass gasifier. *Solar Energy*, *74*(1), 85-91.
- Guan, Y., Luo, S., Liu, S., Xiao, B., & Cai, L. (2009). Steam catalytic gasification of municipal solid waste for producing tar-free fuel gas. *International Journal of Hydrogen Energy*, *34*(23), 9341-9346.
- Guo, F., Dong, Y., Dong, L., & Guo, C. (2014). Effect of design and operating parameters on the gasification process of biomass in a downdraft fixed bed: An experimental study. *International Journal of Hydrogen Energy*, *39*(11), 5625-5633.
- Hanaoka, T., Inoue, S., Uno, S., Ogi, T., & Minowa, T. (2005). Effect of woody biomass components on air-steam gasification. *Biomass and Bioenergy*, *28*(1), 69-76.
- Hernández, J. J., Aranda-Almansa, G., & Bula, A. (2010). Gasification of biomass wastes in an entrained flow gasifier: Effect of the particle size and the residence time. *Fuel Processing Technology*, *91*(6), 681-692.
- Higman, C., & van der Burgt, M. (2008a). Chapter 2 - The Thermodynamics of Gasification. In C. Higman & M. v. d. Burgt (Eds.), *Gasification (Second Edition)* (pp. 11-31). Burlington: Gulf Professional Publishing.
- Higman, C., & van der Burgt, M. (2008b). Chapter 4 - Feedstocks and Feedstock Characteristics. In C. Higman & M. v. d. Burgt (Eds.), *Gasification (Second Edition)* (pp. 47-90). Burlington: Gulf Professional Publishing.
- Higman, C., & van der Burgt, M. (2008c). Chapter 5 - Gasification Processes. In C. Higman & M. v. d. Burgt (Eds.), *Gasification (Second Edition)* (pp. 91-191). Burlington: Gulf Professional Publishing.

- Hosseini, M., Dincer, I., & Rosen, M. A. (2012). Steam and air fed biomass gasification: Comparisons based on energy and exergy. *International Journal of Hydrogen Energy*, 37(21), 16446-16452.
- Jain, A. K., & Goss, J. R. (2000). Determination of reactor scaling factors for throatless rice husk gasifier. *Biomass and Bioenergy*, 18(3), 249-256.
- Jarunthammachote, S., & Dutta, A. (2007). Thermodynamic equilibrium model and second law analysis of a downdraft waste gasifier. *Energy*, 32(9), 1660-1669.
- Jayah, T. H., Aye, L., Fuller, R. J., & Stewart, D. F. (2003). Computer simulation of a downdraft wood gasifier for tea drying. *Biomass and Bioenergy*, 25(4), 459-469.
- Keche, A., Gaddale, A., & Tated, R. (2015). Simulation of biomass gasification in downdraft gasifier for different biomass fuels using ASPEN PLUS. *Clean Technologies and Environmental Policy*, 17(2), 465-473.
- Klass, D. L. (1998a). Chapter 2 - Biomass as an Energy Resource: Concept and Markets. In D. L. Klass (Ed.), *Biomass for Renewable Energy, Fuels, and Chemicals* (pp. 29-50). San Diego: Academic Press.
- Klass, D. L. (1998b). Chapter 9 - Thermal Conversion: Gasification. In D. L. Klass (Ed.), *Biomass for Renewable Energy, Fuels, and Chemicals* (pp. 271-331). San Diego: Academic Press.
- Kumar, A., Jones, D., & Hanna, M. (2009). Thermochemical Biomass Gasification: A Review of the Current Status of the Technology. *Energies*, 2(3), 556-581.
- Kuo, P.-C., Wu, W., & Chen, W.-H. (2014). Gasification performances of raw and torrefied biomass in a downdraft fixed bed gasifier using thermodynamic analysis. *Fuel*, 117, Part B(0), 1231-1241.
- Li, J., Yin, Y., Zhang, X., Liu, J., & Yan, R. (2009). Hydrogen-rich gas production by steam gasification of palm oil wastes over supported tri-metallic catalyst. *International Journal of Hydrogen Energy*, 34(22), 9108-9115.
- Li, X. T., Grace, J. R., Lim, C. J., Watkinson, A. P., Chen, H. P., & Kim, J. R. (2004). Biomass gasification in a circulating fluidized bed. *Biomass and Bioenergy*, 26(2), 171-193.

- Lv, P., Yuan, Z., Ma, L., Wu, C., Chen, Y., & Zhu, J. (2007). Hydrogen-rich gas production from biomass air and oxygen/steam gasification in a downdraft gasifier. *Renewable Energy*, *32*(13), 2173-2185.
- Lv, P. M., Xiong, Z. H., Chang, J., Wu, C. Z., Chen, Y., & Zhu, J. X. (2004). An experimental study on biomass air–steam gasification in a fluidized bed. *Bioresource Technology*, *95*(1), 95-101.
- Maniatis, K. (2008). Progress in Biomass Gasification: An Overview *Progress in Thermochemical Biomass Conversion* (pp. 1-31): Blackwell Science Ltd.
- Martinez, J. D., Mahkamov, K., Andrade, R. V., & Silva Lora, E. E. (2012). Syngas production in downdraft biomass gasifiers and its application using internal combustion engines. *Renewable Energy*, *38*(1), 1-9.
- McKendry, P. (2002a). Energy production from biomass (part 1): overview of biomass. *Bioresource Technology*, *83*(1), 37-46.
- McKendry, P. (2002b). Energy production from biomass (part 2): conversion technologies. *Bioresource Technology*, *83*(1), 47-54.
- Miao, Y., Xue, J., Xia, F., Yin, X., & Wu, C. (2010). Utilization of porous dolomite pellets for the catalytic decomposition of acetic acid. *Biomass and Bioenergy*, *34*(12), 1855-1860.
- Nikoo, M. B., & Mahinpey, N. (2008). Simulation of biomass gasification in fluidized bed reactor using ASPEN PLUS. *Biomass and Bioenergy*, *32*(12), 1245-1254.
- Olgun, H., Ozdogan, S., & Yinesor, G. (2011). Results with a bench scale downdraft biomass gasifier for agricultural and forestry residues. *Biomass and Bioenergy*, *35*(1), 572-580.
- Pérez, J. F., Melgar, A., & Benjumea, P. N. (2012). Effect of operating and design parameters on the gasification/combustion process of waste biomass in fixed bed downdraft reactors: An experimental study. *Fuel*, *96*(0), 487-496.
- Puig-Arnabat, M., Bruno, J. C., & Coronas, A. (2010). Review and analysis of biomass gasification models. *Renewable and Sustainable Energy Reviews*, *14*(9), 2841-2851.



- Ramzan, N., Ashraf, A., Naveed, S., & Malik, A. (2011). Simulation of hybrid biomass gasification using Aspen plus: A comparative performance analysis for food, municipal solid and poultry waste. *Biomass and Bioenergy*, *35*(9), 3962-3969.
- Roy, P. C., Datta, A., & Chakraborty, N. (2009). Modelling of a downdraft biomass gasifier with finite rate kinetics in the reduction zone. *International Journal of Energy Research*, *33*(9), 833-851.
- Ruiz, J. A., Juárez, M. C., Morales, M. P., Muñoz, P., & Mendivil, M. A. (2013). Biomass gasification for electricity generation: Review of current technology barriers. *Renewable and Sustainable Energy Reviews*, *18*(0), 174-183.
- Schuster, G., Löffler, G., Weigl, K., & Hofbauer, H. (2001). Biomass steam gasification – an extensive parametric modeling study. *Bioresource Technology*, *77*(1), 71-79.
- Sharma, A. K. (2008). Equilibrium and kinetic modeling of char reduction reactions in a downdraft biomass gasifier: A comparison. *Solar Energy*, *82*(10), 918-928.
- Sharma, A. K. (2009). Experimental study on 75&#xa0;kWth downdraft (biomass) gasifier system. *Renewable Energy*, *34*(7), 1726-1733.
- Sharma, A. K. (2011). Modeling and simulation of a downdraft biomass gasifier 1. Model development and validation. *Energy Conversion and Management*, *52*(2), 1386-1396.
- Shen, Y., Zhao, P., Shao, Q., Ma, D., Takahashi, F., & Yoshikawa, K. (2014a). In-situ catalytic conversion of tar using rice husk char-supported nickel-iron catalysts for biomass pyrolysis/gasification. *Applied Catalysis B: Environmental*, *152-153*(0), 140-151.
- Shen, Y., Zhao, P., Shao, Q., Ma, D., Takahashi, F., & Yoshikawa, K. (2014b). In-situ catalytic conversion of tar using rice husk char-supported nickel-iron catalysts for biomass pyrolysis/gasification. *Applied Catalysis B: Environmental*, *152-153*(Supplement C), 140-151.
- Sheth, P. N., & Babu, B. V. (2009). Experimental studies on producer gas generation from wood waste in a downdraft biomass gasifier. *Bioresource Technology*, *100*(12), 3127-3133.

- Singh, R. N., Jena, U., Patel, J. B., & Sharma, A. M. (2006). Feasibility study of cashew nut shells as an open core gasifier feedstock. *Renewable Energy*, 31(4), 481-487.
- Skoulou, V., Zabaniotou, A., Stavropoulos, G., & Sakelaropoulos, G. (2008). Syngas production from olive tree cuttings and olive kernels in a downdraft fixed-bed gasifier. *International Journal of Hydrogen Energy*, 33(4), 1185-1194.
- Son, Y.-I., Yoon, S. J., Kim, Y. K., & Lee, J.-G. (2011). Gasification and power generation characteristics of woody biomass utilizing a downdraft gasifier. *Biomass and Bioenergy*, 35(10), 4215-4220.
- Sornkade, P., Atong, D., & Sricharoenchaikul, V. (2013). Enhancement of Cassava Rhizome Gasification Using Mono-Metallic Cobalt Catalysts. *Energy Procedia*, 34(0), 273-281.
- Srinakruang, J., Sato, K., Vitidsant, T., & Fujimoto, K. (2006). Highly efficient sulfur and coking resistance catalysts for tar gasification with steam. *Fuel*, 85(17-18), 2419-2426.
- Sutton, D., Kelleher, B., & Ross, J. R. H. (2001). Review of literature on catalysts for biomass gasification. *Fuel Processing Technology*, 73(3), 155-173.
- Tinaut, F. V., Melgar, A., Pérez, J. F., & Horrillo, A. (2008). Effect of biomass particle size and air superficial velocity on the gasification process in a downdraft fixed bed gasifier. An experimental and modelling study. *Fuel Processing Technology*, 89(11), 1076-1089.
- Waheed, Q. M. K., Wu, C., & Williams, P. T. (2016). Pyrolysis/reforming of rice husks with a Ni-dolomite catalyst: Influence of process conditions on syngas and hydrogen yield. *Journal of the Energy Institute*, 89(4), 657-667.
- Wander, P. R., Altafini, C. R., & Barreto, R. M. (2004). Assessment of a small sawdust gasification unit. *Biomass and Bioenergy*, 27(5), 467-476.
- Wang, D., Yuan, W., & Ji, W. (2011). Char and char-supported nickel catalysts for secondary syngas cleanup and conditioning. *Applied Energy*, 88(5), 1656-1663.
- Wang, J., Cheng, G., You, Y., Xiao, B., Liu, S., He, P., . . . Zhang, G. (2012). Hydrogen-rich gas production by steam gasification of municipal solid waste (MSW) using NiO

supported on modified dolomite. *International Journal of Hydrogen Energy*, 37(8), 6503-6510.

Wang, Y., & Kinoshita, C. M. (1993). Kinetic model of biomass gasification. *Solar Energy*, 51(1), 19-25.

Yoon, S. J., Son, Y.-I., Kim, Y.-K., & Lee, J.-G. (2012). Gasification and power generation characteristics of rice husk and rice husk pellet using a downdraft fixed-bed gasifier. *Renewable Energy*, 42(0), 163-167.

Zainal, Z. A., Rifau, A., Quadir, G. A., & Seetharamu, K. N. (2002). Experimental investigation of a downdraft biomass gasifier. *Biomass and Bioenergy*, 23(4), 283-289.

Zhang, S., Asadullah, M., Dong, L., Tay, H.-L., & Li, C.-Z. (2013). An advanced biomass gasification technology with integrated catalytic hot gas cleaning. Part II: Tar reforming using char as a catalyst or as a catalyst support. *Fuel*, 112(0), 646-653.





APPENDIX

จุฬาลงกรณ์มหาวิทยาลัย  
**CHULALONGKORN UNIVERSITY**



Table A.1 The gas composition from peanut shell gasification.

Peanut shell		total feed (g)		3000.00	g/min	50
Char		total solid (g)		542.00		
Tar		total liquid (g)		70.00	Heat	Recovery Unit
Gas		flow in (m <sup>3</sup> /hr)		1.62	Catalyst	Non-catalyst
Time	CO	CO <sub>2</sub>	CH <sub>4</sub>	H <sub>2</sub>	C <sub>n</sub> H <sub>m</sub>	LHV (MJ/m <sup>3</sup> )
0	0.00	0.00	0.00	0.00	0.00	0.00
1	1.23	4.88	0.24	0.05	0.04	0.26
2	1.32	5.11	0.24	0.10	0.03	0.27
3	1.42	5.48	0.26	0.16	0.04	0.30
4	1.61	7.06	0.30	0.24	0.05	0.35
5	4.01	11.08	0.93	1.49	0.09	1.03
6	6.30	14.06	1.70	2.70	0.03	1.71
7	7.21	15.04	2.07	3.01	0.02	1.98
8	7.82	15.70	2.36	3.19	0.00	2.18
9	7.80	15.91	2.39	3.41	0.01	2.21
10	7.89	16.09	2.35	4.20	0.00	2.29
11	8.14	15.97	2.30	5.30	0.00	2.42
12	8.16	16.14	2.27	5.26	0.00	2.41
13	8.03	16.46	2.29	4.91	0.01	2.37
14	7.97	16.51	2.10	5.39	0.01	2.34
15	9.52	16.57	2.34	7.41	0.03	2.85
16	10.30	16.80	2.63	8.79	0.03	3.20
17	10.71	16.99	2.78	9.38	0.03	3.37
18	10.65	17.30	3.05	9.22	0.06	3.45
19	10.57	17.26	3.14	9.01	0.07	3.46
20	10.47	17.10	3.16	9.76	0.07	3.53
21	10.01	16.86	3.05	9.52	0.07	3.41
22	9.49	16.64	2.89	9.33	0.06	3.26
23	9.43	16.26	2.90	9.80	0.02	3.29

Table A.1 The gas composition from peanut shell gasification (cont.).

Time	CO	CO <sub>2</sub>	CH <sub>4</sub>	H <sub>2</sub>	C <sub>n</sub> H <sub>m</sub>	LHV (MJ/m <sup>3</sup> )
24	9.78	16.48	3.10	9.56	0.03	3.39
25	11.24	17.21	3.51	9.53	0.07	3.73
26	11.39	17.43	3.70	9.72	0.07	3.84
27	11.43	17.36	3.69	10.04	0.09	3.88
28	11.38	17.04	3.57	10.41	0.09	3.87
29	11.00	16.73	3.38	10.71	0.09	3.79
30	10.83	16.41	3.10	11.02	0.06	3.69
31	11.17	15.94	2.81	11.75	0.06	3.71
32	11.33	15.87	2.92	12.53	0.08	3.86
33	11.24	16.15	3.16	12.57	0.05	3.92
34	11.67	16.57	3.46	11.46	0.08	3.98
35	12.33	16.98	4.24	11.01	0.01	4.27
36	12.20	17.40	4.60	10.26	0.11	4.33
37	11.51	17.54	4.51	9.55	0.13	4.14
38	10.91	17.41	4.24	9.44	0.14	3.96
39	11.23	17.15	4.04	9.25	0.12	3.90
40	11.21	16.56	3.39	8.83	0.1	3.62
41	10.12	15.50	2.16	7.55	0.07	2.89
42	10.77	14.44	1.44	6.83	0.04	2.63
43	13.78	13.00	1.31	7.11	0.01	2.98
44	13.94	11.62	1.01	6.13	0.00	2.78
45	13.00	10.74	0.75	4.63	0.01	2.41
46	12.00	11.21	0.61	2.84	0.10	2.08
47	10.72	11.96	0.55	1.97	0.10	1.80
48	7.55	12.96	0.51	1.02	0.01	1.25
49	6.67	13.35	0.51	0.84	0.10	1.15
50	6.18	13.46	0.53	0.94	0.10	1.11
Average	11.17	12.22	3.48	10.26	0.06	3.56

Table A.2 The gas composition from peanut shell gasification.

Peanut shell		total feed (g)		166.84	g/min		51
Char		total solid (g)		20.00			
Tar		total liquid (g)		70.00	Heat	Recovery Unit	
Gas		flow in (m <sup>3</sup> /hr)		1.98	Catalyst	Non-catalyst	
Time	CO	CO <sub>2</sub>	CH <sub>4</sub>	H <sub>2</sub>	C <sub>n</sub> H <sub>m</sub>	LHV (MJ/m <sup>3</sup> )	
0	0.00	0.00	0.00	0.00	0.00	0.00	
1	13.82	14.27	2.53	12.38	0.07	4.01	
2	13.72	14.69	2.53	12.18	0.07	3.98	
3	13.60	15.15	2.55	12.02	0.08	3.96	
4	13.67	15.54	2.66	11.93	0.09	4.00	
5	14.46	15.84	3.06	12.08	0.13	4.27	
6	15.20	16.16	3.50	12.09	0.17	4.54	
7	15.57	16.36	3.78	12.71	0.18	4.76	
8	15.81	16.93	3.90	12.93	0.19	4.86	
9	15.76	16.53	3.98	12.96	0.18	4.88	
10	15.18	17.07	3.90	12.70	0.20	4.75	
11	14.92	16.43	3.56	12.42	0.16	4.56	
12	17.51	15.91	3.20	13.06	0.16	4.82	
13	17.74	16.13	3.59	13.08	0.20	5.01	
14	17.65	16.07	3.56	13.01	0.18	4.97	
15	17.71	15.64	2.93	13.72	0.11	4.81	
16	18.47	14.72	2.17	13.51	0.06	4.59	
17	18.59	14.67	2.21	13.72	0.04	4.64	
18	19.61	14.33	3.28	13.78	0.12	5.18	
19	19.96	14.00	3.11	13.58	0.11	5.14	
20	20.10	13.41	2.60	13.06	0.10	4.92	
21	19.51	13.20	2.26	12.57	0.05	4.65	
22	18.30	13.43	2.04	12.30	0.03	4.38	
23	16.37	14.08	1.93	11.81	0.02	4.04	



Table A.2 The gas composition from peanut shell gasification (cont.).

Time	CO	CO <sub>2</sub>	CH <sub>4</sub>	H <sub>2</sub>	C <sub>n</sub> H <sub>m</sub>	LHV (MJ/m <sup>3</sup> )
24	15.17	14.66	1.90	11.34	0.01	3.82
25	14.85	14.91	1.86	11.26	0.00	3.76
26	14.87	15.78	1.88	11.25	0.02	3.77
27	14.81	15.64	1.96	11.52	0.02	3.82
28	14.55	16.04	2.09	11.54	0.00	3.83
29	14.22	16.50	2.44	11.48	0.05	3.93
30	14.28	16.59	2.64	11.40	0.06	4.00
31	14.18	16.58	2.67	11.18	0.07	3.98
32	13.78	16.55	2.62	11.15	0.07	3.91
33	13.72	16.43	2.62	11.04	0.07	3.89
34	13.68	16.34	2.59	10.94	0.08	3.86
35	13.83	16.18	2.54	10.39	0.09	3.81
36	13.97	15.93	2.51	11.10	0.07	3.89
37	13.85	15.66	2.38	11.11	0.05	3.82
38	13.85	15.63	2.32	11.08	0.05	3.79
39	13.77	15.56	2.25	11.06	0.04	3.75
40	13.63	15.46	2.17	10.88	0.05	3.69
41	13.43	15.45	2.09	10.64	0.04	3.61
42	13.20	15.45	2.01	10.35	0.02	3.51
43	12.90	15.58	2.00	10.33	0.05	3.48
44	12.90	15.63	2.09	10.52	0.02	3.52
45	12.90	15.82	2.02	10.62	0.04	3.51
46	12.99	15.95	2.17	10.38	0.05	3.56
47	13.02	15.98	2.11	10.89	0.04	3.59
48	13.02	16.00	2.24	10.95	0.04	3.64
49	12.88	16.27	2.31	10.72	0.06	3.63
50	12.87	16.23	2.17	10.38	0.01	3.53
51	12.50	16.51	2.79	8.19	0.02	3.47

Table A.2 The gas composition from peanut shell gasification (cont.).

Time	CO	CO <sub>2</sub>	CH <sub>4</sub>	H <sub>2</sub>	C <sub>n</sub> H <sub>m</sub>	LHV (MJ/m <sup>3</sup> )
52	11.11	16.56	1.72	8.79	0.02	2.98
53	9.85	16.57	1.69	8.63	0.02	2.79
54	9.62	16.56	1.62	8.58	0.00	2.72
55	9.39	16.53	1.54	8.38	0.00	2.64
56	9.17	16.50	1.38	8.28	0.00	2.55
57	8.98	16.55	1.28	8.25	0.00	2.48
58	8.57	16.55	1.30	8.33	0.00	2.45
59	8.51	16.53	1.31	8.23	0.00	2.43
60	8.10	16.52	1.34	8.23	0.00	2.39
Average	15.92	15.42	2.53	11.98	0.07	4.23

Table A.3 The gas composition from peanut shell gasification.

Peanut shell	total feed (g)	3000.00	g/min	54.54		
Char	total solid (g)	361.27				
Tar	total liquid (g)	70.00	Heat	Recovery Unit		
Gas	flow in (m <sup>3</sup> /hr)	2.34	Catalyst	Non-catalyst		
Time	CO	CO <sub>2</sub>	CH <sub>4</sub>	H <sub>2</sub>	C <sub>n</sub> H <sub>m</sub>	LHV (MJ/m <sup>3</sup> )
0	0.00	0.00	0.00	0.00	0.00	0.00
1	3.50	6.87	1.21	0.94	0.00	0.98
2	4.98	10.48	1.62	0.51	0.03	1.27
3	5.09	11.34	1.80	0.78	0.03	1.38
4	6.24	12.35	1.44	1.44	0.05	1.48
5	6.30	12.79	2.35	2.26	0.06	1.90
6	5.89	12.99	2.62	2.88	0.05	2.01
7	7.37	13.19	2.35	3.75	0.07	2.20
8	7.23	13.04	2.26	4.24	0.05	2.20
9	7.28	13.38	2.19	5.10	0.05	2.27
10	7.83	13.56	2.41	5.53	0.06	2.47
11	8.22	13.75	2.39	6.00	0.07	2.57

Table A.3 The gas composition from peanut shell gasification (cont.).

Time	CO	CO <sub>2</sub>	CH <sub>4</sub>	H <sub>2</sub>	C <sub>n</sub> H <sub>m</sub>	LHV (MJ/m <sup>3</sup> )
12	8.10	13.87	2.54	6.36	0.04	2.63
13	7.77	14.08	2.51	6.88	0.04	2.64
14	7.56	14.49	2.47	6.98	0.03	2.60
15	7.71	13.92	2.34	7.47	0.02	2.62
16	7.68	13.15	2.35	7.87	0.01	2.66
17	11.46	15.67	4.41	7.07	0.18	3.85
18	10.67	13.95	3.40	8.29	0.14	3.51
19	10.50	13.53	3.23	9.07	0.11	3.50
20	9.91	14.15	3.24	9.45	0.10	3.47
21	9.85	13.17	2.71	9.86	0.10	3.31
22	9.68	13.29	2.38	9.65	0.07	3.14
23	10.08	13.20	2.30	9.83	0.04	3.17
24	10.62	12.80	2.23	10.13	0.03	3.24
25	10.36	13.70	3.31	10.46	0.01	3.63
26	10.77	12.90	2.54	10.86	0.07	3.47
27	11.04	12.45	3.15	10.69	0.05	3.69
28	10.99	12.62	3.45	10.99	0.01	3.81
29	10.63	12.95	3.02	10.08	0.04	3.53
30	10.73	12.97	3.55	10.99	0.05	3.83
31	10.86	12.57	2.24	10.89	0.06	3.37
32	11.07	12.35	2.05	10.07	0.02	3.23
33	11.18	12.37	2.12	10.39	0.01	3.30
34	10.99	12.51	2.57	10.36	0.01	3.43
35	11.36	12.39	2.45	10.03	0.03	3.41
36	11.82	12.10	2.10	10.98	0.02	3.44
37	12.27	12.10	2.90	10.78	0.00	3.75
38	12.46	11.80	1.76	10.86	0.00	3.38
39	12.61	11.51	1.75	10.76	0.00	3.38
40	12.28	11.40	1.65	10.68	0.00	3.30

Table A.3 The gas composition from peanut shell gasification (cont.).

Time	CO	CO <sub>2</sub>	CH <sub>4</sub>	H <sub>2</sub>	C <sub>n</sub> H <sub>m</sub>	LHV (MJ/m <sup>3</sup> )
41	12.50	11.39	1.60	11.39	0.00	3.38
42	12.43	11.28	1.67	11.91	0.00	3.45
43	12.29	11.19	1.66	11.35	0.00	3.37
44	12.30	10.30	1.66	11.21	0.00	3.36
45	11.69	11.33	1.68	10.51	0.00	3.21
46	12.05	11.56	1.78	10.45	0.00	3.29
47	12.30	11.42	1.78	10.25	0.00	3.30
48	12.16	11.94	2.16	12.05	0.00	3.61
49	11.90	11.85	2.04	10.63	0.00	3.38
50	11.87	11.66	1.75	10.88	0.00	3.30
51	11.51	11.63	1.84	10.17	0.00	3.21
52	11.73	11.49	1.67	10.83	0.00	3.25
53	12.30	11.47	1.63	10.78	0.00	3.30
54	12.20	11.61	1.84	10.71	0.00	3.36
55	11.42	11.52	1.86	9.74	0.00	3.16
56	10.86	10.94	1.44	9.18	0.00	2.88
57	10.43	10.69	1.12	8.84	0.00	2.67
58	10.09	10.67	0.91	8.07	0.00	2.47
59	12.84	10.85	0.87	9.36	0.10	2.98
60	15.02	11.55	1.66	7.97	0.00	3.35
Average	11.34	12.42	2.42	10.76	0.03	3.43

Table A.4 The gas composition from peanut shell gasification.

Peanut shell		total feed (g)	3000.00	g/min	50	
Char		total solid (g)	220.33			
Tar		total liquid (g)	40.00	Heat	Recovery Unit	
Gas		flow in (m <sup>3</sup> /hr)	3.05	Catalyst	Non-catalyst	
Time	CO	CO <sub>2</sub>	CH <sub>4</sub>	H <sub>2</sub>	C <sub>n</sub> H <sub>m</sub>	LHV (MJ/m <sup>3</sup> )
0	0.00	0.00	0.00	0.00	0.00	0.00
1	1.83	3.82	0.65	0.00	0.00	0.46
2	3.69	5.82	1.21	0.50	0.05	0.97
3	6.99	14.39	2.13	1.20	0.07	1.80
4	7.51	12.85	2.41	2.91	0.11	2.16
5	8.71	13.47	2.59	3.28	0.11	2.42
6	9.56	13.36	2.95	3.93	0.09	2.72
7	9.74	13.05	2.95	5.57	0.06	2.91
8	10.42	13.16	2.71	7.48	0.10	3.13
9	10.72	14.93	2.73	9.30	0.16	3.39
10	10.33	15.99	3.51	8.52	0.16	3.54
11	10.97	15.61	4.33	10.67	0.15	4.14
12	11.79	13.40	3.91	11.04	0.09	4.11
13	11.79	12.48	2.99	11.34	0.05	3.80
14	11.87	13.04	2.31	11.34	0.04	3.56
15	11.75	12.38	2.46	10.92	0.02	3.55
16	12.01	11.95	1.87	11.12	0.01	3.39
17	12.20	12.70	1.86	12.02	0.01	3.51
18	12.55	13.10	2.46	12.47	0.03	3.82
19	12.26	13.50	2.88	12.58	0.03	3.95
20	12.61	13.25	2.61	12.33	0.04	3.87
21	13.92	12.75	2.52	11.99	0.03	3.97
22	13.50	11.89	2.03	12.73	0.00	3.81
23	13.66	11.64	1.99	13.85	0.00	3.93

Table A.4 The gas composition from peanut shell gasification (cont.).

Time	CO	CO <sub>2</sub>	CH <sub>4</sub>	H <sub>2</sub>	C <sub>n</sub> H <sub>m</sub>	LHV (MJ/m <sup>3</sup> )
24	13.03	11.90	2.41	12.90	0.02	3.91
25	13.19	11.39	2.25	13.55	0.01	3.94
26	13.35	11.07	1.78	13.45	0.00	3.78
27	13.49	11.09	1.70	13.40	0.00	3.76
28	13.40	11.35	1.82	13.20	0.00	3.77
29	13.00	11.48	1.89	13.16	0.00	3.74
30	14.45	12.18	1.89	12.30	0.03	3.84
31	14.30	12.36	2.89	11.60	0.04	4.11
32	14.68	11.56	3.30	11.33	0.01	4.26
33	14.22	10.84	2.53	11.30	0.00	3.92
34	14.29	10.67	1.92	11.29	0.00	3.71
35	14.49	10.41	1.77	11.46	0.00	3.70
36	14.55	10.38	1.62	11.05	0.00	3.61
37	14.57	10.25	1.59	10.81	0.00	3.58
38	14.38	10.06	1.59	11.39	0.00	3.62
39	14.20	10.27	1.48	12.47	0.00	3.67
40	14.37	11.07	1.40	12.10	0.00	3.62
41	13.63	11.86	1.56	11.59	0.00	3.53
42	13.47	11.22	2.12	12.04	0.00	3.76
43	13.71	10.72	1.88	13.56	0.00	3.87
44	13.80	10.81	1.57	13.99	0.00	3.82
45	13.00	11.98	1.68	14.00	0.02	3.76
46	13.95	12.45	2.98	13.50	0.05	4.30
47	13.98	12.74	3.37	11.62	0.04	4.24
48	13.41	12.38	3.45	10.72	0.03	4.10
49	13.27	10.88	3.02	9.59	0.00	3.79
50	13.20	10.41	1.82	10.80	0.00	3.48
Average	12.92	12.07	2.37	11.32	0.03	3.83

Table A.5 The gas composition from peanut shell gasification.

Peanut shell		total feed (g)		3000.00	g/min	45
Char		total solid (g)		166.84		
Tar		total liquid (g)		20.00	Heat	Recovery Unit
Gas		flow in (m <sup>3</sup> /hr)		3.54	Catalyst	Non-catalyst
Time	CO	CO <sub>2</sub>	CH <sub>4</sub>	H <sub>2</sub>	C <sub>n</sub> H <sub>m</sub>	LHV (MJ/m <sup>3</sup> )
0	0.00	0.00	0.00	0.00	0.00	0.00
1	0.88	1.95	0.34	0.00	0.06	0.25
2	1.68	2.98	0.41	0.00	0.06	0.38
3	2.47	6.37	0.42	0.00	0.05	0.48
4	2.10	7.88	0.04	0.00	0.05	0.30
5	3.37	9.19	0.97	0.22	0.00	0.80
6	9.64	12.97	3.34	4.17	0.09	2.89
7	11.50	14.33	4.36	5.41	0.15	3.65
8	11.71	14.07	4.47	6.40	0.16	3.83
9	11.53	13.43	4.11	7.38	0.14	3.77
10	11.16	12.93	3.66	8.49	0.11	3.67
11	11.54	13.41	3.99	8.83	0.11	3.88
12	10.57	12.98	3.29	8.84	0.07	3.49
13	9.96	12.64	3.29	8.87	0.05	3.41
14	10.21	12.77	2.92	9.46	0.05	3.37
15	9.91	12.64	3.20	9.02	0.07	3.39
16	9.17	11.36	3.01	8.23	0.06	3.14
17	8.87	11.12	2.90	8.09	0.03	3.04
18	9.85	10.42	2.77	8.42	0.04	3.16
19	11.09	10.22	2.22	9.89	0.00	3.26
20	10.75	10.93	2.20	10.06	0.01	3.23
21	10.44	11.44	2.75	10.23	0.04	3.42
22	10.92	11.78	3.25	10.69	0.06	3.72
23	12.19	11.99	2.51	10.69	0.02	3.60

Table A.5 The gas composition from peanut shell gasification (cont.).

Time	CO	CO <sub>2</sub>	CH <sub>4</sub>	H <sub>2</sub>	C <sub>n</sub> H <sub>m</sub>	LHV (MJ/m <sup>3</sup> )
24	13.04	11.89	2.05	10.65	0.00	3.53
25	13.25	12.36	2.04	10.77	0.00	3.57
26	12.95	12.35	2.08	11.02	0.00	3.57
27	12.04	12.45	1.89	10.35	0.00	3.31
28	10.89	11.99	1.83	9.45	0.00	3.05
29	10.70	11.89	1.67	8.79	0.00	2.90
30	11.10	12.33	1.28	7.66	0.00	2.69
31	11.18	12.56	1.08	7.10	0.00	2.57
32	9.98	12.56	1.67	6.76	0.00	2.59
33	9.24	12.45	1.12	6.58	0.00	2.28
34	9.89	11.11	0.91	6.28	0.09	2.29
35	10.41	11.29	0.84	6.12	0.10	2.31
36	11.51	11.24	0.74	6.60	0.09	2.46
37	12.78	10.98	0.69	5.90	0.07	2.52
38	13.74	10.62	0.66	5.78	0.08	2.63
39	14.54	10.14	0.64	5.49	0.07	2.68
40	14.68	9.77	0.59	4.34	0.06	2.56
41	13.65	10.14	0.70	3.69	0.07	2.40
42	13.05	10.34	0.88	4.90	0.08	2.52
43	12.16	10.66	0.88	4.09	0.09	2.33
44	12.08	10.56	0.71	3.60	0.00	2.17
45	12.07	10.34	0.71	3.50	0.00	2.16
46	12.03	10.23	0.90	3.90	0.00	2.26
47	12.05	10.44	0.80	3.50	0.00	2.19
48	12.10	10.20	0.60	3.00	0.00	2.07
49	12.10	10.56	0.36	3.20	0.00	2.00
50	12.09	10.22	0.90	4.90	0.00	2.38
Average	11.95	11.90	2.35	10.56	0.02	3.51



Table A.6 The gas composition from cassava rhizome ( $\leq 5\text{mm}$ ) gasification.

Cassava rhizome		total feed (g)	3100.00	g/min	100	
Char		total solid (g)	620.00			
Tar		total liquid (g)	63.00	Heat	Recovery Unit	
Gas		flow in ( $\text{m}^3/\text{hr}$ )	2.50	Catalyst	Non-catalyst	
Time	CO	CO <sub>2</sub>	CH <sub>4</sub>	H <sub>2</sub>	C <sub>n</sub> H <sub>m</sub>	LHV ( $\text{MJ}/\text{m}^3$ )
0	0.00	0.00	0.00	0.00	0	0.00
1	6.11	6.46	0.26	1.15	0.04	1.00
2	5.31	4.04	0.67	2.70	0.09	1.23
3	8.10	4.91	1.20	4.51	0	1.94
4	12.18	6.75	1.89	5.01	0.03	2.77
5	14.84	8.40	2.29	6.35	0.07	3.40
6	16.39	9.16	2.48	7.02	0.09	3.75
7	17.40	9.49	2.58	7.47	0.09	3.96
8	18.19	9.54	2.61	7.70	0.11	4.10
9	18.70	9.46	2.62	7.85	0.11	4.19
10	19.04	9.42	2.61	7.97	0.11	4.24
11	19.29	9.32	2.65	8.16	0.12	4.31
12	19.54	9.21	2.64	8.33	0.13	4.36
13	19.64	9.15	2.60	8.35	0.12	4.36
14	20.04	8.97	2.54	8.31	0.12	4.38
15	20.31	8.99	2.55	8.40	0.13	4.43
16	20.45	9.09	2.70	8.92	0.13	4.56
17	20.27	9.24	2.92	9.17	0.12	4.64
18	20.16	9.30	2.93	10.02	0.14	4.73
19	19.76	9.35	2.88	10.29	0.13	4.68
20	19.17	9.44	2.82	10.57	0.12	4.61
21	18.75	9.59	2.81	10.58	0.14	4.57
22	18.54	9.71	2.82	10.54	0.13	4.54
23	18.41	9.79	2.79	10.22	0.14	4.48

Table A.6 The gas composition from cassava rhizome ( $\leq 5\text{mm}$ ) gasification (cont.).

Time	CO	CO <sub>2</sub>	CH <sub>4</sub>	H <sub>2</sub>	C <sub>n</sub> H <sub>m</sub>	LHV (MJ/m <sup>3</sup> )
24	18.52	9.83	2.76	9.98	0.14	4.45
25	18.54	9.93	2.80	9.92	0.14	4.46
26	18.67	9.95	2.83	9.88	0.15	4.49
27	18.57	9.91	2.83	9.81	0.13	4.46
28	18.54	9.90	2.84	9.80	0.15	4.47
29	18.57	9.89	2.82	9.81	0.14	4.46
30	18.53	9.88	2.84	9.82	0.14	4.47
31	18.56	9.94	2.84	11.25	0.14	4.63
32	18.59	9.89	2.83	11.31	0.14	4.63
33	18.54	9.89	2.85	11.33	0.16	4.64
34	18.59	9.90	2.85	11.33	0.15	4.65
35	18.53	9.87	2.85	11.40	0.14	4.64
36	18.52	9.86	2.85	11.46	0.15	4.65
37	18.44	9.90	2.86	11.32	0.15	4.63
38	18.53	9.86	2.85	11.42	0.14	4.64
39	18.51	9.87	2.86	11.48	0.15	4.65
40	18.50	9.86	2.86	11.43	0.15	4.65
41	18.28	9.86	2.87	11.47	0.15	4.63
42	18.37	9.87	2.86	11.53	0.14	4.64
43	18.42	9.77	2.88	9.64	0.14	4.45
44	18.29	9.73	2.87	9.63	0.15	4.43
45	18.36	9.73	2.88	9.64	0.14	4.44
46	18.28	9.70	2.87	9.63	0.15	4.43
47	18.29	9.72	2.87	9.62	0.14	4.43
48	18.27	9.66	2.90	9.61	0.14	4.43
49	18.29	9.65	2.88	9.60	0.14	4.43
50	18.27	9.63	2.87	11.42	0.15	4.62
51	18.20	9.59	2.89	9.65	0.14	4.42

Table A.6 The gas composition from cassava rhizome ( $\leq 5\text{mm}$ ) gasification (cont.).

Time	CO	CO <sub>2</sub>	CH <sub>4</sub>	H <sub>2</sub>	C <sub>n</sub> H <sub>m</sub>	LHV (MJ/m <sup>3</sup> )
52	18.27	9.63	2.88	9.50	0.15	4.42
53	18.26	9.58	2.91	9.49	0.15	4.43
54	18.27	9.59	2.87	9.47	0.15	4.41
55	18.32	9.55	2.90	9.44	0.15	4.42
56	18.27	9.57	2.90	9.40	0.16	4.42
57	18.17	9.57	2.92	11.03	0.15	4.58
58	18.20	9.47	2.90	10.94	0.13	4.56
59	18.18	9.49	2.92	9.16	0.14	4.38
60	18.20	9.48	2.93	9.12	0.14	4.38
Average	18.82	9.66	2.81	10.11	0.14	4.5

Table A.7 The gas composition from cassava rhizome (5-10mm) gasification (cont.).

Cassava rhizome	total feed (g)	3000.00	g/min	50		
Char	total solid (g)	712.00				
Tar	total liquid (g)	40.00	Heat	Recovery Unit		
Gas	flow in (m <sup>3</sup> /hr)	2.50	Catalyst	Non-catalyst		
Time	CO	CO <sub>2</sub>	CH <sub>4</sub>	H <sub>2</sub>	C <sub>n</sub> H <sub>m</sub>	LHV (MJ/m <sup>3</sup> )
0	0.00	0.00	0.00	0.00	0.00	0.00
1	2.96	6.71	0.34	0.00	0.07	0.52
2	2.97	7.25	0.36	0.00	0.08	0.53
3	2.70	7.19	0.36	0.00	0.00	0.47
4	2.26	6.13	0.34	0.00	0.08	0.44
5	5.79	5.49	1.40	1.13	0.00	1.35
6	14.22	11.89	3.24	9.13	0.14	3.99
7	16.29	12.97	3.53	9.05	0.18	4.36
8	16.87	12.89	3.52	8.87	0.19	4.42
9	17.53	12.86	3.41	7.40	0.18	4.30
10	18.06	12.82	3.52	7.04	0.23	4.38

Table A.7 The gas composition from cassava rhizome (5-10mm) gasification (cont.).

Time	CO	CO <sub>2</sub>	CH <sub>4</sub>	H <sub>2</sub>	C <sub>n</sub> H <sub>m</sub>	LHV (MJ/m <sup>3</sup> )
11	18.31	13.00	3.69	6.82	0.24	4.45
12	18.28	12.80	3.86	6.85	0.24	4.51
13	18.06	12.44	3.94	7.31	0.25	4.57
14	18.96	12.34	3.72	7.77	0.23	4.65
15	18.99	12.29	3.54	7.81	0.22	4.59
16	18.76	12.14	3.41	7.53	0.20	4.47
17	18.86	12.11	3.40	7.30	0.20	4.46
18	18.64	12.66	3.46	7.86	0.21	4.52
19	18.56	12.59	3.44	8.49	0.19	4.56
20	18.75	12.99	3.40	9.24	0.19	4.65
21	18.46	12.89	3.29	10.58	0.18	4.72
22	17.66	12.76	3.17	10.95	0.17	4.61
23	16.14	12.88	3.10	11.41	0.16	4.44
24	16.99	12.76	3.01	11.84	0.14	4.55
25	16.78	12.10	2.98	12.06	0.14	4.54
26	16.85	12.32	2.99	12.32	0.12	4.57
27	16.75	12.49	2.96	12.50	0.14	4.57
28	16.79	12.63	2.94	12.58	0.13	4.58
29	16.86	12.67	2.94	12.69	0.13	4.60
30	16.99	12.66	2.94	12.90	0.12	4.63
31	16.23	12.77	2.89	12.99	0.12	4.53
32	16.21	12.78	2.81	13.12	0.11	4.51
33	16.20	12.79	2.80	13.11	0.12	4.51
34	15.42	12.85	2.78	13.17	0.12	4.41
35	15.23	12.76	2.75	13.14	0.12	4.37
36	15.86	12.77	2.74	13.14	0.12	4.45
37	15.43	12.68	2.71	13.42	0.12	4.41
38	15.00	12.69	2.68	13.16	0.11	4.31
39	15.21	12.64	2.65	13.01	0.10	4.31

Table A.7 The gas composition from cassava rhizome (5-10mm) gasification (cont.).

Time	CO	CO <sub>2</sub>	CH <sub>4</sub>	H <sub>2</sub>	C <sub>n</sub> H <sub>m</sub>	LHV (MJ/m <sup>3</sup> )
40	15.01	12.63	2.64	13.00	0.10	4.28
41	15.06	12.59	2.61	13.21	0.09	4.29
42	15.05	12.57	2.60	13.15	0.08	4.28
43	15.03	12.54	2.62	13.19	0.09	4.29
44	15.98	12.62	2.84	13.82	0.08	4.56
45	15.76	12.94	3.30	13.55	0.08	4.66
46	16.88	13.53	3.69	13.33	0.10	4.93
47	16.94	14.09	3.94	12.09	0.14	4.90
48	16.97	14.29	3.97	10.66	0.19	4.78
49	16.93	14.46	3.93	10.15	0.19	4.71
50	17.07	14.23	4.02	8.59	0.21	4.60
51	17.11	14.23	4.00	8.03	0.24	4.54
52	16.87	14.56	3.64	8.03	0.24	4.39
53	16.37	14.89	3.42	9.56	0.24	4.41
54	15.90	14.89	3.24	10.47	0.24	4.38
55	15.51	13.56	3.09	11.24	0.19	4.35
56	15.42	13.55	2.96	11.69	0.19	4.34
57	15.32	13.21	2.91	12.16	0.19	4.36
58	15.15	13.22	2.85	12.40	0.16	4.33
59	15.01	13.24	2.80	12.45	0.16	4.30
60	14.89	13.11	2.78	12.35	0.16	4.27
Average	16.39	13.02	3.18	11.08	0.16	4.5

Table A.8 The gas composition from cassava rhizome (10-15mm) gasification.

Cassava rhizome		total feed (g)		2700.00	g/min	64.28
Char		total solid (g)		340.00		
Tar		total liquid (g)		70.00	Heat	Recovery Unit
Gas		flow in (m <sup>3</sup> /hr)		2.50	Catalyst	Non-catalyst
Time	CO	CO <sub>2</sub>	CH <sub>4</sub>	H <sub>2</sub>	C <sub>n</sub> H <sub>m</sub>	LHV (MJ/m <sup>3</sup> )
0	0.00	0.00	0.00	0.00	0.00	0.00
1	0.21	3.83	0.14	0.00	0.04	0.09
2	7.29	6.64	1.76	3.61	0.02	1.95
3	9.72	9.78	1.97	5.98	0.04	2.59
4	9.81	11.07	1.40	5.98	0.01	2.39
5	8.60	11.33	0.93	4.17	0.00	1.87
6	8.25	12.87	1.44	4.67	0.01	2.07
7	10.58	13.66	2.47	7.87	0.07	3.09
8	11.95	13.45	2.75	9.49	0.10	3.55
9	12.90	13.17	2.63	10.86	0.09	3.78
10	12.65	12.82	2.41	10.63	0.07	3.63
11	12.15	12.94	2.19	10.38	0.06	3.46
12	11.42	12.77	2.02	10.05	0.06	3.27
13	11.51	12.41	2.24	10.77	0.06	3.44
14	11.56	12.79	2.25	11.67	0.06	3.55
15	11.67	13.13	2.27	11.60	0.07	3.56
16	12.10	13.81	2.76	12.00	0.10	3.85
17	10.27	14.21	2.70	11.85	0.12	3.59
18	10.29	14.53	2.99	11.33	0.13	3.64
19	12.18	14.58	3.02	10.80	0.14	3.83
20	12.45	14.44	3.07	10.25	0.15	3.83
21	12.65	14.32	3.08	9.89	0.16	3.82
22	13.11	14.26	3.12	9.58	0.16	3.86
23	13.50	13.95	3.10	9.32	0.16	3.88

Table A.8 The gas composition from cassava rhizome (10-15mm) gasification (cont.).

Time	CO	CO <sub>2</sub>	CH <sub>4</sub>	H <sub>2</sub>	C <sub>n</sub> H <sub>m</sub>	LHV (MJ/m <sup>3</sup> )
24	13.95	13.81	3.05	9.15	0.15	3.89
25	14.35	13.40	2.95	9.02	0.16	3.90
26	14.79	13.14	2.82	9.09	0.14	3.91
27	15.89	12.37	2.67	9.23	0.12	4.00
28	16.25	12.20	2.54	9.87	0.14	4.08
29	16.44	11.97	2.49	9.92	0.12	4.08
30	16.57	11.92	2.48	9.98	0.12	4.10
31	16.64	11.75	2.48	10.01	0.12	4.11
32	17.16	11.46	2.53	10.12	0.12	4.21
33	17.25	11.81	2.56	10.09	0.13	4.23
34	17.34	11.74	2.57	10.09	0.13	4.25
35	17.45	11.67	2.58	10.08	0.12	4.26
36	17.62	11.73	2.59	10.09	0.13	4.29
37	17.84	11.82	2.69	10.38	0.13	4.38
38	18.11	12.02	2.94	10.73	0.14	4.55
39	18.45	12.10	3.21	10.85	0.14	4.70
40	18.24	12.34	3.40	10.39	0.18	4.71
41	18.01	12.43	3.44	9.70	0.18	4.62
42	17.62	12.40	3.22	9.47	0.20	4.47
43	17.35	12.38	3.52	9.51	0.19	4.55
44	17.28	12.10	3.12	9.70	0.17	4.41
45	17.32	11.71	2.90	10.37	0.15	4.40
46	17.40	11.70	2.81	10.71	0.14	4.41
47	17.09	11.76	2.67	11.12	0.12	4.36
48	17.09	11.83	2.63	11.15	0.12	4.35
49	16.93	11.59	2.60	11.39	0.11	4.34
50	16.77	11.57	2.61	11.53	0.11	4.34
51	16.73	11.48	2.61	11.63	0.12	4.35
52	16.79	11.60	2.61	11.64	0.11	4.35

Table A.8 The gas composition from cassava rhizome (10-15mm) gasification (cont.).

Time	CO	CO <sub>2</sub>	CH <sub>4</sub>	H <sub>2</sub>	C <sub>n</sub> H <sub>m</sub>	LHV (MJ/m <sup>3</sup> )
53	16.79	11.82	2.62	11.59	0.12	4.35
54	16.57	11.71	2.62	11.49	0.11	4.31
55	16.24	11.76	2.58	11.53	0.12	4.26
56	16.04	11.66	2.58	11.45	0.11	4.22
57	15.75	11.95	2.62	11.60	0.11	4.22
58	15.60	11.97	2.60	11.76	0.12	4.21
59	15.68	12.14	2.97	12.17	0.13	4.40
60	15.99	12.19	3.05	11.89	0.14	4.44
Average	15.68	12.35	2.80	10.67	0.13	4.18

Table A.9 The gas composition from peanut shell gasification with 5%Ni/dolomite.

Cassava rhizome	total feed (g)	1800.00	g/min	32		
Char	total solid (g)	321.00	Catalyst	300g		
Tar	total liquid (g)	69.00	Heat	Recovery Unit		
Gas	flow in (m <sup>3</sup> /hr)	1.62				
Time	CO	CO <sub>2</sub>	CH <sub>4</sub>	H <sub>2</sub>	C <sub>n</sub> H <sub>m</sub>	LHV (MJ/m <sup>3</sup> )
0	0.00	0.00	0.00	0.00	0.00	0.00
1	3.79	1.51	0.45	2.00	0.14	0.86
2	5.62	7.99	1.52	3.77	0.00	1.66
3	8.75	10.19	1.59	5.46	0.00	2.26
4	9.93	11.14	1.89	6.17	0.00	2.60
5	10.18	12.43	2.00	4.97	0.01	2.54
6	10.38	12.73	2.25	5.03	0.02	2.66
7	11.22	12.98	2.70	5.33	0.02	2.96
8	12.03	12.56	3.19	5.28	0.10	3.23
9	11.76	12.63	3.07	6.30	0.09	3.26
10	11.14	12.43	2.75	7.53	0.08	3.20
11	10.43	12.16	2.49	5.69	0.07	2.82
12	10.37	13.06	2.58	8.02	0.08	3.10



Table A.9 The gas composition from peanut shell gasification with 5%Ni/dolomite  
(cont.).

Time	CO	CO <sub>2</sub>	CH <sub>4</sub>	H <sub>2</sub>	C <sub>n</sub> H <sub>m</sub>	LHV (MJ/m <sup>3</sup> )
13	10.35	13.28	2.78	8.46	0.00	3.21
14	10.27	12.25	2.16	8.27	0.14	2.96
15	11.13	10.84	1.51	8.14	0.00	2.83
16	11.18	10.27	1.27	8.14	0.00	2.75
17	10.26	10.78	1.97	7.93	0.00	2.86
18	10.77	11.25	2.47	8.02	0.01	3.11
19	10.77	11.25	2.47	8.02	0.02	3.11
20	13.01	12.01	4.06	9.30	0.02	4.10
21	12.47	10.93	2.88	9.43	0.10	3.62
22	12.38	9.97	2.00	9.39	0.09	3.29
23	12.56	9.22	1.50	9.37	0.08	3.14
24	12.90	8.86	1.41	9.39	0.07	3.15
25	12.59	8.87	1.26	9.41	0.08	3.06
26	12.42	9.19	1.35	9.51	0.05	3.08
27	12.64	9.54	1.81	9.61	0.04	3.28
28	13.25	9.63	2.23	10.10	0.00	3.56
29	13.07	9.45	2.10	10.00	0.02	3.48
30	13.49	9.52	2.84	10.20	0.02	3.82
31	13.49	9.52	2.84	10.20	0.05	3.68
32	12.31	11.31	3.36	8.60	0.05	3.21
33	11.77	10.23	2.18	8.73	0.15	2.88
34	11.68	9.27	1.30	8.69	0.11	2.72
35	11.86	8.52	0.80	8.67	0.05	2.73
36	12.20	8.16	0.71	8.69	0.02	2.64
37	11.89	8.17	0.56	8.71	0.00	2.67
38	11.72	8.49	0.65	8.81	0.00	2.87
39	11.94	8.84	1.11	8.91	0.00	3.15
40	12.55	8.93	1.53	9.40	0.00	3.07
Average	11.78	10.70	2.19	8.76	0.05	3.23

Table A.10 The gas composition from cassava rhizome (10-15mm) gasification with 5%Ni/dolomite.

Cassava rhizome		total feed (g)	2000.00	g/min	40	
Char		total solid (g)	240.00	300g		
Tar		total liquid (g)	30.00	Heat	Recovery Unit	
Gas		flow in (m <sup>3</sup> /hr)	1.98			
Time	CO	CO <sub>2</sub>	CH <sub>4</sub>	H <sub>2</sub>	C <sub>n</sub> H <sub>m</sub>	LHV (MJ/m <sup>3</sup> )
0	0.00	0.00	0.00	0.00	0.00	0.00
1	8.79	7.89	1.95	1.93	0.00	0.00
2	14.49	14.67	1.14	5.42	0.15	2.02
3	15.01	15.56	1.52	6.56	0.10	2.82
4	15.06	15.76	1.03	8.07	0.13	3.15
5	14.81	15.61	1.04	9.07	0.10	3.14
6	14.41	15.21	1.03	12.95	0.12	3.22
7	13.99	14.74	1.3	13.56	0.16	3.59
8	13.78	14.52	1.12	15.98	0.14	3.70
9	14.48	12.36	1.15	15.47	0.10	3.87
10	14.96	12.56	1.14	15.84	0.10	3.91
11	14.86	12.45	1.1	15.68	0.10	4.01
12	14.46	12.65	1.17	15.98	0.10	3.96
13	15.75	12.58	1.84	15.64	0.10	3.97
14	15.49	13.24	1.36	15.36	0.10	4.34
15	15.99	13.25	1.31	15.46	0.10	4.10
16	15.25	13.26	1.35	15.68	0.10	4.16
17	15.56	13.42	1.47	15.98	0.10	4.10
18	15.42	12.56	1.85	15.64	0.10	4.22
19	15.26	12.54	1.23	15.46	0.10	4.30
20	16.48	12.89	1.36	15.86	0.10	4.04
21	16.68	12.87	1.96	15.95	0.10	4.28
22	16.34	12.36	1.52	15.68	0.12	4.53

Table A.10 The gas composition from cassava rhizome (10-15mm) gasification with 5%Ni/dolomite (cont.).

Time	CO	CO <sub>2</sub>	CH <sub>4</sub>	H <sub>2</sub>	C <sub>n</sub> H <sub>m</sub>	LHV (MJ/m <sup>3</sup> )
23	16.49	12.45	1.95	15.46	0.15	4.45
24	16.79	12.84	1.26	15.26	0.15	4.22
25	17.6	12.02	1.26	13.6	0.15	4.14
26	13.91	14.71	0.14	8.17	0.10	2.69
27	13.51	14.31	0.13	12.05	0.10	3.06
28	13.09	13.84	0.4	12.66	0.10	3.16
29	12.88	13.62	0.22	15.08	0.10	3.34
30	13.58	11.46	0.25	14.57	0.10	3.38
31	14.06	11.66	0.24	14.94	0.10	3.48
32	13.96	11.55	0.2	14.78	0.10	3.43
33	13.56	11.75	0.27	15.08	0.10	3.44
34	14.85	11.68	0.94	14.74	0.10	3.80
35	14.59	12.34	0.46	14.46	0.10	3.57
36	15.09	12.35	0.41	14.56	0.10	3.63
37	14.35	12.36	0.45	14.78	0.10	3.57
38	14.66	12.52	0.57	15.08	0.10	3.69
39	14.52	11.66	0.95	14.74	0.10	3.77
40	14.36	11.64	0.33	14.56	0.10	3.51
Average	15.11	12.95	1.34	15.68	0.10	4.08

Table A.11 The gas composition from peanut shell gasification

Gas composition (%)	Non-Heat Recovery				
Air flow (m <sup>3</sup> /hr)	1.62	1.98	2.34	3.05	3.54
H <sub>2</sub>	10.26	11.98	10.76	11.32	10.56
CO	11.17	15.92	11.34	12.92	11.95
CO <sub>2</sub>	12.22	15.42	12.42	12.07	11.90
CH <sub>4</sub>	3.55	2.60	2.45	2.40	2.36
C <sub>x</sub> H <sub>y</sub>	0.06	0.07	0.03	0.03	0.02
LHV (MJ/m <sup>3</sup> )	3.79	4.23	3.47	3.71	3.49
	Heat Recovery				
H <sub>2</sub>	10.26	11.98	10.76	11.32	10.56
CO	11.17	15.92	11.34	12.92	11.95
CO <sub>2</sub>	12.22	15.42	12.42	12.07	11.90
CH <sub>4</sub>	3.55	2.60	2.45	2.40	2.36
C <sub>x</sub> H <sub>y</sub>	0.06	0.07	0.03	0.03	0.02
LHV (MJ/m <sup>3</sup> )	3.79	4.23	3.47	3.72	3.49

Table A.12 The gas composition from cassava rhizome (5-10mm) gasification

Sizes	Gas composition (%)		Heat Recovery			
	Air flow (m <sup>3</sup> /hr)					
1-5 mm	H <sub>2</sub>	14.77	17.23	18.82	14.49	
	CO	15.66	13.27	9.66	11.92	
	CO <sub>2</sub>	2.94	3.24	2.81	2.70	
	CH <sub>4</sub>	14.41	10.38	10.11	10.97	
	C <sub>x</sub> H <sub>y</sub>	0.11	0.16	0.14	0.13	
	LHV (MJ/m <sup>3</sup> )	4.55	4.57	4.52	4.05	
5-10 mm	H <sub>2</sub>	14.82	13.69	16.39	17.82	
	CO	15.62	15.62	13.02	11.80	
	CO <sub>2</sub>	3.07	2.84	3.18	3.19	
	CH <sub>4</sub>	15.31	12.79	11.08	11.11	
	C <sub>x</sub> H <sub>y</sub>	0.11	0.11	0.16	0.14	
	LHV (MJ/m <sup>3</sup> )	4.71	4.18	4.50	4.70	
10-15 mm	H <sub>2</sub>	13.54	15.07	15.68	16.91	
	CO	14.81	12.54	12.35	11.70	
	CO <sub>2</sub>	2.89	2.76	2.80	3.01	
	CH <sub>4</sub>	9.37	11.14	10.67	10.91	
	C <sub>x</sub> H <sub>y</sub>	0.13	0.12	0.13	0.13	
	LHV (MJ/m <sup>3</sup> )	4.00	4.19	4.18	4.41	

Table A.13 Ultimate analysis of char from gasification of peanut shell

unit	(%wt.)	Air flow rate (m <sup>3</sup> /hr)			
		1.98	2.34	.250	3.06
Heat Recovery	C	12.83	7.7	4.88	3.7
	H	0.53	0.33	0.15	0.12
	N	0.25	0.21	0.1	0.07
	S	0.12	0.13	0.11	0.21
	O	15.04	15.36	14.61	11.49
	Other*	71.23	76.27	80.15	84.41
Non-Heat Recovery	C	18.65	15.91	3.66	3.58
	H	0.71	0.65	0.13	0.13
	N	0.39	0.32	0.06	0.07
	S	0.21	0.22	0.18	0.19
	O	15.3	16.05	9.27	10.59
	Other*	64.74	66.85	86.7	85.44

Table A.14 Ultimate analysis of char from cassava rhizome gasification.

Particle size		Air flow rate (m <sup>3</sup> /hr)			
(mm)	(%wt.)	1.98	2.34	.250	3.06
1-5	C	7.85	11.77	12.77	6.92
	H	0.29	0.53	0.24	0.04
	N	0.12	0.24	0.04	0.56
	S	0.03	0.04	0.01	0.04
	O	0.36	0.56	0.42	0.35
	Other*	92.96	89.61	88.33	93.89
5-10	C	6.46	9.34	9.42	4.78
	H	0.26	0.45	0.37	0.20
	N	0.11	0.15	0.18	0.09
	S	0.01	0.07	0.07	0.01
	O	0.4	0.48	0.49	0.27
	Other*	94.32	91.80	91.69	95.79
10-15	C	6.76	5.86	5.73	5.52
	H	0.27	0.18	0.21	0.19
	N	0.15	0.12	0.10	0.09
	S	0.00	0.01	0.02	0.00
	O	0.30	0.31	0.30	0.02
	Other*	93.65	94.77	94.90	94.78

\*Other (mainly inorganics) by difference

Table A.15 The chemical compounds identified by GC-MS analysis in tar (peanut shell gasification).

Compound	Area (%)	Formula
Phenol	1.68	C <sub>6</sub> H <sub>6</sub> O
Azulene	1.47	C <sub>10</sub> H <sub>8</sub>
Phenol, 4-methyl-	5.89	C <sub>7</sub> H <sub>8</sub> O
2-Methoxy-4-methylphenol	1.15	C <sub>8</sub> H <sub>10</sub> O <sub>2</sub>
Phenol, 2,4-dimethyl-	3.4	C <sub>8</sub> H <sub>10</sub> O
Phenol, 4-ethyl-	1.4	C <sub>8</sub> H <sub>10</sub> O
Phenol, 3,5-dimethyl-	1.41	C <sub>8</sub> H <sub>10</sub> O
Naphthalene, 2-methyl-	2.3	C <sub>11</sub> H <sub>10</sub>
Phenol, 4-ethyl-2-methoxy-	1.98	C <sub>9</sub> H <sub>12</sub> O <sub>2</sub>
2-Methoxy-4-vinylphenol	1.67	C <sub>9</sub> H <sub>10</sub> O <sub>2</sub>
Phenol, 2,6-dimethoxy-	4.3	C <sub>8</sub> H <sub>10</sub> O <sub>3</sub>
Biphenylene	4	C <sub>12</sub> H <sub>8</sub>
Phenol, 2-methoxy-4-(1-propenyl)-	5.74	C <sub>10</sub> H <sub>12</sub> O <sub>2</sub>
1,2,4-Trimethoxybenzene	1.89	C <sub>9</sub> H <sub>12</sub> O <sub>3</sub>
Dibenzofuran	0.94	C <sub>12</sub> H <sub>8</sub> O
1-Hexadecene	1.36	C <sub>16</sub> H <sub>32</sub>
5-tert-Butylpyrogallol	2.14	C <sub>10</sub> H <sub>14</sub> O <sub>3</sub>
9H-Fluorene	1.8	C <sub>13</sub> H <sub>10</sub>
Ethanone, 1-(4-hydroxy-3-methoxyphenyl)-	3.34	C <sub>9</sub> H <sub>10</sub> O <sub>3</sub>
1,2-Benzenedicarboxylic acid, diethyl ester	1.63	C <sub>12</sub> H <sub>14</sub> O <sub>4</sub>
Phenol, 2-methoxy-4-propyl-	2.02	C <sub>10</sub> H <sub>14</sub> O <sub>2</sub>
1-Heptadecene	7.29	C <sub>17</sub> H <sub>34</sub>
Phenol, 2,6-dimethoxy-4-(2-propenyl)-	4.21	C <sub>11</sub> H <sub>14</sub> O <sub>3</sub>
1,6-Anhydro-.beta.-D-glucopyranose (levoglucosan)	5.03	C <sub>6</sub> H <sub>10</sub> O <sub>5</sub>
Propennitrile, 2-(benzoxazol-2-yl)-3-hydroxy-	1.03	C <sub>10</sub> H <sub>6</sub> N <sub>2</sub> O <sub>2</sub>
Anthracene	4.88	C <sub>14</sub> H <sub>10</sub>
Decanoic acid, methyl ester	1.03	C <sub>11</sub> H <sub>22</sub> O <sub>2</sub>



Table A.15 The chemical compounds identified by GC-MS analysis in tar (peanut shell gasification).

Compound	Area (%)	Formula
Ethanone, 1-(4-hydroxy-3,5-dimethoxyphenyl)-	1.85	C <sub>10</sub> H <sub>12</sub> O <sub>4</sub>
2-Bromo dodecane	1.08	C <sub>12</sub> H <sub>25</sub> Br
1-Nonadecene	4	C <sub>19</sub> H <sub>38</sub>
9-Octadecenoic acid (Z)-, methyl ester	1.4	C <sub>19</sub> H <sub>36</sub> O <sub>2</sub>
2-Bromo dodecane	1.65	C <sub>12</sub> H <sub>25</sub> Br
Eicosane	0.98	C <sub>20</sub> H <sub>42</sub>
Oxacycloheptadec-8-en-2-one	1.52	C <sub>16</sub> H <sub>28</sub> O <sub>2</sub>
1-Hexadecanesulfonyl chloride	2.07	C <sub>16</sub> H <sub>33</sub> ClO <sub>2</sub> S
Pyrene	2.43	C <sub>16</sub> H <sub>10</sub>
Tributyl acetylcitrate	2.12	C <sub>20</sub> H <sub>34</sub> O <sub>8</sub>
1-Nonadecene	6.16	C <sub>19</sub> H <sub>38</sub>

Table A.16 The chemical compounds identified by GC-MS analysis in tar (cassava rhizome gasification).

Compound	Area (%)	Formula
Phenol	1.98	C <sub>6</sub> H <sub>6</sub> O
Azulene	1.77	C <sub>10</sub> H <sub>8</sub>
Phenol, 4-methyl-	6.19	C <sub>7</sub> H <sub>8</sub> O
2-Methoxy-4-methylphenol	1.45	C <sub>8</sub> H <sub>10</sub> O <sub>2</sub>
Phenol, 2,4-dimethyl-	3.7	C <sub>8</sub> H <sub>10</sub> O
Phenol, 4-ethyl-	1.7	C <sub>8</sub> H <sub>10</sub> O
Phenol, 3,5-dimethyl-	1.71	C <sub>8</sub> H <sub>10</sub> O
Naphthalene, 2-methyl-	2.6	C <sub>11</sub> H <sub>10</sub>
Phenol, 4-ethyl-2-methoxy-	2.28	C <sub>9</sub> H <sub>12</sub> O <sub>2</sub>
2-Methoxy-4-vinylphenol	1.97	C <sub>9</sub> H <sub>10</sub> O <sub>2</sub>
Phenol, 2,6-dimethoxy-	4.6	C <sub>8</sub> H <sub>10</sub> O <sub>3</sub>

Table A.16 The chemical compounds identified by GC-MS analysis in tar (cassava rhizome gasification) (cont.).

Compound	Area (%)	Formula
Biphenylene	4.3	C <sub>12</sub> H <sub>8</sub>
Phenol, 2-methoxy-4-(1-propenyl)-	6.04	C <sub>10</sub> H <sub>12</sub> O <sub>2</sub>
1,2,4-Trimethoxybenzene	2.19	C <sub>9</sub> H <sub>12</sub> O <sub>3</sub>
Dibenzofuran	1.24	C <sub>12</sub> H <sub>8</sub> O
1-Hexadecene	1.66	C <sub>16</sub> H <sub>32</sub>
5-tert-Butylpyrogallol	2.44	C <sub>10</sub> H <sub>14</sub> O <sub>3</sub>
9H-Fluorene	2.1	C <sub>13</sub> H <sub>10</sub>
Ethanone, 1-(4-hydroxy-3-methoxyphenyl)-	3.64	C <sub>9</sub> H <sub>10</sub> O <sub>3</sub>
1,2-Benzenedicarboxylic acid, diethyl ester	1.93	C <sub>12</sub> H <sub>14</sub> O <sub>4</sub>
Phenol, 2-methoxy-4-propyl-	2.32	C <sub>10</sub> H <sub>14</sub> O <sub>2</sub>
1-Heptadecene	7.59	C <sub>17</sub> H <sub>34</sub>
Phenol, 2,6-dimethoxy-4-(2-propenyl)-	4.51	C <sub>11</sub> H <sub>14</sub> O <sub>3</sub>
1,6-Anhydro-.beta.-D-glucopyranose (levoglucosan)	5.33	C <sub>6</sub> H <sub>10</sub> O <sub>5</sub>
Propennitrile, 2-(benzoxazol-2-yl)-3-hydroxy-	1.33	C <sub>10</sub> H <sub>6</sub> N <sub>2</sub> O <sub>2</sub>
Anthracene	5.18	C <sub>14</sub> H <sub>10</sub>
Decanoic acid, methyl ester	1.33	C <sub>11</sub> H <sub>22</sub> O <sub>2</sub>
Ethanone, 1-(4-hydroxy-3,5-dimethoxyphenyl)-	2.15	C <sub>10</sub> H <sub>12</sub> O <sub>4</sub>
2-Bromo dodecane	1.38	C <sub>12</sub> H <sub>25</sub> Br
1-Nonadecene	4.3	C <sub>19</sub> H <sub>38</sub>
9-Octadecenoic acid (Z)-, methyl ester	1.7	C <sub>19</sub> H <sub>36</sub> O <sub>2</sub>
2-Bromo dodecane	1.95	C <sub>12</sub> H <sub>25</sub> Br

Table A.16 The chemical compounds identified by GC-MS analysis in tar (cassava rhizome gasification) (cont.).

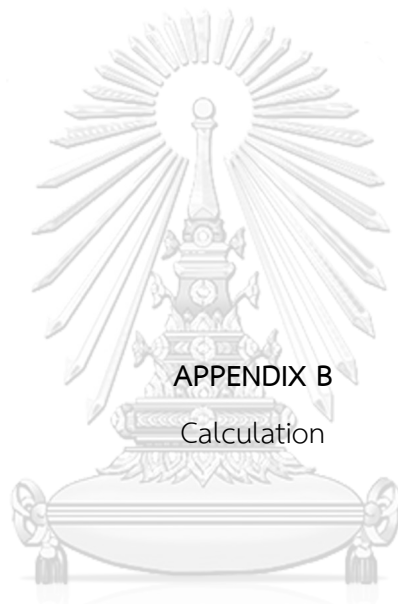
Compound	Area (%)	Formula
2-Bromo dodecane	1.95	C <sub>12</sub> H <sub>25</sub> Br
Eicosane	1.28	C <sub>20</sub> H <sub>42</sub>
Oxacycloheptadec-8-en-2-one	1.82	C <sub>16</sub> H <sub>28</sub> O <sub>2</sub>
1-Hexadecanesulfonyl chloride	2.37	C <sub>16</sub> H <sub>33</sub> ClO <sub>2</sub> S
Pyrene	2.73	C <sub>16</sub> H <sub>10</sub>
Tributyl acetylcitrate	2.42	C <sub>20</sub> H <sub>34</sub> O <sub>8</sub>
1-Nonadecene	6.46	C <sub>19</sub> H <sub>38</sub>

Table A.17 The gas composition and the efficiency of gasifier-cogeneration system from peanut shell gasification.

Gas composition (%)	1	2	3	Average	SD
H <sub>2</sub>	8.20	11.84	11.74	10.59	2.07
CO	14.51	14.25	14.05	14.27	0.23
CO <sub>2</sub>	8.27	13.21	13.43	11.64	2.92
CH <sub>4</sub>	3.00	2.22	2.91	2.71	0.43
C <sub>x</sub> H <sub>y</sub>	0.13	0.11	0.15	0.13	0.02
LHV (MJ/m <sup>3</sup> )	3.79	3.89	4.08	3.92	0.15
Cold gas efficiency (%)	53.66	54.76	57.73	55.38	2.11
The efficiency of generation (%)	11.03	10.61	10.49	10.71	0.28
The efficiency of gasifier-cogeneration system (%)	11.84	11.62	12.11	11.86	0.25

Table A.18 The gas composition and the efficiency of gasifier-cogeneration system from cassava rhizome (10-15mm) gasification.

Gas composition (%)	1	2	3	Average	SD
H <sub>2</sub>	10.92	11.21	11.24	11.12	0.18
CO	15.37	15.97	13.49	14.94	1.29
CO <sub>2</sub>	10.12	12.93	12.77	11.94	1.58
CH <sub>4</sub>	2.98	3.23	2.83	3.01	0.20
C <sub>x</sub> H <sub>y</sub>	0.18	0.15	0.15	0.16	0.02
LHV (MJ/m <sup>3</sup> )	4.19	4.37	3.93	4.16	0.22
Cold gas efficiency (%)	54.92	53.90	50.61	53.14	2.25
The efficiency of generation (%)	11.29	10.42	10.77	10.83	0.44
The efficiency of gasifier-cogeneration system (%)	12.40	11.23	10.90	11.51	0.79



APPENDIX B  
Calculation

จุฬาลงกรณ์มหาวิทยาลัย  
CHULALONGKORN UNIVERSITY

### Equivalent Ratio, ER

ER is the ratio of actual mole of oxygen to the stoichiometric mole of oxygen for particular oxidation process.

$$ER = \frac{\text{Actual mole of Oxygen}}{\text{Stoichiometric mole of Oxygen}}$$

### Carbon and Hydrogen Conversion

Carbon conversion is the percentage of carbon mole in raw material convert to the carbon mole of gaseous products. The carbon conversion can calculate in many terms such as carbon conversion to carbon-monoxide, carbon conversion to carbon-dioxide.

$$\text{Carbon conversion} = \frac{\text{carbon mole of gaseous products}}{\text{carbon mole in raw material}}$$

Hydrogen conversion is the percentage in hydrogen mole of raw material convert to the hydrogen mole of gaseous products. The hydrogen conversion can calculate in many terms such as hydrogen conversion to hydrogen gas, hydrogen conversion to methane.

$$\text{Hydrogen conversion} = \frac{\text{hydrogen mole of gaseous products}}{\text{hydrogen mole in raw material}}$$

### Portable GAS3100P Syngas Analyser

Syngas production methods include steam reforming of natural gas or liquid hydrocarbons to produce hydrogen, the gasification of coal and biomass or Plasma gasification process (produces rich syngas including H<sub>2</sub> and CO)

- Coal chemical process
- Steel making process as
- Blast furnace top gas
- Converter
- Coking
- Direct iron ore smelting reduction processes
- Coal or Biomass gasification
- Others

### Standard measuring ranges

GAS 3100 Syngas

CO: 0-100%

CO<sub>2</sub>: 0-50%

CH<sub>4</sub>: 0-10%

C<sub>n</sub>H<sub>m</sub>: 0-10%

H<sub>2</sub>: 0-50%

Detector	CO, CO <sub>2</sub> , CH <sub>4</sub> , C <sub>n</sub> H <sub>m</sub> : proprietary dual beam NDIR detectors O <sub>2</sub> : industrial electrochemical cell H <sub>2</sub> : proprietary thermal conductivity detector Other ranges customizable on request without price increase
Resolution	0.01%
Accuracy	≤} 2% FS
Repeatability	≤ 2%
Zero	Auto-zeroing function via keyboard interface
Flow	0.7 to 1.2L/min, internal gas sampling pump
Inlet pressure	2 to 50 kPa
Gas conditions	No dust, no water vapour, no tar

Operating conditions Tamb : 0-50°C / Pamb : 86 to 108 kPa / RH : 0-95% non-condensing

Response time (T90) ≤ 15 sec

Warm-up time 15 min

Communication RS232 (real time and memory data download software included)

Power supply External 220 VAC-50Hz

Data logging Up to 1500 sets of 7 data

Possibility to identify 10 different sites and up to 100 measuring points

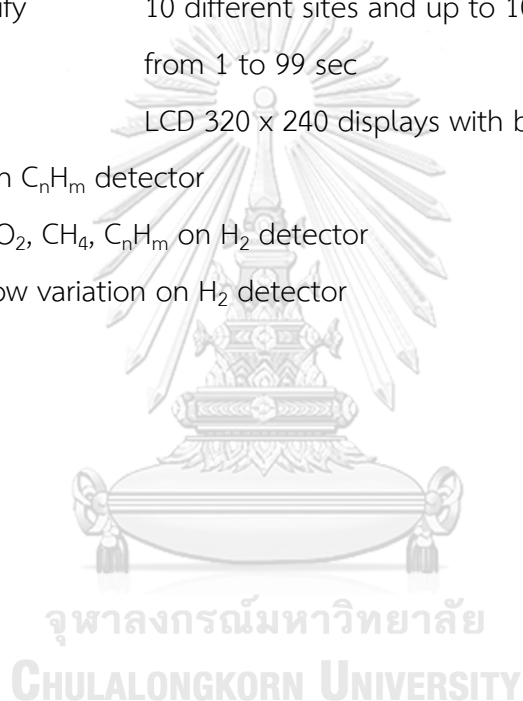
Logging rate from 1 to 99 sec

Display LCD 320 x 240 displays with back-lit function

No effect of CH<sub>4</sub> on C<sub>n</sub>H<sub>m</sub> detector

No effect of CO, CO<sub>2</sub>, CH<sub>4</sub>, C<sub>n</sub>H<sub>m</sub> on H<sub>2</sub> detector

No effect of gas flow variation on H<sub>2</sub> detector







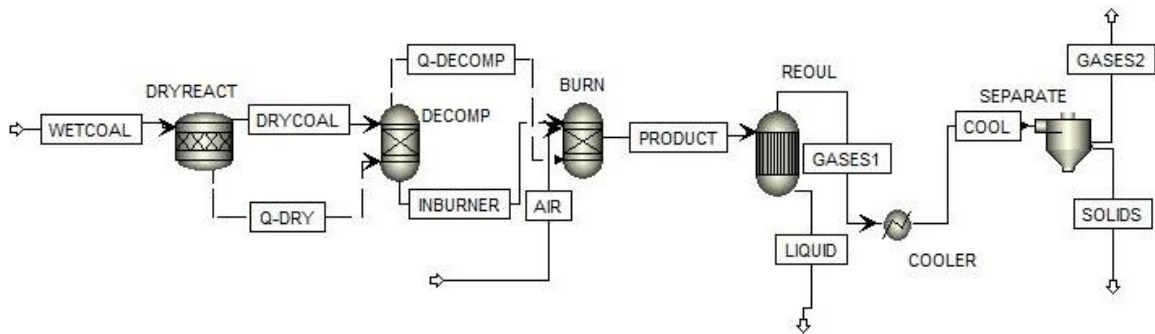
APPENDIX C

Model

จุฬาลงกรณ์มหาวิทยาลัย  
**CHULALONGKORN UNIVERSITY**

## Modeling Coal Drying and Coal Combustion

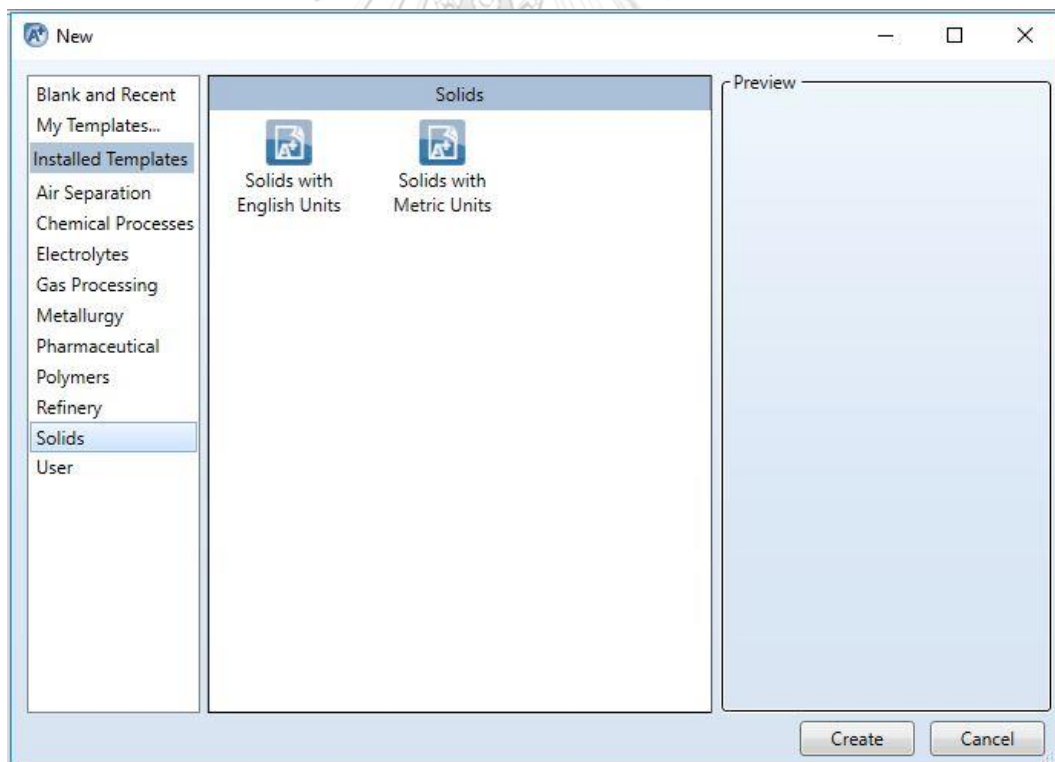
### 1. Flowsheet



### 2. To start Aspen Plus

2.1 Open Aspen Plus V8.8

2.2 Select the Solids with English Units template. (To Specify the Application Type and Run Type for the New Run)

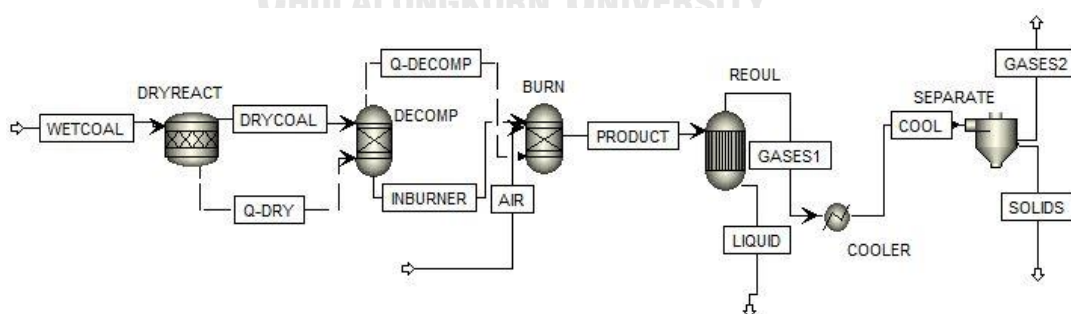


2.3 Click Create to apply this option

### 3. Drawing the Graphical Simulation Flowsheet

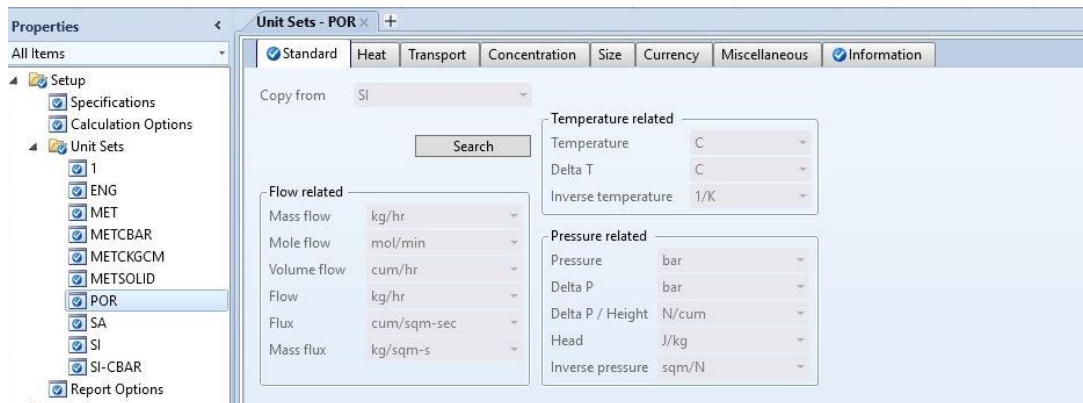
The simulation flowsheet shown in the following figure feeds the WETCOAL stream to an RStoic model. In the RStoic block (DRYREACT), a portion of the coal reacts to form water. Because the RStoic model has a single outlet stream (DRYCOAL).

Use the RGibbs model to simulate combustion of the dry coal. RGibbs models chemical equilibrium by minimizing Gibbs free energy. However, the Gibbs free energy of coal cannot be calculated because it is a nonconventional component. Before feeding the dried coal to the RGibbs block, BURN, decompose the coal into its constituent elements. This is done in the RYield block, DECOMP. The heat of reaction associated with the decomposition of coal must be considered in the coal combustion. Use a heat stream to carry this heat of reaction from the RStoic to RYield block and from the RYield block to the RGibbs block. Then, the product from BURN block move to the Requil block, REQUIL to react the reaction of gasification. The liquid and Gas products was separate in this block. The gas product move to the cooler system. Finally, separate the combustion gases from the ash using the Aspen Plus model SSplit, SEPARATE, for this separation.



#### 4. Specifying Unit set

4.1 In the Data Browser window. The Setup | Specifications | Unit Sets Use this sheet to review unit sets that were set in my simulation. Set the unit as the following figure.

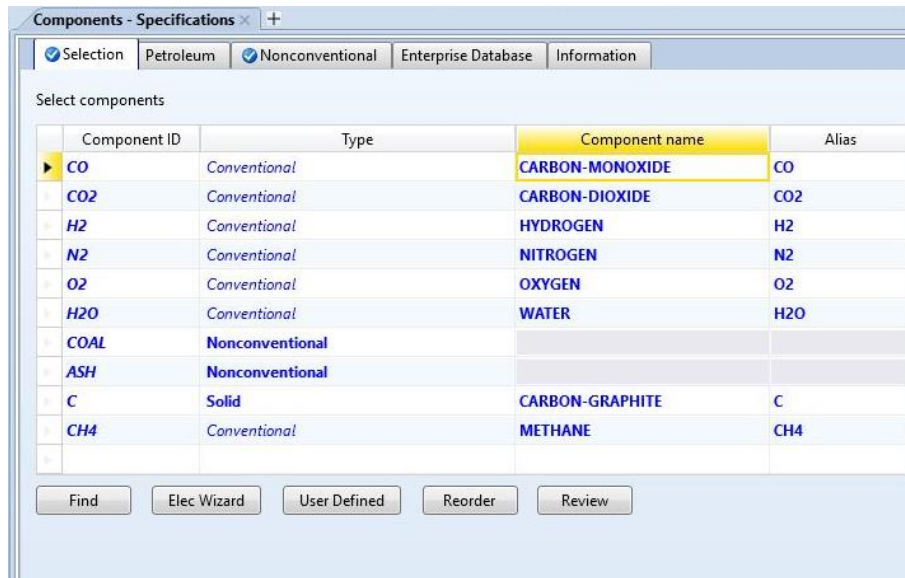


#### 5. Specifying Components

The Components | Specifications | Selection sheet is used to enter the components present in the simulation. The components in this simulation are CO, CO<sub>2</sub>, H<sub>2</sub>, N<sub>2</sub>, O<sub>2</sub>, H<sub>2</sub>O, C, CH<sub>4</sub>.COAL and ASH

5.1 Add the components listed below:


Component ID	Type	Component Name
CO	Conventional	CARBON-MONOXIDE
CO <sub>2</sub>	Conventional	CARBON-DIOXIDE
H <sub>2</sub>	Conventional	HYDROGEN
N <sub>2</sub>	Conventional	NITROGEN
O <sub>2</sub>	Conventional	OXYGEN
H <sub>2</sub> O	Conventional	WATER
CH <sub>4</sub>	Conventional	METHANE
COAL	Nonconventional	
ASH	Nonconventional	
C	Solid	CARBON-GRAPHITE

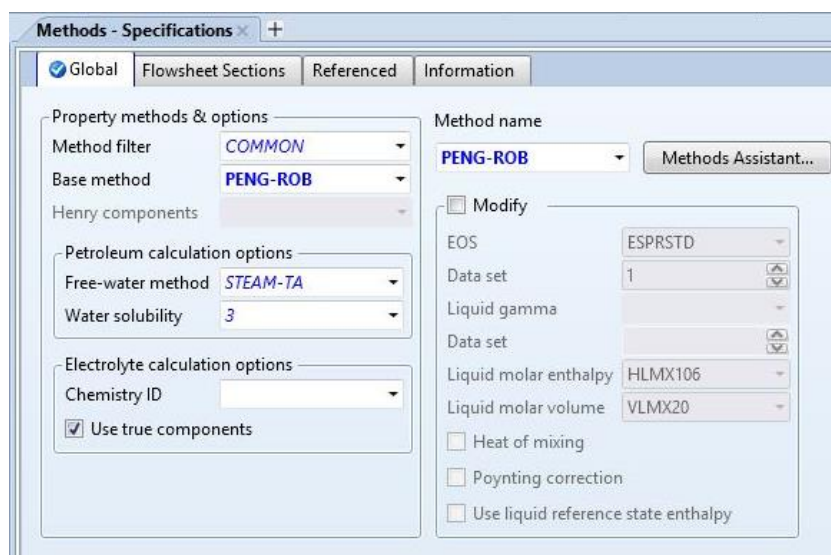


## 6. Specifying Methods

The Properties | Methods | Specifications | Global sheet is used to select the thermodynamic methods used to calculate properties such as K-values, enthalpy, and density. Property methods in Aspen Plus are categorized into various process types.

Because the physical property methods for solid components are the same for all property methods, select a property method based on the conventional components in the simulation.

6.1 In the Base method field, click  and select PENG-ROB.



## 7. Specifying Methods for Calculating COAL Properties

The Properties | Methods | NC Props | Property Methods sheet is used to specify the models used to calculate the nonconventional solid properties.

Because nonconventional components are heterogeneous solids that do not participate in chemical or phase equilibrium, the only physical properties that are calculated for *nonconventional* components are enthalpy and density.

In this simulation, use the HCOALGEN and the DCOALIGT models to calculate the enthalpy and density of coal and ash.

### 7.1 In the Model name field for Enthalpy, click and select HCOALGEN.

The component attributes PROXANAL, ULTANAL, and SULFANAL are automatically included in the Required component attributes for the selected models field for coal when you select HCOALGEN. Also, four Option code value fields with values of 1 appear change it to code 6 1 1 1.

Aspen Plus uses component attributes to represent nonconventional components in terms of a set of identifiable constituents needed to calculate physical properties. HCOALGEN uses the proximate analysis, ultimate analysis, and sulfur analysis to calculate the enthalpy of coal.

The Option code value fields define how the HCOALGEN model calculates the heat of combustion, the standard heat of formation, the heat capacity, and the enthalpy basis for coal.

7.2 In the Model name field for Density, click and select DCOALIGT.

Methods - NC Props

Property Methods Information

Component: COAL

Property models for nonconventional components

Property	Model name	Option codes											
Enthalpy	HCOALGEN	6	1	1	1								
Density	DCOALIGT												

Required component attributes

PROXANAL ULTANAL SULFANAL

## 8. Specifying Methods for Calculating Ash Properties

You must also specify how Aspen Plus calculates the enthalpy and density of ASH.

8.1 In the Component field, click and select ASH.

8.2 In the Model name field for Enthalpy, click and select HCOALGEN. The Option code value defaults of 1, 1, 1, and 1 are acceptable for ASH.

8.3 In the Model name field for Density, click and select DCOALIGT.

Property Methods Information

Component: ASH

Property models for nonconventional components

Property	Model name	Option codes											
Enthalpy	HCOALGEN	1	1	1	1								
Density	DCOALIGT												

Required component attributes

PROXANAL ULTANAL SULFANAL

## 9. Specifying the Heat of Combustion for Coal

We just specified that Aspen Plus will use a user-specified value for the heat of combustion of coal. Now you must specify that value.

9.1 From the Data Browser, select the Properties | Methods | Parameters | Pure Component folder. Click New. The New Pure Component Parameters dialog box appears. The heat of combustion for coal is a *Nonconventional* type.

9.2 Select the Nonconventional option.

9.3 Delete the default name NC-1 and enter *HEAT* as the new name in the Enter new name or accept default field.

9.4 Click OK. The Properties | Methods | Parameters | Pure Component | HEAT | Input sheet appears.

9.5 In the Parameter field, click  and select HCOMB.

Note that the prompt indicates that HCOMB is the heat of combustion on a dry basis. Use the following equation to convert the heat of combustion on a wet basis to a dry basis:

$$\text{HCOMB} = \text{Heat of Combustion (wet)} \times \frac{100}{100 - \% \text{Moisture}}$$

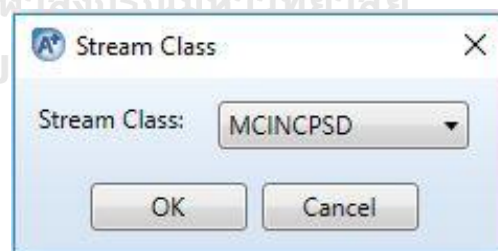
9.6 In the first line under the Nonconventional component parameter column, click  and select COAL.

9.7 In the parameter value field directly below COAL, enter the heat of combustion on a dry basis: 14.47 KJ/kg.

## 10. Defining the Stream class

10.1 Click (right click) at the stream line in Main flowsheet.

10.2 Select Change stream class, the window of Stream Class will appear.



10.3 Click to select Stream Class MCINCPSD

10.4 Click OK

10.5 Change all stream line to the MCINCPSD Stream Class

## 11. Entering Stream Data



The Simulation | Streams | AIR | Input sheet is used to specify a stream, Aspen Plus requires two thermodynamic specifications, and enough information to calculate the flow rate of each component.

### 11.1 Specifying the AIR Stream as follow data:

Specifications

Flash Type: Temperature, Pressure

State variables

Temperature: 30 C

Pressure: 1.01353 bar

Vapor fraction:

Total flow basis: Volume

Total flow rate: 51 l/min

Solvent:

Reference Temperature

Volume flow reference temperature: C

Component concentration reference temperature: C

Composition

Mole-Frac

Component	Value
CO	
CO2	
H2	
N2	0.79
O2	0.21
H2O	
C	
CH4	
Total	1

### Specifying the WETCOAL Stream as follow data:

Specifications

Substream name: NCPD

Temperature: 30 C

Pressure: 1.01353 bar

Total flow basis: Mass

Total flow rate: 3.6 kg/hr

Composition

Mass-Frac

Component	Value
COAL	1
ASH	
Total	1

Component Attribute

Component ID: COAL

Attribute ID: PROXANAL

Element	Value
MOISTURE	11.41
FC	17.34
VM	65.65
ASH	5.96

Particle Size Distribution

PSD mesh ID: PSD Units: mm

Interval	Lower limit	Upper limit	Weight fraction	Cumulative weight fraction
1	1	5	1	1

11.2 Change the attribute ID to ULTANAL

11.3 Change the attribute ID to SULFANAL

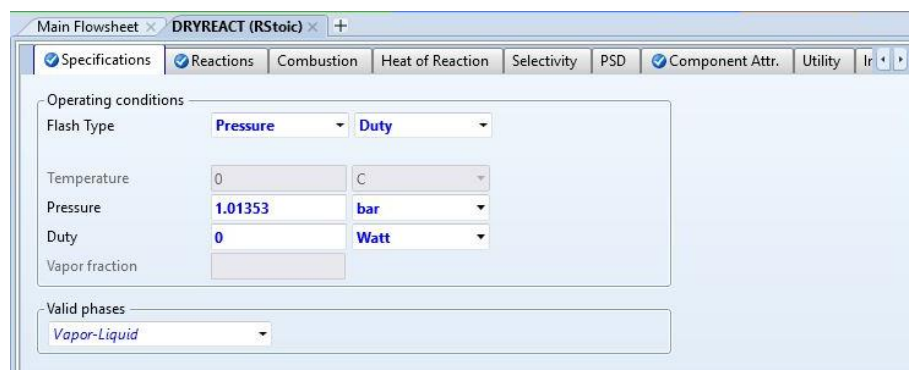
## 12. Specifying the RStoic Block (DRYREACT)

In the Simulation | Blocks | DRYREACT | Setup | Specifications sheet

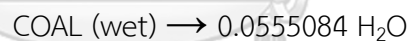
12.1 In the Pressure field, enter 1.01353 bar.

12.2 In the second operating conditions field, Flash Type, click and select Pressure duty.

12.3 In the duty field, enter 0 Watt.



This RStoic block models the drying of coal. Although coal drying is not normally considered a chemical reaction, you are using an RStoic block to convert a portion of the coal to form water. The following equation is the chemical reaction for coal drying:



Aspen Plus treats all nonconventional components as if they have a molecular weight of 1.0. The reaction indicates that 1 mole (or 1 lb.) of coal reacts to form 0.0555084 mole (or 1 lb.) of water.

12.4 To Enter the Reaction Stoichiometry

1) In Reaction Tab, Click New, The Edit Stoichiometry dialog box appears.

A reaction number of 1 is automatically chosen.

2) In the Reactants Component field, click and select COAL.

3) In the Reactants Coefficient field, enter 1.

Note that the stoichiometric coefficient for reactants is displayed as negative.

4) In the Products Component field, click and select H2O.

- 5) In the Products Coefficient field, enter .0555084.

The conversion for this reaction must be set to achieve the proper amount of drying.

- 6) In the Products generation section, select the Fractional conversion option.

- 7) In the Fractional conversion field, enter 0.2 and in the of component field, click and select COAL.

The fraction conversion of Coal of 0.2 is a temporary value that you will override later with a Calculator block.

Edit Stoichiometry

Reaction No. 1

Reactants	
Component	Coefficient
COAL	-1

Products	
Component	Coefficient
H2O	0.0555084

Products generation

Molar extent  mol/min

Fractional conversion  of component

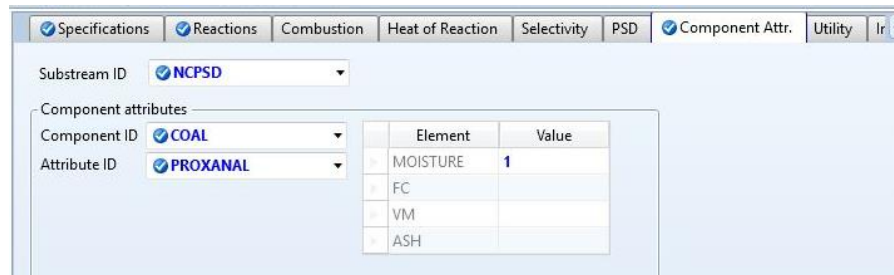
OK Close

### 13. Specifying the Moisture Content of COAL

Drying the coal changes its component attribute for moisture in the Proximate Analysis. Since the other elements of PROXANAL, ULTANAL, and SULFANAL are on a dry basis, drying the coal does not change these attributes.

- 1) Click the Blocks | DRYREACT | Setup | Component Attr. Component Attr. Tab sheet. This sheet, enter the values for component attributes that change in this RStoic block. If you do not enter an attribute value, the attribute does not change.
- 2) In the Substream field, click and select *NCPSD*.

- 3) In the Component ID field, click and select *COAL*.
- 4) In the Attribute ID field, click and select *PROXANAL*.
- 5) In the Moisture field, enter a value of 1.0. (The moisture content of 1.0 is a temporary value that you will override later with a Fortran block.)



#### 14. Using a Calculator Block to Control Drying

The material balance equations for this process define relations between the following quantities:

- Water content of the feed coal.
- Fractional conversion of coal to water.
- Water content of the dried coal.

$$\text{CONV} = (\text{H}_2\text{OIN} - \text{H}_2\text{ODRY}) / (100 - \text{H}_2\text{ODRY})$$

Where:  $\text{H}_2\text{OIN}$  = Percent moisture in the coal in stream WET-COAL

$\text{H}_2\text{ODRY}$  = Percent moisture in the coal in stream IN-DRIER

$\text{CONV}$  = Fractional conversion of coal to  $\text{H}_2\text{O}$  in the block DRY-REAC

Use this equation in a Calculator block to ensure these three specifications are consistent.

The Calculator block specifies the moisture content of the dried coal and calculates the corresponding conversion of coal to water.

Using a Calculator block to set specifications allows you to run different cases easily.

- 1) From the Data menu, select Flowsheeting Options | Calculator.
- 2) Click New to create a new Calculator block. Fill WATER to define this calculation in The Enter ID block and click OK. The Flowsheeting Options |

Calculator | WATER | Input | Define sheet appears. Use this sheet to access the flow sheet variables you want to use in the Calculator block. Define the three Calculator variables from the equation: H2OIN, H2ODRY, and CONV. H2OIN is the water content of the feed coal. The H2OIN variable accesses the first element (percent moisture) of the component attribute PROXANAL for component COAL in the NCPD substream of stream WETCOAL.

#### 14.1 Creating the H2OIN Variable

- 1) Click New. The Create new Variable dialog box appears.
- 2) In the Variable name field, enter H2OIN and click OK.  
The Variable Definition dialog box appears.
- 3) Under Category, select Streams.
- 4) In the Reference frame, in the Type field, click and select Compattr-Var since the variable is a component attribute. When you are specifying variables, Aspen Plus displays the other fields necessary to complete the variable definition. In this case, the Stream field appears.
- 5) In the Stream field, click and select WETCOAL.  
The Substream and Component fields appear. In this example, do not modify the default choice of NCPD in the Substream field.
- 6) In the Component field, click and select COAL.  
The Attribute field appears.
- 7) In the Attribute field, click and select PROXANAL.
- 8) In the Element field, enter 1. Press Enter.
- 9) In the Information flow frames, Click Import Variable.

Main Flowsheet x WATER x +

Define Calculate Sequence Tears Stream Flash Information

Active

Sampled variables (drag and drop variables from form to the grid below)

Variable	Information flow	Definition
H2OIN	Import variable	Compattr-Var Stream=WETCOAL Substream=NCPD Component=COAL Attribute=PROXANAL Element=1
H2ODRY		Block-Var Block=DRYREACT Variable=COMPATT Sentence=COMP-ATTR ID1=NCPD ID2=COAL ID3=PROXANAL Element=1
CONV	Export variable	Block-Var Block=DRYREACT Variable=CONV Sentence=CONV ID1=1

New... Delete Copy Paste Move Up Move Down View Variables

Edit selected variable

Variable: H2OIN

Category:  All  Blocks  Streams  Model Utility  Property Parameters  Reactions

Reference:

Type: Compattr-Var  
Stream: WETCOAL  
Substream: NCPD  
Component: COAL  
Attribute: PROXANAL  
Element: 1

Information flow:  Import variable  Export variable  Tear variable

EO input

Open variable:

Description:

## 14.2 Creating the Other Variables

### 1) H2ODRY

Edit selected variable

Variable: H2ODRY

Category:  All  Blocks  Streams  Model Utility  Property Parameters  Reactions

Reference:

Type: Block-Var  
Block: DRYREACT  
Variable: COMPATT  
Sentence: COMP-ATTR  
ID1: NCPD  
ID2: COAL  
ID3: PROXANAL  
Element: 1

Information flow:  Import variable  Export variable  Tear variable

EO input

Open variable:

Description:

### 2) CONV

Edit selected variable

Variable: CONV

Category:  All  Blocks  Streams  Model Utility  Property Parameters  Reactions

Reference:

Type: Block-Var  
Block: DRYREACT  
Variable: CONV  
Sentence: CONV  
ID1: 1

Information flow:  Import variable  Export variable  Tear variable

EO input

Open variable:

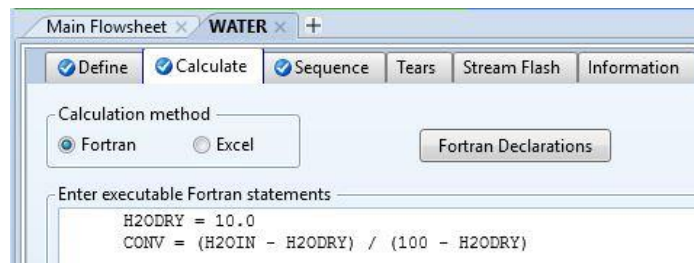
Description:

### 14.3 Calculating the Conversion Variable

The Calculator | WATER | Input | Calculate sheet. Use this sheet to enter the Fortran statements you want Aspen Plus to execute to set H2ODRY and to calculate CONV from equation.

- 3) Enter the following Fortran statements:

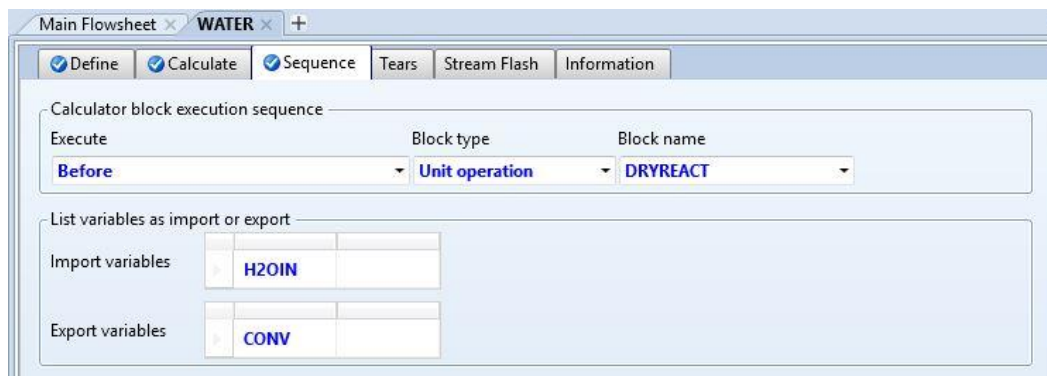
$$H2ODRY = 10.0$$

$$CONV = (H2OIN - H2ODRY) / (100 - H2ODRY)$$


### 14.4 Specifying When the Calculator Block Should Run

The Calculator | WATER | Input | Sequence sheet. Use this sheet to specify when Aspen Plus should execute this Calculator block. Since you have used inline Fortran to modify the specifications for the RStoic block DRYREACT, this Calculator block should execute immediately prior to DRYREACT.

- 4) In the Execute field, click and select Before.
- 5) In the Block type field, click and select Unit operation.
- 6) In the Block name field, click and select DRYREACT.



## 15. Specifying the RYield Reactor Model



The Simulation | Blocks | DECOMP | Setup | Specifications sheet . RYield is used to simulate a reactor with a known yield, and does not require reaction stoichiometry and kinetics.

- 1) On the DECOMP | Setup | Specifications sheet, enter the pressure and temperature: Pressure 1.01353 bar, Temperature 300 °C

The screenshot shows the 'DECOMP (RYield)' specifications sheet. The 'Operating conditions' section includes the following fields:

- Flash Type: Temperature (dropdown), Pressure (dropdown)
- Temperature: 300 (input), C (dropdown)
- Temperature change: (input), C (dropdown)
- Pressure: 1.01353 (input), bar (dropdown)
- Duty: 0 (input), Watt (dropdown)
- Vapor fraction: (input)

The 'Valid phases' section is set to 'Vapor-Liquid' (dropdown).

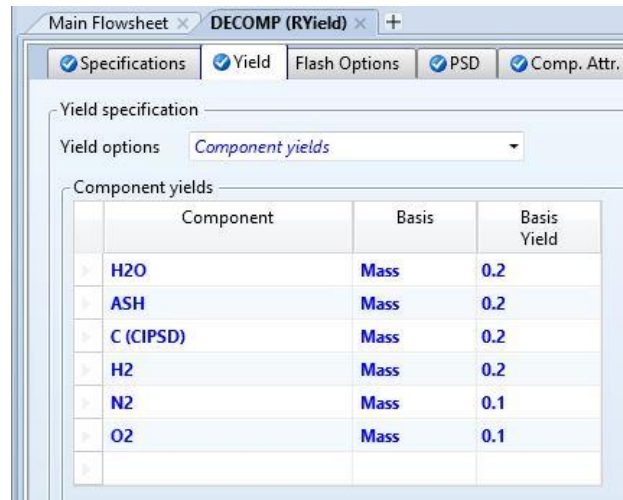
- 2) The Yield sheet appears.

For this simulation, the yield distribution you enter on this sheet is not the true yield distribution. Use a Calculator block to calculate the actual yield distribution from the component attributes for coal in the feed stream to the RYield model (stream DRY-COAL).

- 3) Enter the component yields as follows:

Component	Basis	Yield
H <sub>2</sub> O	Mass	0.2
ASH	Mass	0.2
C (CIPSD)	Mass	0.2
H <sub>2</sub>	Mass	0.2
N <sub>2</sub>	Mass	0.1
O <sub>2</sub>	Mass	0.1

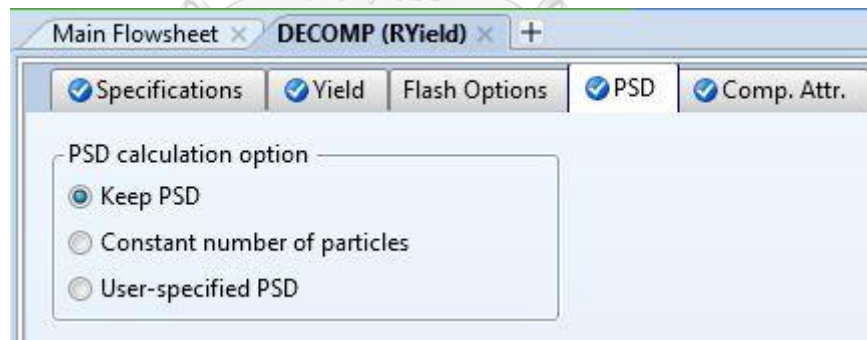




In addition to the MIXED substream products, this RYield block forms carbon in the CIPSD substream and ash in the NCPD substream. To fully specify the yield, specify the particle size distributions of the CIPSD and NCPD substream and the component attributes of the ash that is formed.

#### 16. Specifying the Particle Size Distributions

- 1) Click the PSD tab
- 2) In the PSD calculation option, click Keep PSD.



#### 17. Specifying the Component Attributes for Ash

- 3) Click the Comp. Attr. tab.

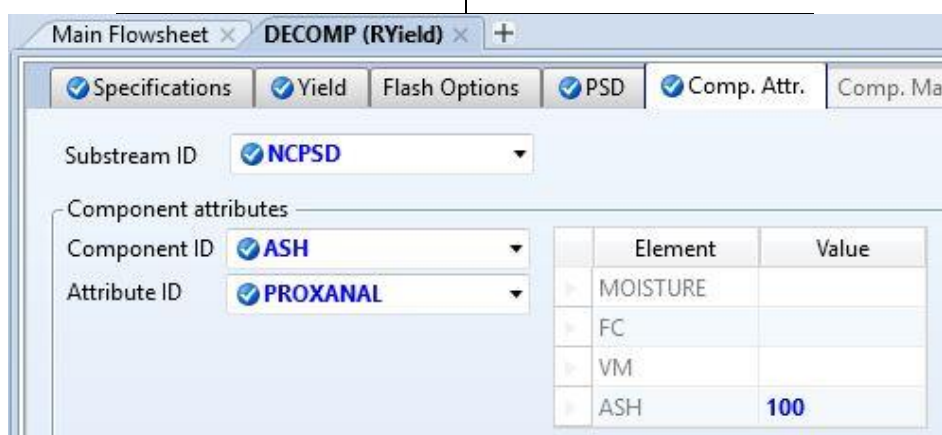
The attributes PROXANAL, ULTANAL, and SULFANAL are required for RYield to calculate the enthalpy and density of ash.

- 4) In the Substream ID field, click  and select *NCPD*.
- 5) In the Component ID field, click  and select *ASH*. ASH has the attributes PROXANAL, ULTANAL, and SULFANAL.

6) In the Attribute ID field, click  and select PROXANAL.

7) For the attribute PROXANAL, enter these values:

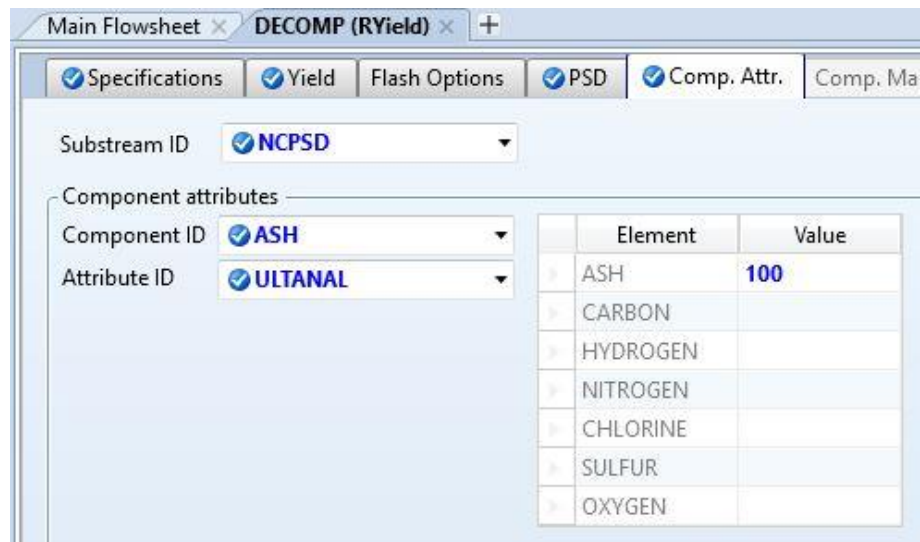
Element	Value
Moisture	0
FC	0
VM	0
Ash	100



8) In the Attribute ID field, click  and select *ULTANAL*.

9) For the attribute *ULTANAL*, enter these values:

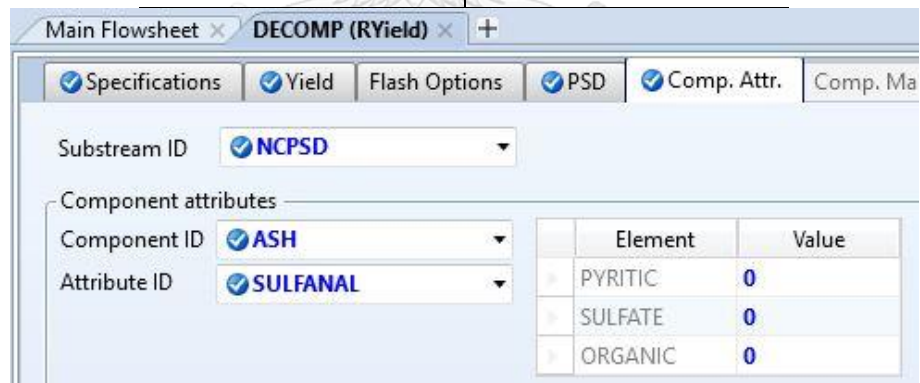
Element	Value
Ash	100
Carbon	0
Hydrogen	0
Nitrogen	0
Chlorine	0
Sulfur	0
Oxygen	0



10) In the Attribute ID field, click  and select *SULFANAL*.

11) For the attribute *SULFANAL*, enter these values:

Element	Value
Pyritic	0
Sulfate	0
Organic	0



#### 18. Using a Calculate Block to Control decomposition of COAL

You have completed enough specifications to run the simulation. However, the yields you specified in the RYield block were only temporary placeholders. You could directly enter the correct yields on the RYield | Setup | Yield sheet. However, by defining a Calculator block to calculate the yields based on the component

attributes of the feed coal, you will be easily able to run different cases (such as different feed coals).

### 18.1 Create the Calculator Block

- 1) From the Aspen Plus menu bar, select Data | Flowsheeting Options | Calculator. The Calculator object manager appears.
- 2) Click New to create a new Calculator block. The Create new ID dialog box appears with an automatically generated ID, C-1.
- 3) In the Create new ID dialog box, enter *COMBUST* as the ID and click OK.

### 18.2 Creating the Calculator Variables

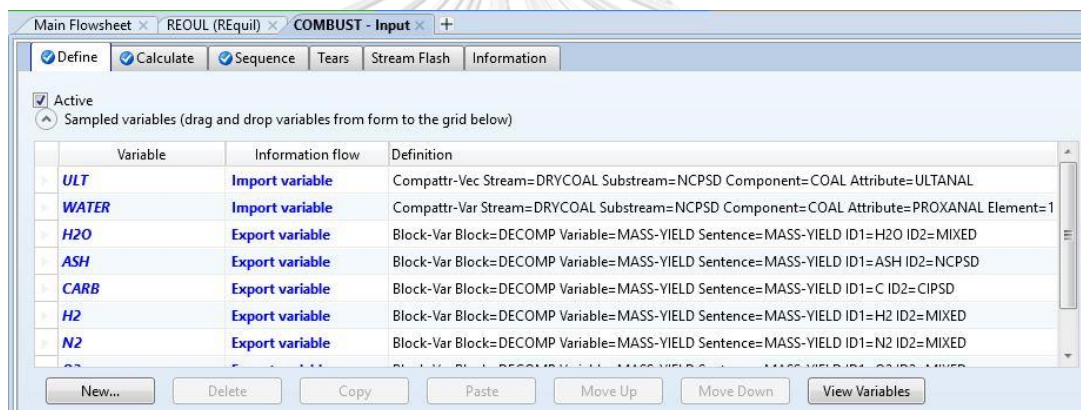
The Simulation | Flowsheeting Options | Calculator | COMBUST | Input | Define sheet. Use this sheet to access the flowsheet variables you want to use in the Fortran block. In this simulation, access the ultimate analysis of coal in stream DRY-COAL as a component attribute vector. Also define variables to access the moisture content of coal and the yield of each component in the DECOMP block.

- 4) Create and define the following two variables:

Variable Name	Type	Stream	Substream	Component	Attribute	Element
ULT	Compattr-Vec	DRY-COAL	NCPSD	COAL	ULTANAL	
WATER	Compattr-Var	DRY-COAL	NCPSD	COAL	PROXANA L	1

5) Also define the following eight mass yield variables.

Variable Name		ID1	ID2
H <sub>2</sub> O		H2O	MIXED
ASH	Type <i>Block-Var</i>	ASH	NCPSD
CARB	Block <i>DECOMP</i>	C	CIPSD
H <sub>2</sub>	Variable <i>MASS-</i>	H2	MIXED
N <sub>2</sub>	<i>YIELD</i>	N2	MIXED
Cl <sub>2</sub>	For all eight	CL2	MIXED
SULF	variables	S	MIXED
O <sub>2</sub>		O2	MIXED



6) Click the Calculate tab.

### 18.3 Specify the Calculations to be Performed

The Simulation | Flowsheeting Options | Calculator | COMBUST | Input | Calculate sheet appears.

ULTANAL is defined as the ultimate analysis on a dry basis. The variable WATER, defined as the percent H<sub>2</sub>O in the PROXANAL for coal, is used to convert the ultimate analysis to a wet basis. The remaining eight variables (H<sub>2</sub>O through O<sub>2</sub>) are defined as the individual component yields of various species in the RYield block. ULT and WATER can then be used to calculate the yield of the individual species in the RYield block.

7) Enter the following Fortran statements:

C FACT IS THE FACTOR TO CONVERT THE ULTIMATE ANALYSIS TO A WET BASIS.

FACT = (100 - WATER) / 100

H2O = WATER / 100

ASH = ULT(1) / 100 \* FACT

CARB = ULT(2) / 100 \* FACT

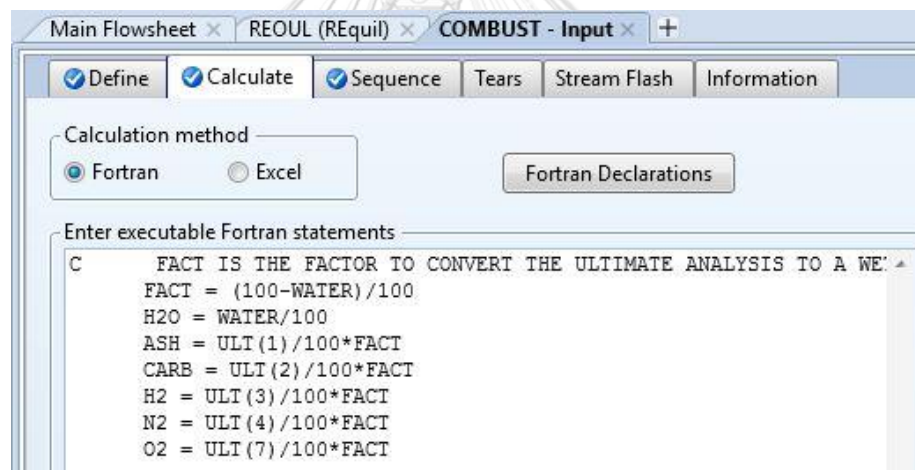
H2 = ULT(3) / 100 \* FACT

N2 = ULT(4) / 100 \* FACT

CL2 = ULT(5) / 100 \* FACT

SULF = ULT(6) / 100 \* FACT

O2 = ULT(7) / 100 \* FACT



8) Click the Sequence tab.

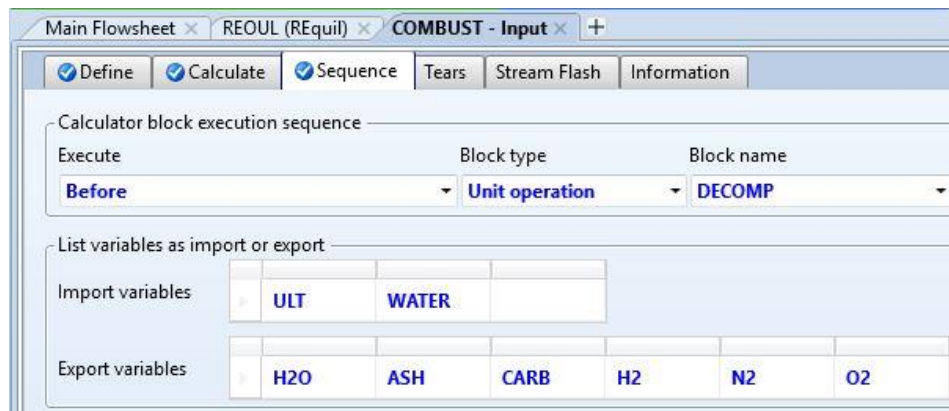
#### 18.4 Specify When the Calculator Block Should be Run

The Simulation | Flowsheeting Options | Calculator | COMBUST | Input | Sequence sheet appears. Since this Calculator block sets values in block DECOMP, the Calculator block must execute before DECOMP.

9) In the Execute field, click  and select Before.

10) In the Block type field, click  and select Unit operation.

11) In the Block name field, click  and select *DECOMP*.



12) Close the Data Browser window.

### 19. Specifying the RGibbs Reactor Model

RGibbs is used to model reactions that come to chemical equilibrium. RGibbs calculates chemical equilibrium and phase equilibrium by minimizing the Gibbs free energy of the system. Therefore, you do not need to specify the reaction stoichiometry

On the Simulation | Blocks | BURN | Setup | Specifications sheet, enter your thermodynamic specifications. This reactor will be at atmospheric pressure.

- 1) In the Pressure field, enter 1.01353 bar and temperature 700 °C. The heat duty for this reactor is specified by the heat stream Q-DECOMP.
- 2) In the Calculation options box, select Restrict chemical equilibrium.
- 3) Select the Products tab. The BURN | Setup | Products sheet. On this sheet, enter the list of products that may exist at equilibrium.

By default, RGibbs assumes that all of the components that are listed on the Components | Specifications | Selection sheet are potential products in the vapor phase or the liquid phase. This default is not appropriate for this simulation, since any carbon that remains after combustion would be solid.

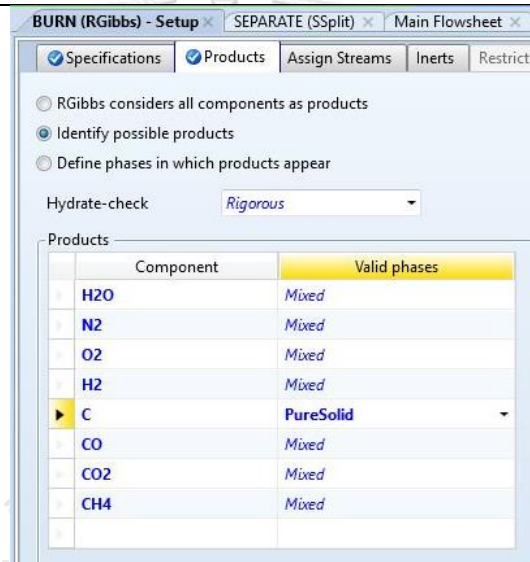
- 4) Select Identify possible products. The Products list appears.

For this simulation, all components are potential MIXED substream products, except for carbon, which is a solid product. Carbon must be assigned a phase

of Pure Solid. This means that any carbon that forms will be present as a pure, solid phase, not present as a solid solution or alloy.

- 5) In the products list, enter the component species and phases shown below:  
(Be sure to change the Phase for C to Pure Solid.)

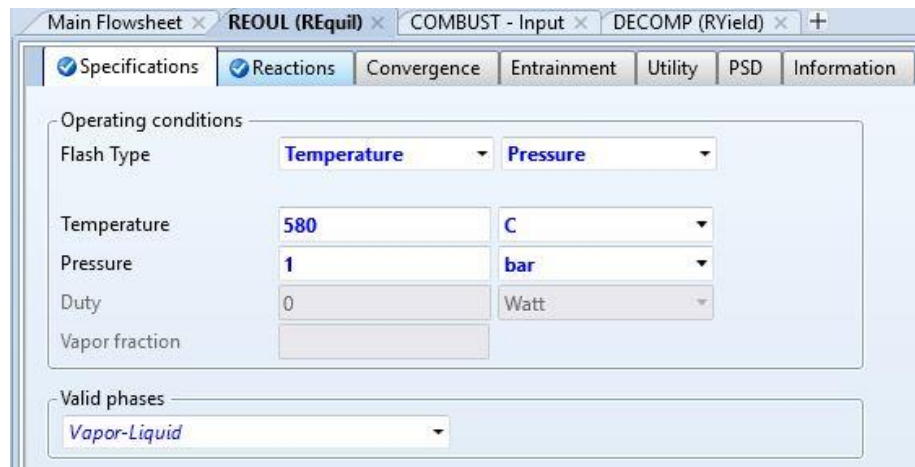
Component	Phase	Component	Phase
H <sub>2</sub> O	Mixed	C	Pure Solid
N <sub>2</sub>	Mixed	CO	Mixed
O <sub>2</sub>	Mixed	CO <sub>2</sub>	Mixed
H <sub>2</sub>	Mixed	CH <sub>4</sub>	Mixed



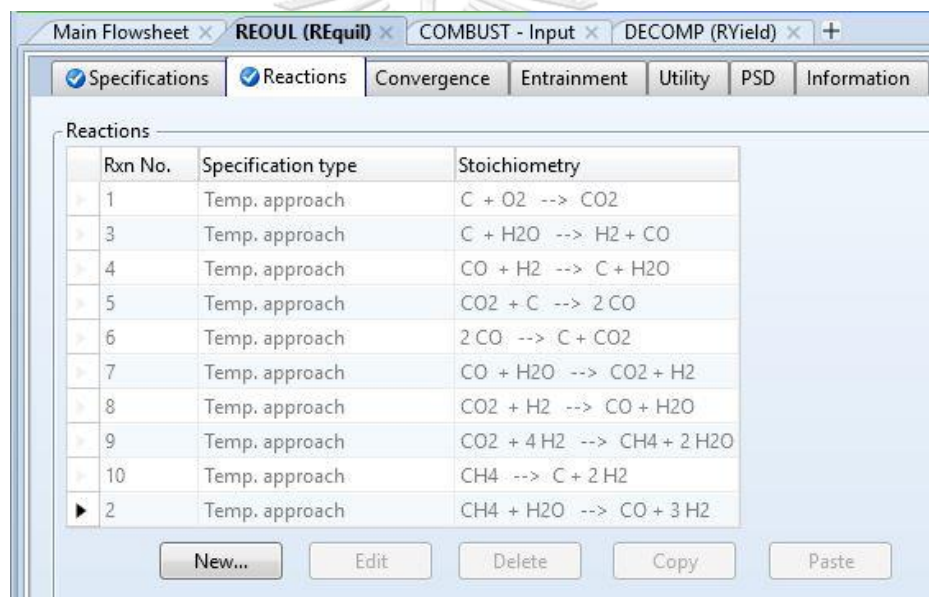
## 20. Specifying the REQU for the REquil Block

- 1) Define the following data in the The simulation | Blocks | REQU | Input | Specifications





- 2) Define the following data in the The simulation | Blocks | REOUL | Input | Reaction



## 21. Specifying the COOLER for the Heater Block

- 1) Define the following data in the The simulation | Blocks | COOLER | Input | Specifications

The screenshot shows the 'Specifications' tab of the 'COOLER (Heater)' dialog. The 'Flash specifications' section includes:

- Flash Type: Temperature (dropdown)
- Pressure: (dropdown)
- Temperature: 25 (input), C (dropdown)
- Temperature change: (input), C (dropdown)
- Degrees of superheating: (input), C (dropdown)
- Degrees of subcooling: (input), C (dropdown)
- Pressure: 1 (input), bar (dropdown)
- Duty: (input), Watt (dropdown)
- Vapor fraction: (input)
- Pressure drop correlation parameter: (input)
- Always calculate pressure drop correlation parameter

The 'Valid phases' section shows 'Vapor-Liquid' (dropdown).

## 22. Specifying the Splits for the SSplit Block

The simulation | Blocks | SEPARATE | Input | Specifications sheet. SSplit mixes all of its feed streams, then splits the resulting mixture into two or more streams according to substream specifications.

In this simulation, the SSplit block provides perfect separation between the gaseous products of combustion (MIXED substream) and the solid products of combustion (CIPSD and NCPSD substreams).


- 1) Enter the following split fraction values for the GASES2 outlet stream:

Substream Name	Specification	Value
MIXED	Split fraction	1.0
CIPSD	Split fraction	0.0
NCPSD	Split fraction	0.0

Substream Name	Specification	Basis	Value	Units	Key Comp No
MIXED	Split fraction		1		
CIPSD	Split fraction		0		
NCPD	Split fraction		0		

2) Close the Data Browser window.

### 23. Running the Simulation

1) Click  to run the simulation.

The Control Panel window appears, allowing you to monitor and interact with the Aspen Plus simulation calculations. As Aspen Plus performs the analysis, status messages display in the Control Panel. The simulation completes without warnings or errors. When the calculations finish, the message Results Available appears in the status area at the bottom right of the main window.

2) When the Simulation Run Completed message appears in the status bar, close the Control Panel window.

3) Examine the results of your simulation.

### 24. Examining Simulation Results

From the Control Panel, click .The Results Summary | Run Status | Streams

sheet to View the Stream Results

Material	AIR	COOL	DRYCOAL	GASES1	GASES2	INBURNER	LIQUID	PRODUCT	SOLIDS	WETCOAL
Substream: MIXED										
Mole Flow mol/min										
CO	0	0.835419	0	0.835419	0.835419	0	0	0.389691	0	0
CO2	0	0.755074	0	0.755074	0.755074	0	0	0.98247	0	0
H2	0	0.942466	0	0.942466	0.942466	1.70545	0	0.514868	0	0
N2	1.62092	1.63619	0	1.63619	1.63619	0.0152682	0	1.63619	0	0
O2	0.430877	1.1842e-25	0	1.1842e-25	1.1842e-25	0.7152	0	7.4274e-28	0	0
H2O	0	0.280509	0.0521779	0.280509	0.280509	0.333922	0	0.271444	0	0
C	0	3.2322e-35	0	3.2322e-35	3.2322e-35	0	0	6.1485e-39	0	0
CH4	0	0.408197	0	0.408197	0.408197	0	0	0.626528	0	0
Mass Flow kg/hr										
CO	0	1.40402	0	1.40402	1.40402	0	0	0.654924	0	0
CO2	0	1.99384	0	1.99384	1.99384	0	0	2.5943	0	0
H2	0	0.113994	0	0.113994	0.113994	0.206278	0	0.0622747	0	0
N2	2.72445	2.75012	0	2.75012	2.75012	0.0256629	0	2.75012	0	0
O2	0.827253	2.2736e-25	0	2.2736e-25	2.2736e-25	1.37313	0	1.426e-27	0	0
H2O	0	0.303206	0.0563999	0.303206	0.303206	0.360942	0	0.293408	0	0
C	0	2.3293e-35	0	2.3293e-35	2.3293e-35	0	0	4.431e-39	0	0
CH4	0	0.392916	0	0.392916	0.392916	0	0	0.603074	0	0
Total Flow mol/min	2.05179	4.85785	0.0521779	4.85785	4.85785	2.76984	0	4.42119	0	0

## VITA

Jurarat Nisamaneenate was born in Lampang, Thailand, on November 20th, 1984. After finishing high school in 2004, she entered the University in King Mongkut's Institute of Technology Ladkrabang, Thailand. In May of 2007, she completed a Bachelor of Science in Environmental Resources Chemistry. In September 2010, she completed at Chulalongkorn University in Master degree of Engineering (Environmental Engineering).

### Publications:

Nisamaneenate, J., Atong, D., Sornkade, P., Sricharoenchaikul, V. 2015. Fuel gas production from peanut shell waste using a modular downdraft gasifier with the thermal integrated unit. *Renewable Energy*, 79: 45–50.

Nisamaneenate, J., Atong, D., Sornkade, P., Sricharoenchaikul, V. 2015. Advanced reforming of agro-waste by modular gasifier for fuel generation. *Chemical Engineering Journal*, 282:170-178.

Sricharoenchaikul, V., Atong, D., Sornkade, P., Nisamaneenate, J. 2016. Performance of Ni/dolomite pellet catalyst on gas distribution from cassava rhizome gasification with a modular fixed-bed gasifier. *Environmental Technology*, 38: 1176-1183.

### Permanent Address:

8 RTS CONDO Viphawadee 16/28

Dindang, Dindang

Bangkok, Thailand 10400